NASA Contractor Report 165274

A CONCEPTUAL STUDY OF THE POTENTIAL FOR AUTOMOTIVE-DERIVED AND FREE-PISTON STIRLING ENGINES IN 30- TO 400-KILOWATT STATIONARY POWER APPLICATIONS

Arthur Vatsky, H. S. Chen, and John Dineen

Mechanical Technology Incorporated
Latham, New York

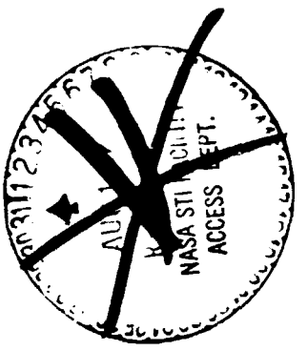

May 1982

Prepared for

NATIONAL AERONAUTICS AND SPACE ADMINISTRATION
Lewis Research Center
Under Contract NAS3-21291

TABLE OF CONTENTS

TABLE OF CONTENTS (Cont'd.)

TABLE OF CONTENTS (Cont'd.)

SUMMARY

The objective of this study was to characterize free-piston and kinematic Stirling engines for stationary applications up to brake powers of 400 kilowatts. Comparison and evaluation of the designs were made on the basis of mechanical feasibility and engine performance: the influences of various working fluids, life cycle, heater head material, and optimized engine geometries on engine design were examined. The proposed engine designs for both the free-piston and the kinematic Stirling engine were found to be mechanically acceptable for the designated 50,000 hour life criteria, and could be developed for stationary applications, achieving brake efficiency ranging from 34 percent for a 30 kW automotive-derived kinematic engine to 46 percent efficiency in the 400 kW power class. Other performance results are:

- A Stirling engine using an advanced variable-stroke output control system is a viable stationary alternative to the presently developed mean pressure control system for automotive applications by offering a multiple of operational and performance advantages.

- The conversion of a kinematic engine design into a free-piston counterpart was achieved through the use of a new hydraulic output system, which shows significant advantages for direct drive of hydraulic loads.

- With common component materials an automotive-derived stationary kinematic engine utilizing helium as the working fluid achieves the brake efficiency of 36.3 percent, whereas a stationary engine designed exclusively for this application reaches a value of 40.5 percent.

- Hydrogen as a working fluid offers at least a 2 percent benefit over helium.

- Free-piston Stirling engines over the power classes considered, and incorporating hydraulic fluid output, reached within two percentage points of similar-sized kinematic engines with common materials. The 400 kW engines were not optimized within this study, thus further efficiency gains would be expected.

While significant gains in efficiency were achieved with the kinematic engines optimized exclusively for the stationary application, automotive-derived engines would counterbalance this performance with cost advantages deriving from both a mature technology base and parts commonality.

The free-piston Stirling engines, on the other hand while achieving comparable performance, offer potentially extended life design advantages over the kinematic engine, by eliminating the need for high pressure differential rod seals.

In conclusion, the inherent high efficiency and the multi-fuel characteristics of Stirling engines demonstrate these designs are potentially major contributors in relieving U.S. dependence on imported petroleum quotas. Future design and development work should be pursued, especially when today's Stirling engine technology (automotive) has reached a level of maturity which proves its suitability for a multiplicity of applications, including stationary power plants.

1.0 INTRODUCTION

This report contains the results of a nine-month study contract awarded to Mechanical Technology Incorporated (MTI) by the NASA/Lewis Research Center (NASA/LeRc) to assess the potential of Stirling engines for stationary applications at power levels up to 400 kW. Both kinematic (crank-driven) and free-piston engines were analyzed in terms of mechanical feasibility and performance, which includes the parameters of life, efficiency, and feasibility. Stirling engines offer high efficiency, low noise, and multi-fuel capability and, in stationary power applications, they can contribute significantly to the national goal of reducing our dependence on petroleum resources. The engine configurations include a 30 kW kinematic Stirling engine derived from automotive application, a 400 kW conceptual kinematic design, and two conceptual free-piston stationary engines utilizing hydraulic fluid output.

The starting point of the kinematic engine evaluation was to modify the automotive Stirling engine generated under Contract DEN 3-32, which has been under development since 1979: this engine is described as the Reference Engine System Design (RESD). Basically, the design was not changed, but downrated to meet the stationary engine life requirement of 50,000 hours and all unnecessary automotive accessories and auxiliaries were removed or modified to match the stationary engine requirements. After evaluation of the downrated version, the automotive-derived engine was optimized exclusively for the stationary application to evaluate performance potential. Changes were limited to those components which could be incorporated without interfering or influencing the major components in the RESD production line. The objective was to evaluate the performance of a stationary engine that in essence could be "pulled" from an automotive production line without special production or development requirements.

To determine the impact on design and performance of a higher output power, a 400 kW optimized kinematic engine was developed to achieve peak efficiency and was not constrained by the RESD production criteria. These engines were evaluated with both hydrogen and helium as the engine working fluid and also alternate component materials were considered.

Similarly, free-piston Stirling engines (FPSE) incorporating a hydraulic fluid output were designed to match the power output of the optimized stationary kinematic engine counterparts. Here the working gas was helium and no variations in material were included. The 37.5 kW and 400 kW engines were scaled from the 37.5 kW kinematic optimized engine.

The complete matrix of engine designs is summarized in Table 1. It should be noted, all the designs utilized the same analytical codes and have the equivalent mechanical design background. Except for the baseline automotive-derived kinematic engine, the designs contained in this study are classified as conceptual configurations requiring further detailed analysis and development test verification.

TABLE 1

Summary of Stationary Stirling Engines

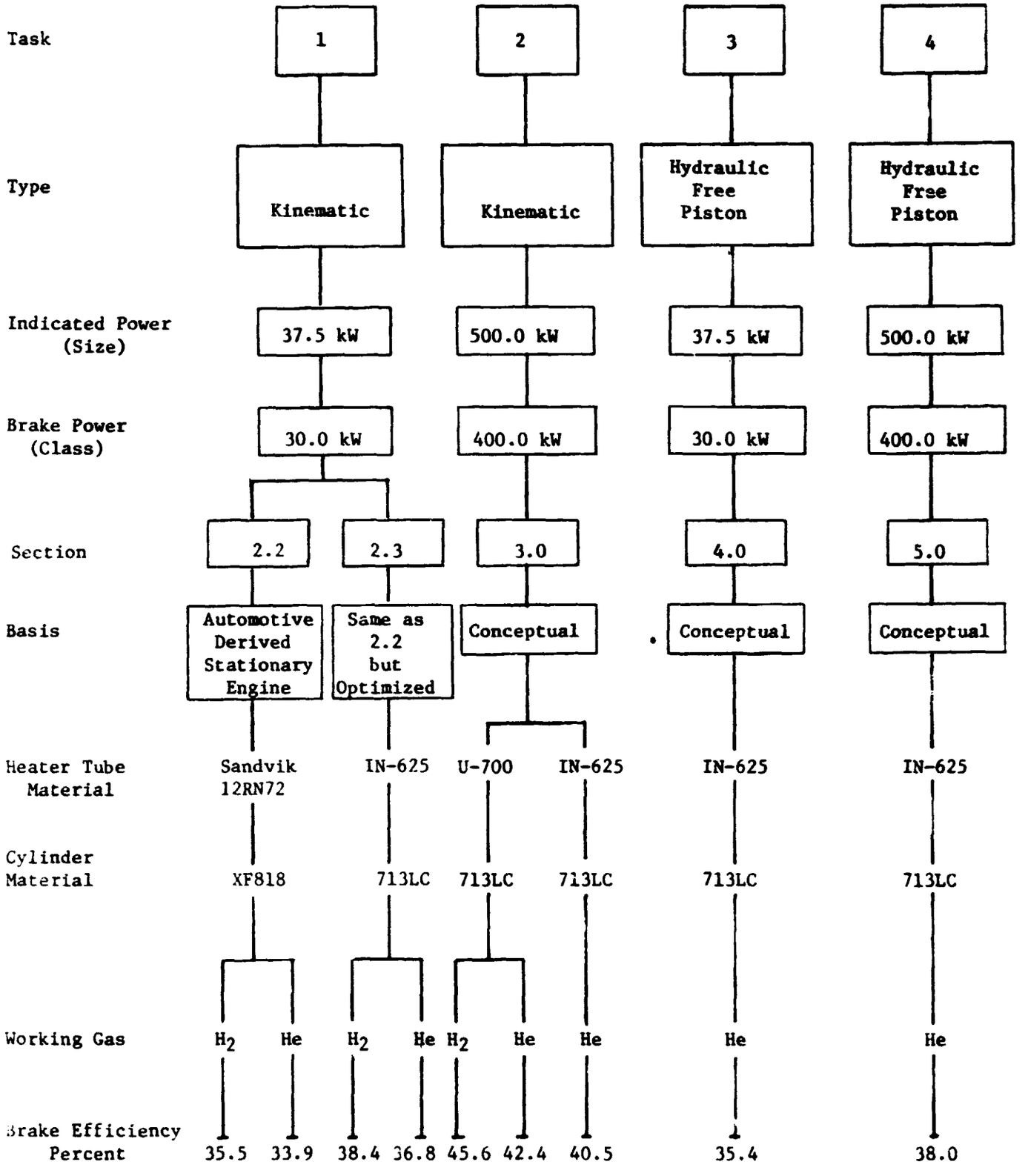

2.0 40 kW KINEMATIC STIRLING ENGINE

2.1 Introduction

Task 1 within this Section evaluates the feasibility of adapting automotive-derived Stirling engines with kinematic output drives to stationary applications in the 40 kW power class. Two engines are considered: automotive-derived with minor external modifications only and an optimum configuration with limited engine geometry and material modifications. In both cases the performance influences of using either hydrogen or helium gas as a working fluid are discussed.

2.2 37.5 kW Reference Engine (Baseline Engine)

2.2.1 Design Approach

This engine is a direct application of the Automotive Stirling Reference Engine designed and developed under the D.O.E. Development Contract (DEN 3-32). To achieve high life requirements, the automotive-derived engine was derated with only minor component changes. Additionally, this approach has a lower cost potential by maintaining parts commonality with a mature engine which offers, in turn, an available production source. The Automotive Reference Engine System (RESD) design is shown in Figure 2.2.1 and, for the stationary application, has no internal engine design changes. Only the actual engine steady state operating conditions of temperature, pressure, and rpm will be derated to extend the automotive engine design life of 3500 hours (simulated automotive duty cycle) to a 50,000-hour stationary engine life (single point, steady state). Under these conditions, an extension of the design parameters of creep life in the hot engine parts and a reduction in wear in the seal area are selected as the primary criteria. Fatigue was not a prime consideration, due to the reduced daily start-stop occurrences in the stationary application, as compared with the 3500-hour life of the automotive engine. The complete automotive engine performance and design is contained in the "Automotive Stirling Reference Engine Design Report" Reference 1.

The Automotive Reference Engine provides 60 kW brake output power at a maximum speed of 4000 rpm and a mean pressure of 15 MPa. To achieve maximum mileage, the peak brake efficiency of 43.5 percent is reached at the part-power condition of 22.1 kW, 1100 rpm, 15 MPa.

By the direct interrelationship of engine weight and volume with vehicle drag and weight, automotive engine installations tend to constrain the engine size and demand high power density. These limitations can be relaxed in the stationary engine installation wherever optional or performance gains can be realized. Design changes are proposed, therefore, to the base Reference Engine in the external heating system to take advantage of this condition.

While the study includes the influence of hydrogen and helium as working gases, the final selection will depend upon the engine application and performance objectives. An analysis of all possible working gases shows that hydrogen and helium are better than any other gas for the Stirling Engine. Hydrogen has the highest thermal conductivity and the lowest viscosity, which are the key characteristics for the efficient Stirling cycle. But, hydrogen permeates easily through metal and can degrade material properties through embrittlement. Also, highly effective sealing designs are required to diminish the potential for leakage of this gas. On the other hand, helium, with twice the molecular weight,

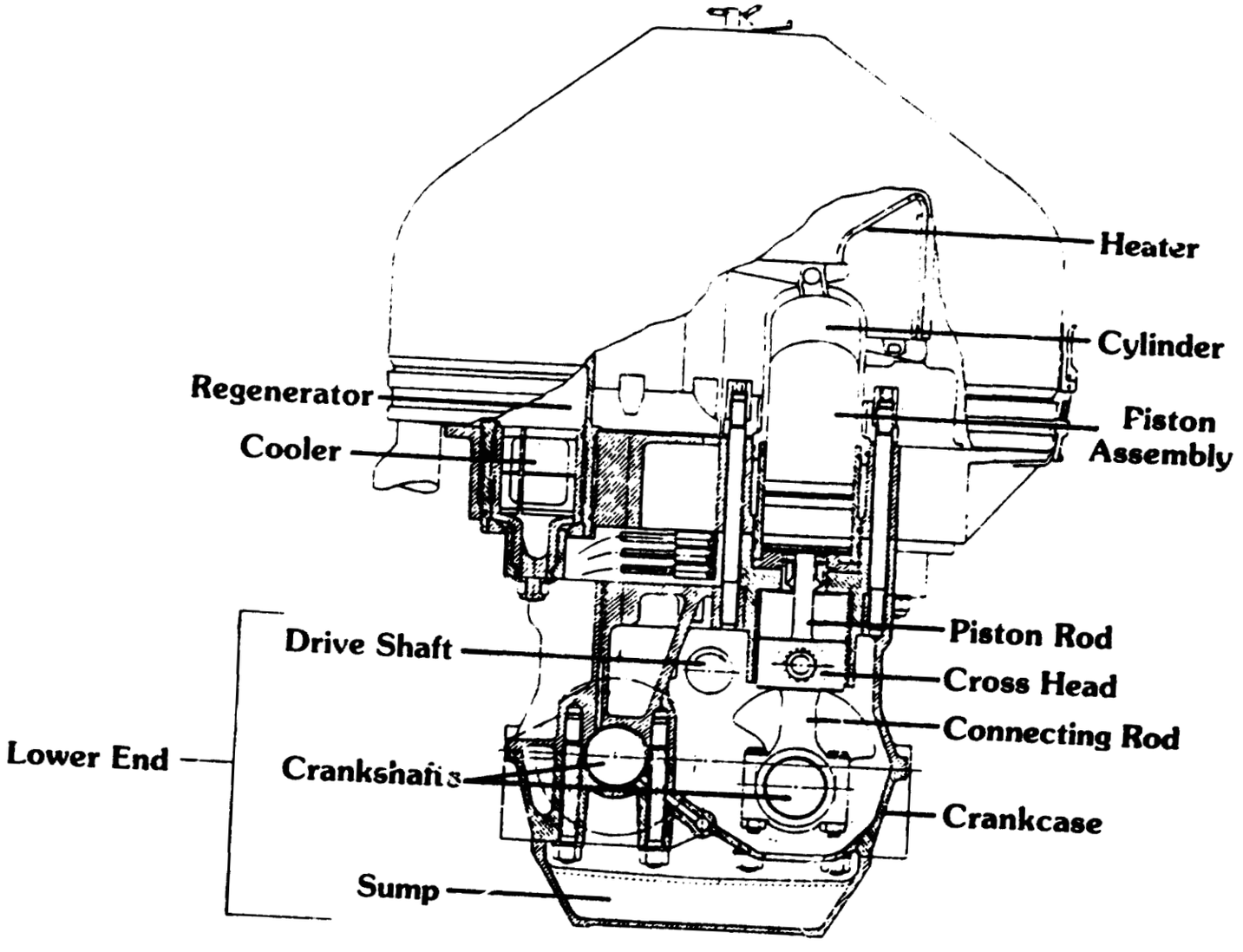

Fig. 2.2-1 Automotive Reference Engine System Design

can be contained more readily. Its thermal conductivity is almost as good as hydrogen, but its viscosity is twice as high, which results in higher flow losses and loss in efficiency. It follows, therefore, that an engine designed to run with hydrogen as a working gas runs poorly with helium as a direct-substitute working gas. But, to minimize these influences, each design was optimized exclusively with the selected working gas.

2.2.2 Cylinder and Heater Tube Life

The primary life-limited components on the Automotive Reference Engine shown in Figure 2.2-1 are the piston cylinder housing and the heater tube network. Using the existing materials and design of this engine, the required limiting operating parameters were determined to extend the 3500-hour automotive life to 50,000 hours. With strength properties of the cylinder material of XF818 at the 1 percent creep strength for selected metal temperatures, the limiting charge pressures were calculated and presented in Table 2.2-1.

The strength and stress of the Multimet N-155 (or 12RN72) heater tubes were checked at the given derated pressure, temperature, and rotational speed conditions using the Larson-Miller parameter for this material at 50,000 hours life. Material properties were taken in part from Reference 2. The criteria of acceptance was the safety factor, which must equal or exceed the existing Automotive Reference Engine value of 1.65 at its average operating point.

2.2.3 Seal Life/Engine Speed

Engine operating speed and operating environment have a direct influence on seal life in the Automotive Reference System Design (RESD) and applying the durability relationship of piston speed to stroke imposed in Reference 3 to meet 50,000 hours of life, the maximum RESD rotational speed of 4000 rpm should be reduced to 2200 rpm for the automotive-derived stationary engine. The variation of power and efficiency with rpm at the comparable pressure and cylinder temperature for the life criteria is shown in Figure 2.2-2. Essentially any rpm below 2200 rpm can be selected, but constant speed operation below 2200 rpm on a fixed size engine results in excessive power derating, causing unattractive power to weight and volume ratios. To provide direct drive capability with three-phase electric generators, the selected operating speed for this study was set at 1800 rpm, setting the power class at an indicated level of 37.5 kilowatts.

2.2.4 Selection of Design Point and Operating Conditions

At the selected rpm and life criteria, the variations of power and efficiency with cylinder head temperature and pressure are plotted in Figure 2.2-3. As illustrated, the near-maximum brake efficiency for the least cylinder temperature (~649°C) occurs at the indicated power around 40 kW, where the limiting cylinder pressure reads 123 bar. This condition was selected as the design point for comparisons with other configurations and is summarized as follows:

- 1800 rpm
- 669°C heater tube temperature
- 37.5 kW indicated power
- 649°C cylinder temperature
- 123 bar charge pressure
- hydrogen as the working fluid

TABLE 2.2-1

LIMITING TEMPERATURE/PRESSURE COMBINATIONS PROVIDING 50,000-HOUR LIFE FOR XF818 CYLINDER MATERIAL

Temperature ^{o}C (^{o}F)	593 (1,100)	649 (1,200)	677 (1,250)	704 (1,300)	760 (1,400)
1% Creep Strength MPa (psi)	310 (45,000)	203 (29,500)	148 (21,500)	110 (16,000)	63 (9,200)
Working Stress MPa (psi)	207 (30,000)	136 (19,667)	99 (14,333)	74 (10,667)	42 (6,133)
Peak Pressure MPa (psi)	25 (3,687)	17 (2,417)	12 (1,762)	9 (1,311)	5.2 (753)
Charge Pressure MPa (psi)	18.8 (2,738)	12.4 (1,795)	9 (1,308)	6.7 (973)	5.9 (559)

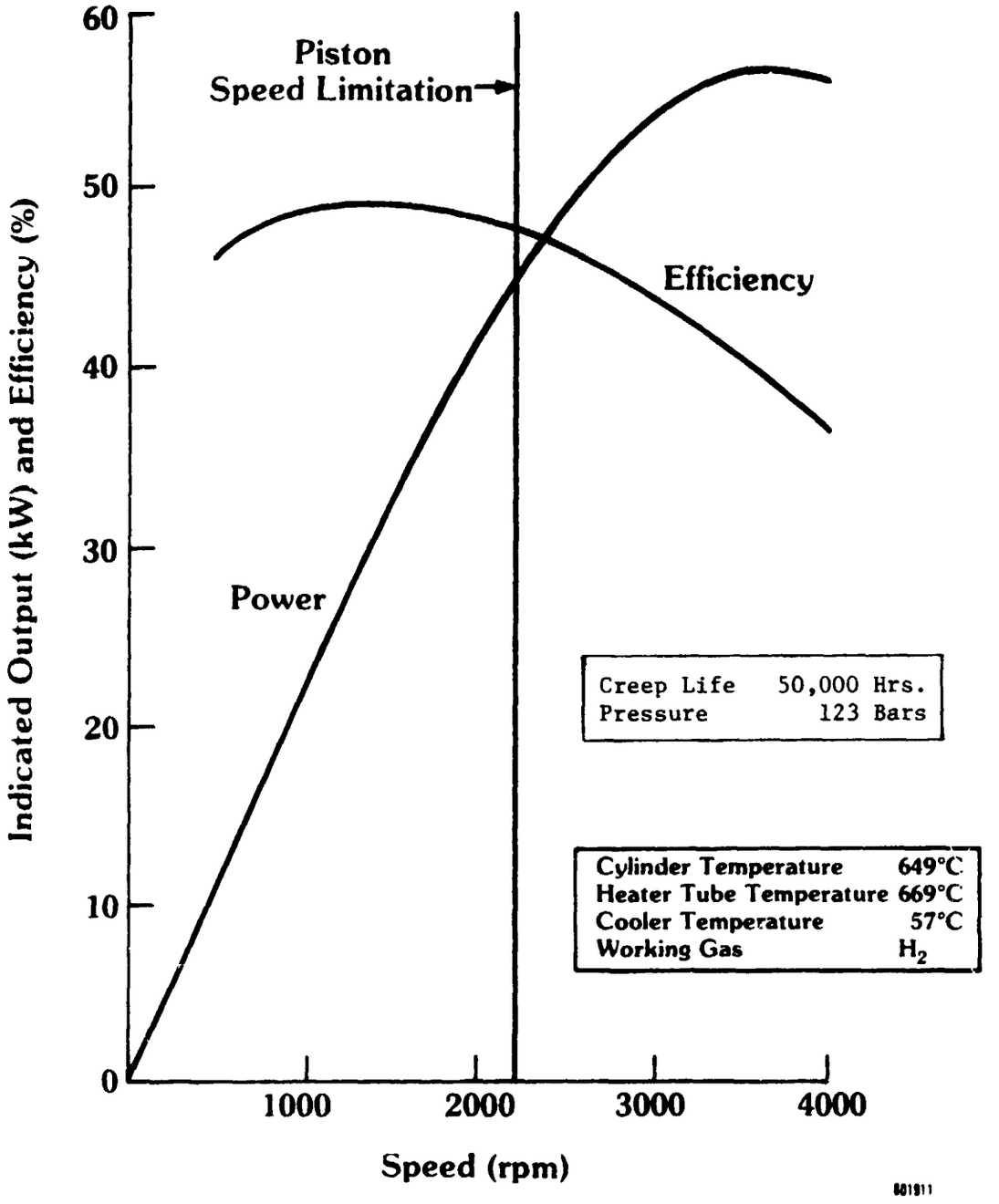

Fig. 2.2-2 Performance of Automotive Reference Engine - Variable RPM, Fixed Temperature

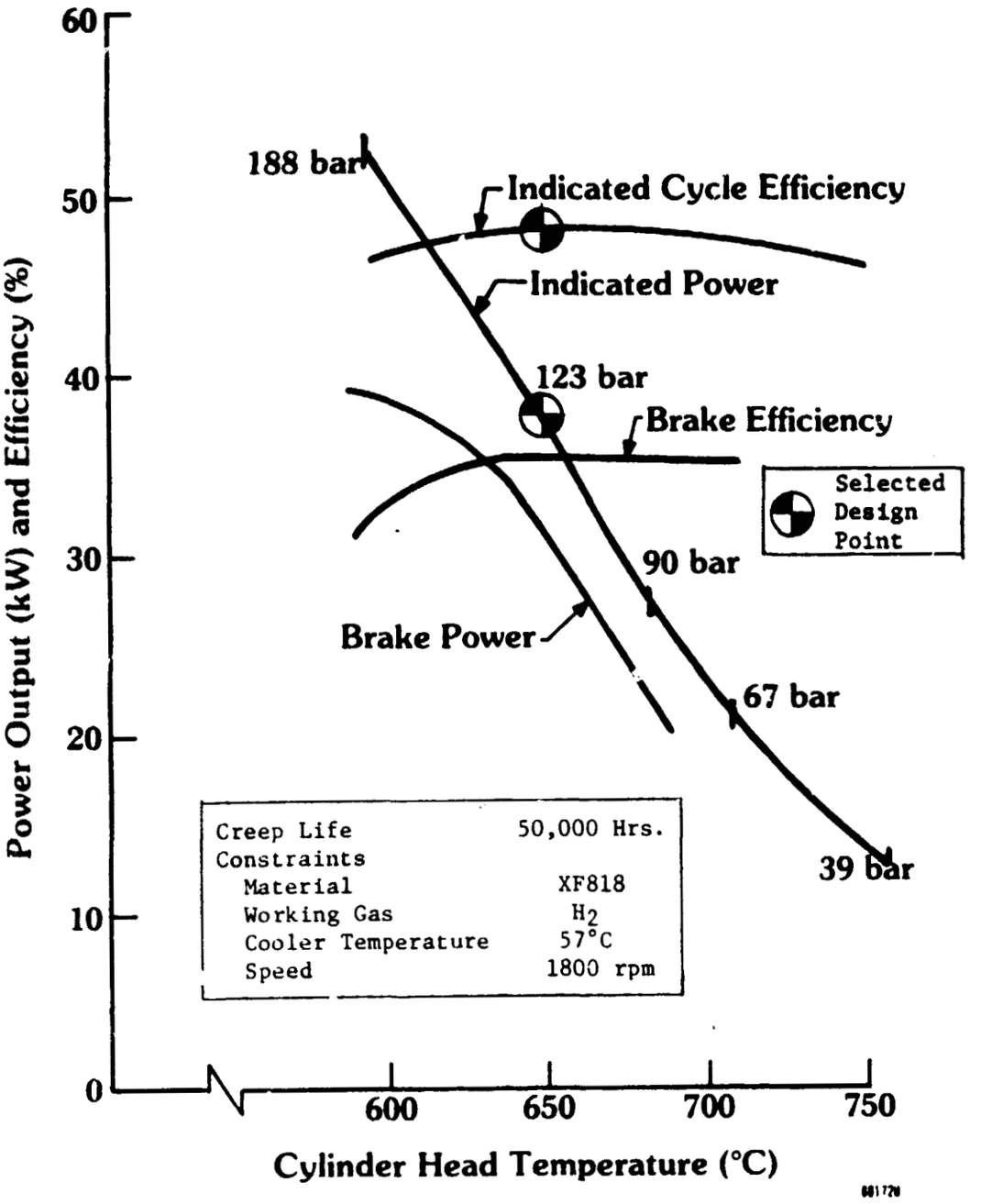

Fig. 2.2-3 Performance of Automotive Reference Engine - Fixed RPM, Variable Temperature

Performance for H_2 and He working fluids are compared in Table 2.2-2. At constant tube temperature and fixed geometry, the introduction of helium as a working gas results in about a 5 percent loss in brake power and a drop of about 1.6 to 2.0 percentage points in brake efficiency.

2.2.5 Auxiliary Loads

Auxiliary components are supportive systems necessary for the complete operation of the Stirling engine. Although the integrated system design of the auxiliaries and controls for stationary applications are outside the scope of this report, their actual load requirements are included in the performance quotations. Certain vehicle auxiliaries are not applicable to the stationary installations, thus providing small gains in engine output power and efficiency. Table 2.2-3 summarizes the auxiliary requirements of the Automotive Reference Engine and those required for the stationary engine system. Car accessories such as the steering and brake pumps are eliminated, and also the variator drive system for the combustor air blower can be removed for this application. The derated engine allows resizing of the working gas compressor, air blower, and alternator. Cooling and lubricating systems would be unchanged. Figure 2.2-4 illustrates the modified auxiliary installation for the stationary engine when viewed from the front.

2.2.6 Preheater and Combustor Evaluation and Optimization

The original automotive engine external heating system design was reviewed to determine if improvements can be made exclusively for the stationary power system. This system includes the preheater, ducting, exhaust, combustor, and heater tube components and the results are discussed in the following sections.

2.2.6.1 Preheater

Without a preheater, all the heat energy in the exhaust is lost to the atmosphere. A preheater allows recovery of part of this rejected heat by providing a heat exchanger between the exhaust gas and the incoming ambient air. By raising the temperature of the ambient air prior to the combustion process less fuel is required to raise the temperature up to the design operating temperature.

Evaluation of the preheater disclosed that two areas could be improved for a stationary application where volume, diameter, and height restrictions do not exist as they do in an automobile. The two areas are:

1. Reduced pressure drop - achieved by increasing preheater volume.

2. Reduced conduction loss - achieved through increased insulation.

Doubling the inner and outer diameters of the preheater was found to improve heat transfer efficiency by almost six points from 84 to 89.8 percent, while the area exposed to outside heat loss increased only 30 percent. Therefore, a large preheater is recommended for the stationary engine application.

2.2.6.2 External Heating System

Three areas were reviewed for possible improvement for the Automotive Reference Engine in the stationary application. Consideration for compatibility with existing production parts was included in conjunction with the desire for low cost impact changes.

TABLE 2.2-2

REFERENCE ENGINE MODIFIED AND DOWNRATED FOR 50,000-HOUR LIFE

Section		2.2	2.2
Engine Type		Kinematic	Kinematic
Working Fluid		H_2	He
Temperature Heater Tube	^oC	669	669
Temperature Cylinder	^oC	649	649
Temperature Cooler	^oC	57	57
Pressure	Bar	123	123
Speed	rpm	1800	1800
Displacement Engine	cm^3	453	453
No. of Cylinders		4	4
Indicated Power	kW	37.5	35.71
Auxiliary Power	kW	2.25	2.25
Drive Power	kW	4.64	4.64
Brake Power	kW	30.61	28.82
Indicated Efficiency	%	48.34	46.61
Combustion Efficiency	%	90.0	90.0
Brake Efficiency	%	35.51	33.87
Heater Tube Material		12RN72	12RN72
Cylinder Material		XF818	XF818
Heat Input	kW	86.2	85.09
sfc	kg/kW	0.24	0.25
Torque	Nm	162.2	152.7

TABLE 2.2-3

AUXILIARY COMPONENTS AND POWER REQUIREMENTS AT BASELINE ENGINE OPERATING POINT

- Eliminated
  - Variator Drive System for Combustion Air Blower
- Optimized
  - Working Gas Compressor (Electrically Activated) 0.343 kW
  - Combustion Air Blower (Fixed Ratio Drive) 0.524 kW
  - Alternator 0.242 kW
- Unchanged
  - Cooling System:
    - Water Pump 0.181 kW
    - Radiator Fan 0.980 kW
  - Lubrication Pump 0.220 kW
- Operating Point
  - 123 Bar
  - 1800 rpm Speed

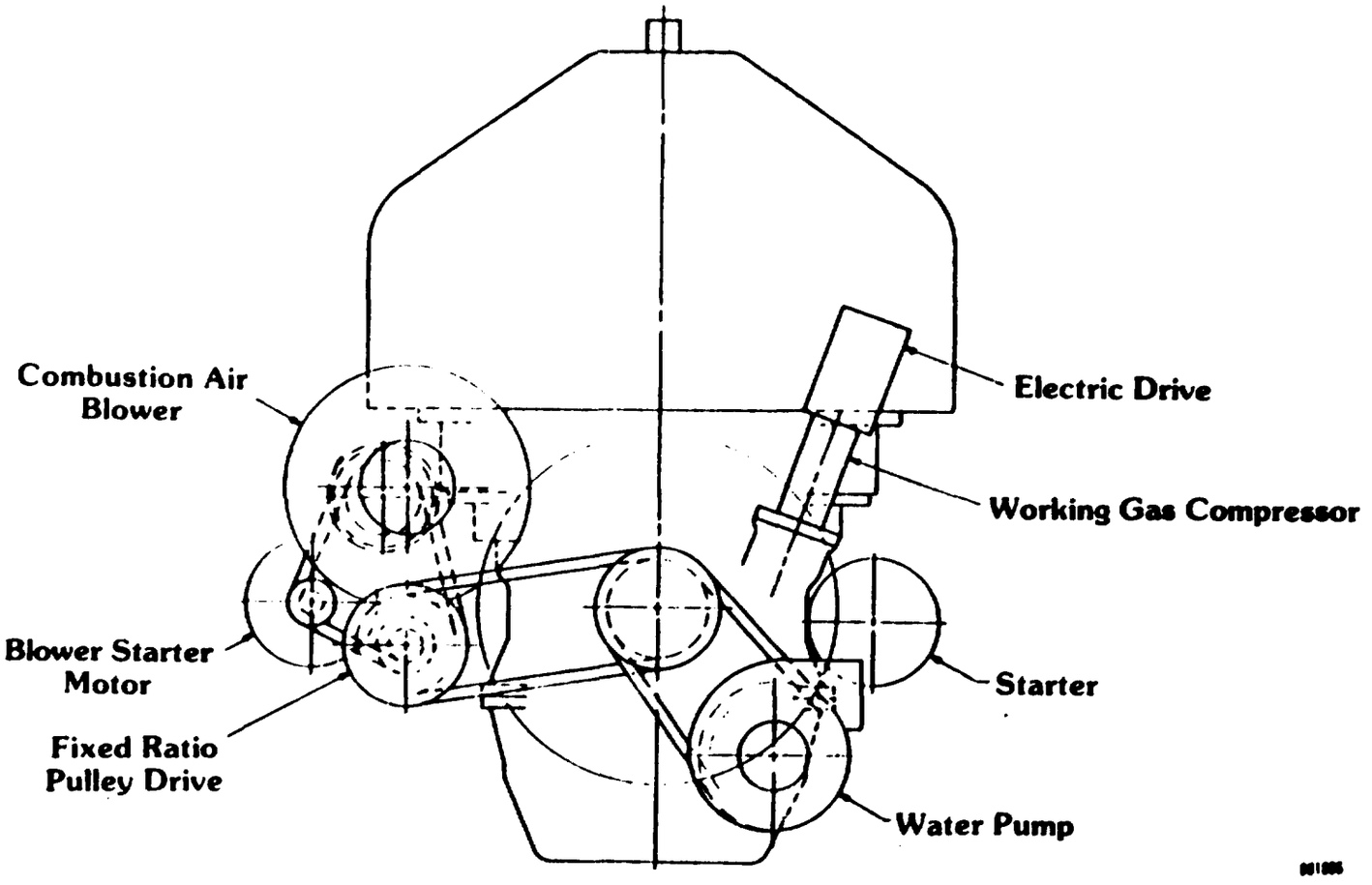

Fig. 2.2-4 Modified Auxiliary Configuration

The effort explored:

- Combustor loading
- Combustor dynamics
- Heater tubes heat transfer

Combustor volume loading for the existing automotive RESD engine is already relatively low when compared to recuperative small gas turbine engine combustors, therefore, no change is proposed for the stationary engine application.

In the evaluation of the gas dynamics through the combustor to the heat tubes in the existing RESD engine, a recontoured combustor using a ceramic material to control diffusion ratio would be recommended.

Heat transfer was calculated for a typical automotive RESD combustor to determine the effect of a skewed inlet velocity profile. A flat profile entering the heater tubes was compared to one in which various flow rates were concentrated across 50 percent of the tube area. The net effect, shown in Table 2.2-4 for the first row of tubes only, was a reduction in heat transfer of 21.4 percent at low power and 26 percent at high power. It can be assumed that some of this heat would be recovered by the second heater tube row and also by the preheater. With the volume restrictions of the automotive Stirling combustor, it is assumed the stationary application will allow a design giving uniform velocity resulting in performance gains by improved aerodynamic matching. Furthermore, if these improved designs result in shorter heater tubes there is an added efficiency advantage by reducing dead volume and friction loss.

The results of the estimated heat system analysis for the stationary engine combustor is illustrated in Figure 2.2-5 and shows two major design changes:

- An enlarged preheater with extra insulation to recover more heat from the combustor exhaust.
- A recontoured combustor using a ceramic material to control diffusion ratio and unify the velocity distribution around the heater tubes.

2.2.7 Performance Map Generation

By use of an MTI performance prediction code, described in Appendix A, a family of indicated power, cycle efficiency, and cylinder life trends as a function of charge pressure (Figures 2.2-6 to 2.2-11) were developed at the following operating conditions:

Cylinder Heat Temperature:	538°C	649°C	760°C
Heater Tube Temperature:	558°C	669°C	780°C
Cooler Temperature:	27°C	57°C	87°C

TABLE 2.2-4

EFFECT OF FLOW DISTRIBUTION ON HEATER SYSTEM PERFORMANCE

	Mass Flow Rate (g/s)	Skewed Flow Condition 2/3 Flow for L/2 1/3 Flow for L/2 Percent Heat Transfer Loss Due to Flow Skew	Concentrated Flow Condition All Flow for L/2 No Flow for L/2 Percent Heat Transfer Loss Due to Flow Skew
Low Power	10	Negligible	21.4%
Intermediate	40	1.5%	25.4%
High Power	80	2.0%	26.0%

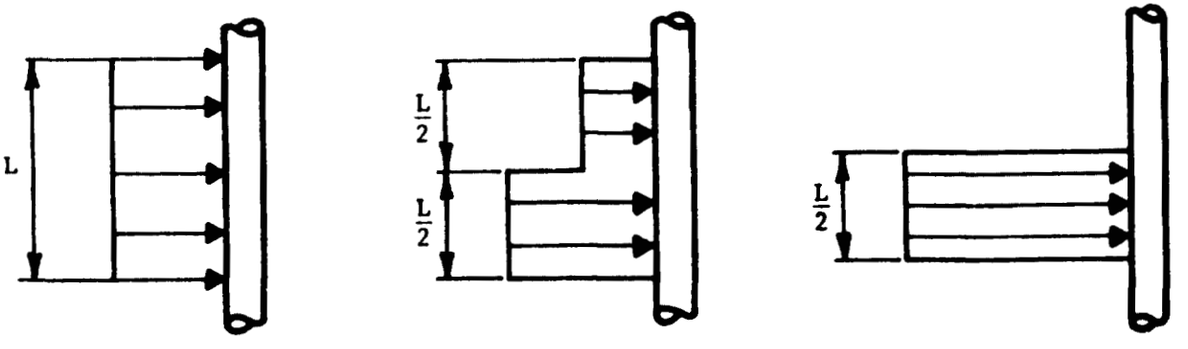

811723

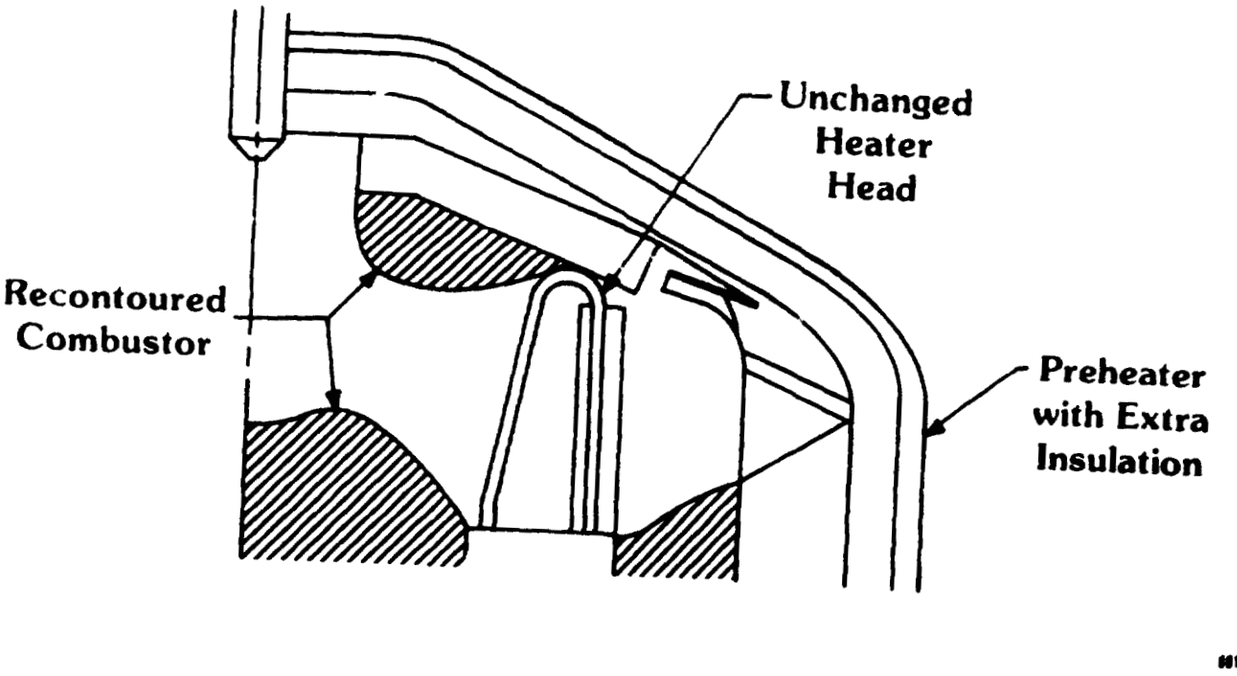

Fig. 2.2-5 Modified Reference Engine Combustor for Stationary Engine

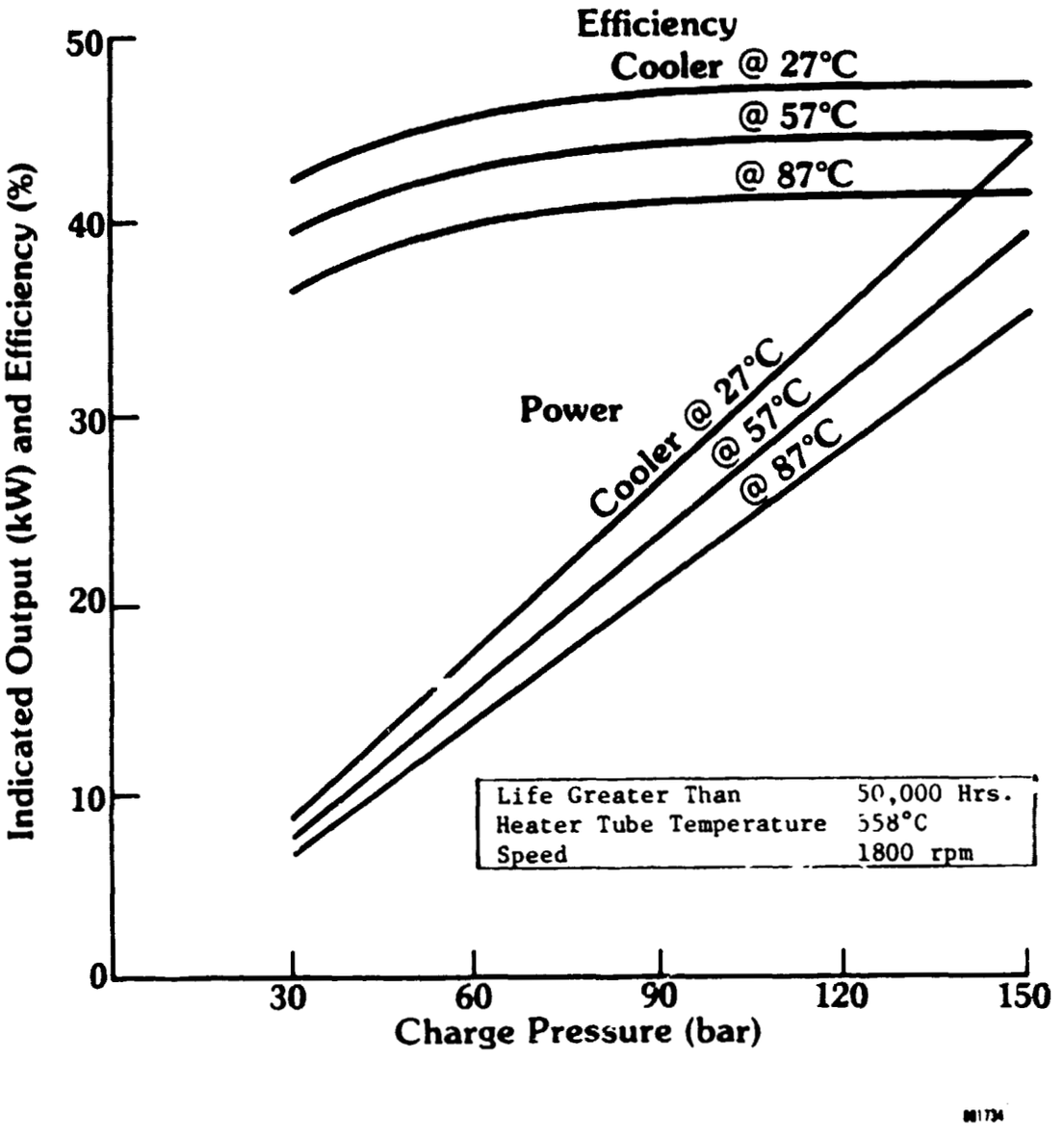

Fig. 2.2-6 H_2 Reference Engine, Indicated Power and Cycle Efficiency vs Charge Pressure, Cylinder Temperature = 538°C

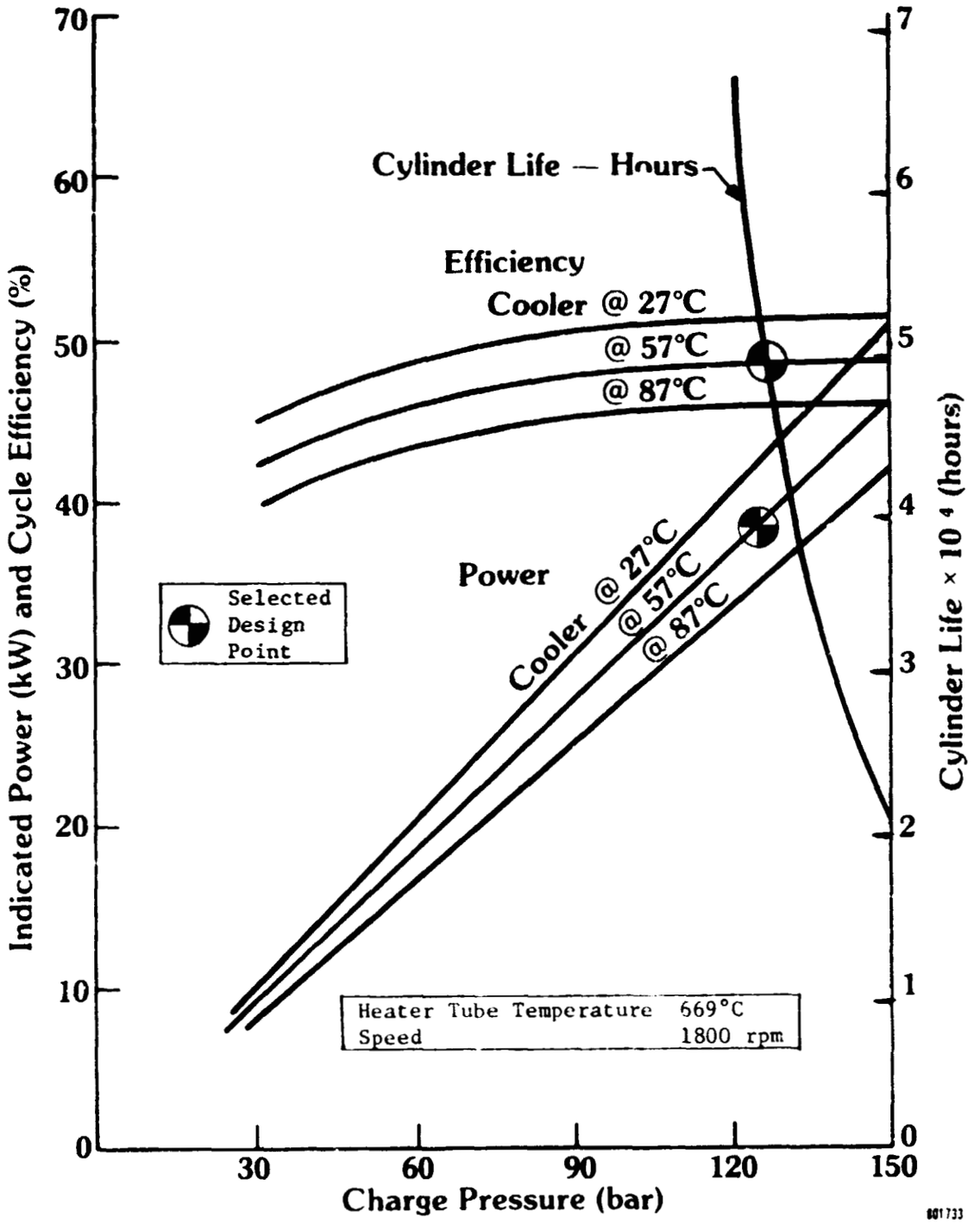

Fig. 2.2-7 H_2 Reference Engine, Indicated Power and Cycle Efficiency vs Charge Pressure, Cylinder Temperature = 649°C

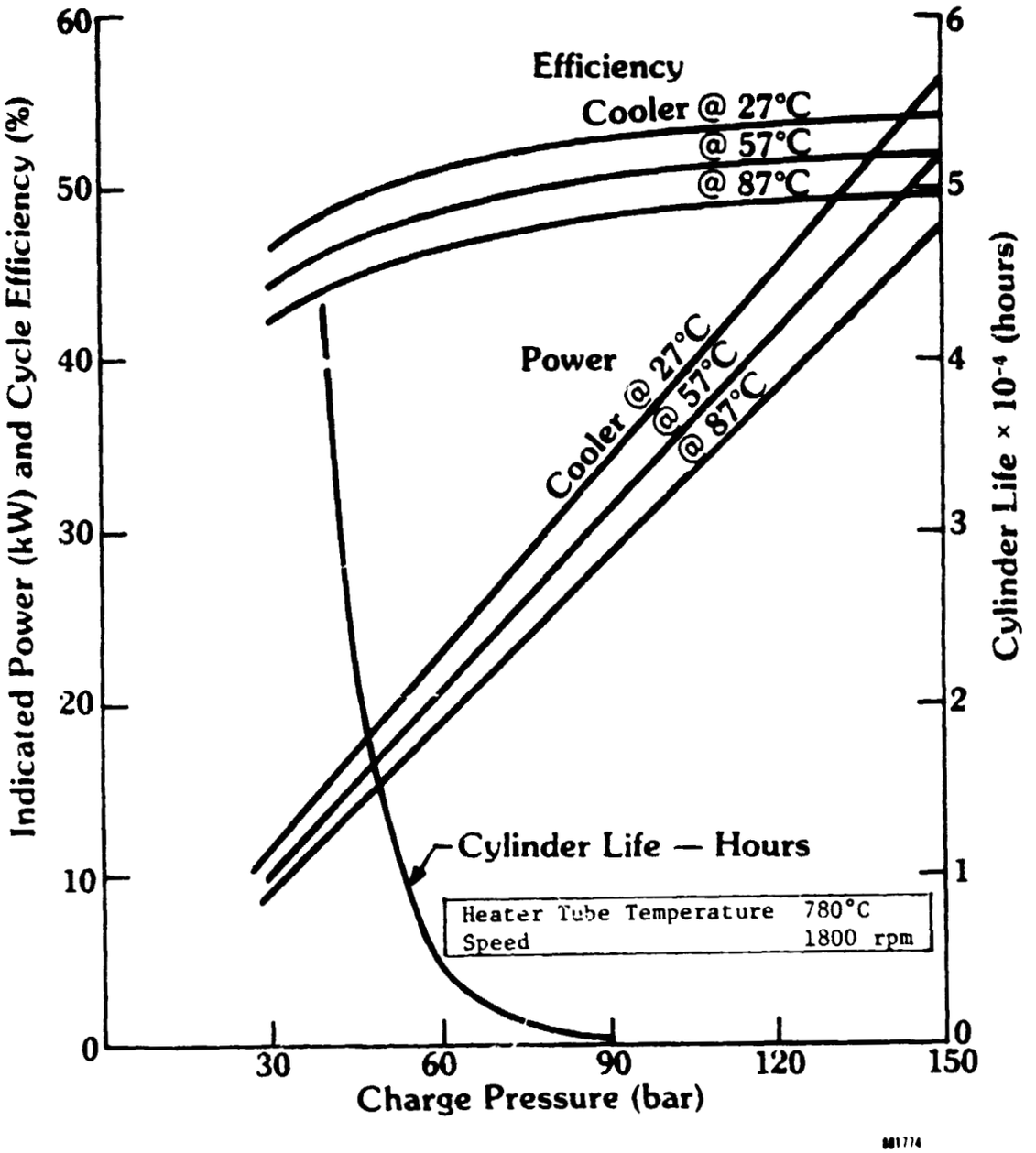

Fig. 2.2-8 H_2 Reference Engine, Indicated Power and Cycle Efficiency vs Charge Pressure, Cylinder Temperature = 760°C

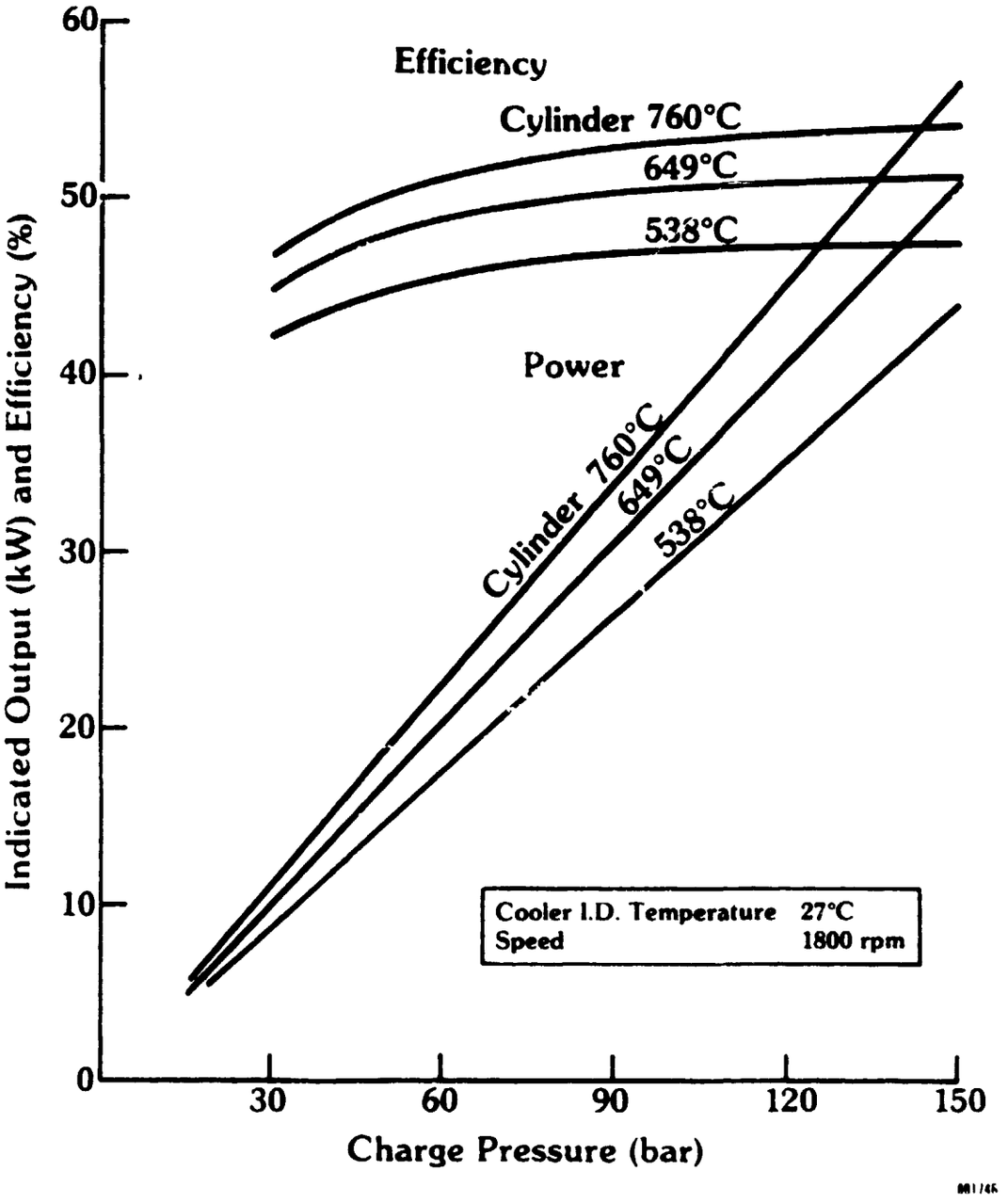

Fig. 2.2-9 H_2 Reference Engine, Indicated Power and Cycle Efficiency vs Charge Pressure, Cooler Temperature = 27°C

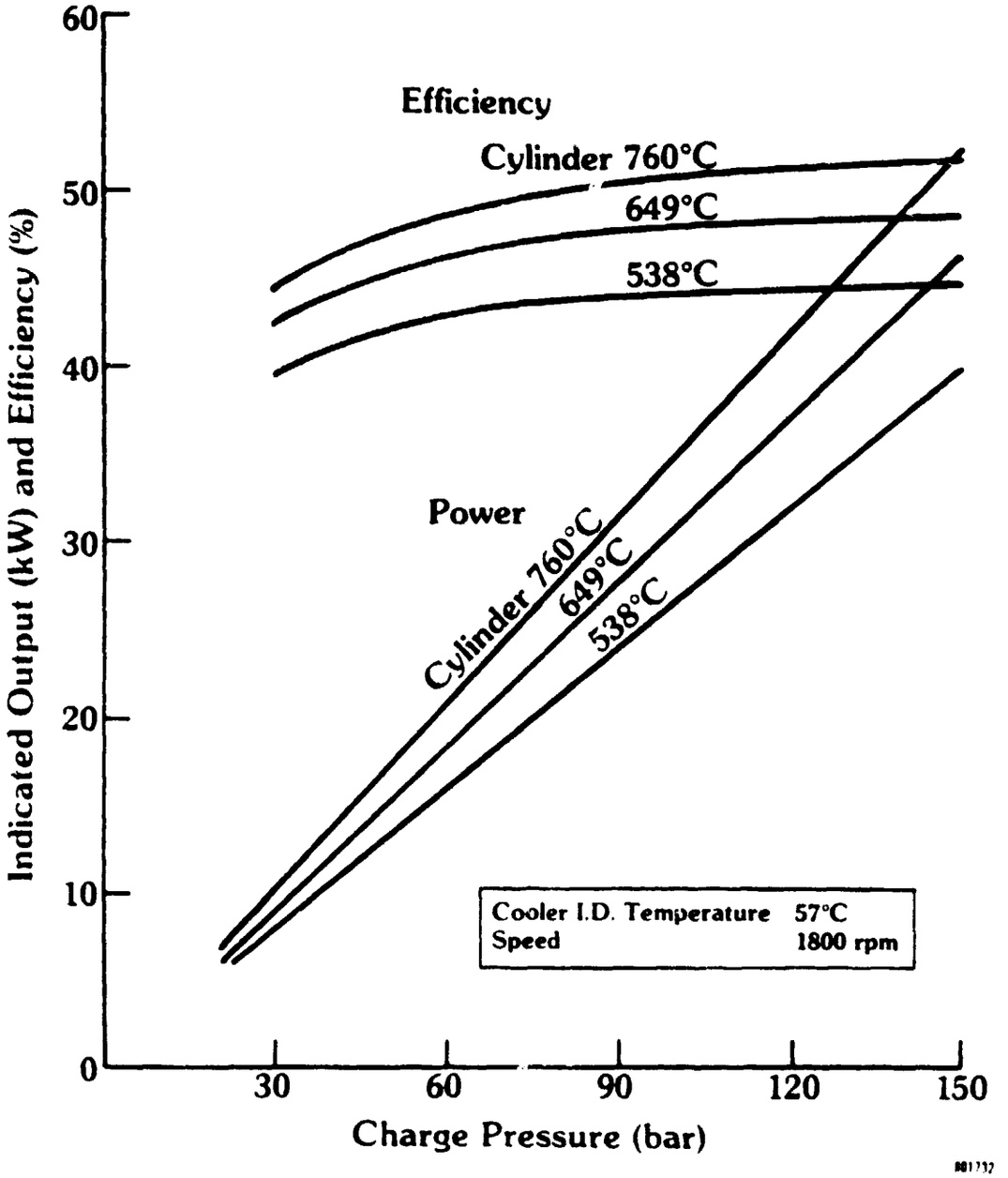

Fig. 2.2-10 H_2 Reference Engine, Indicated Power and Cycle Efficiency vs Charge Pressure, Cooler Temperature = 57°C

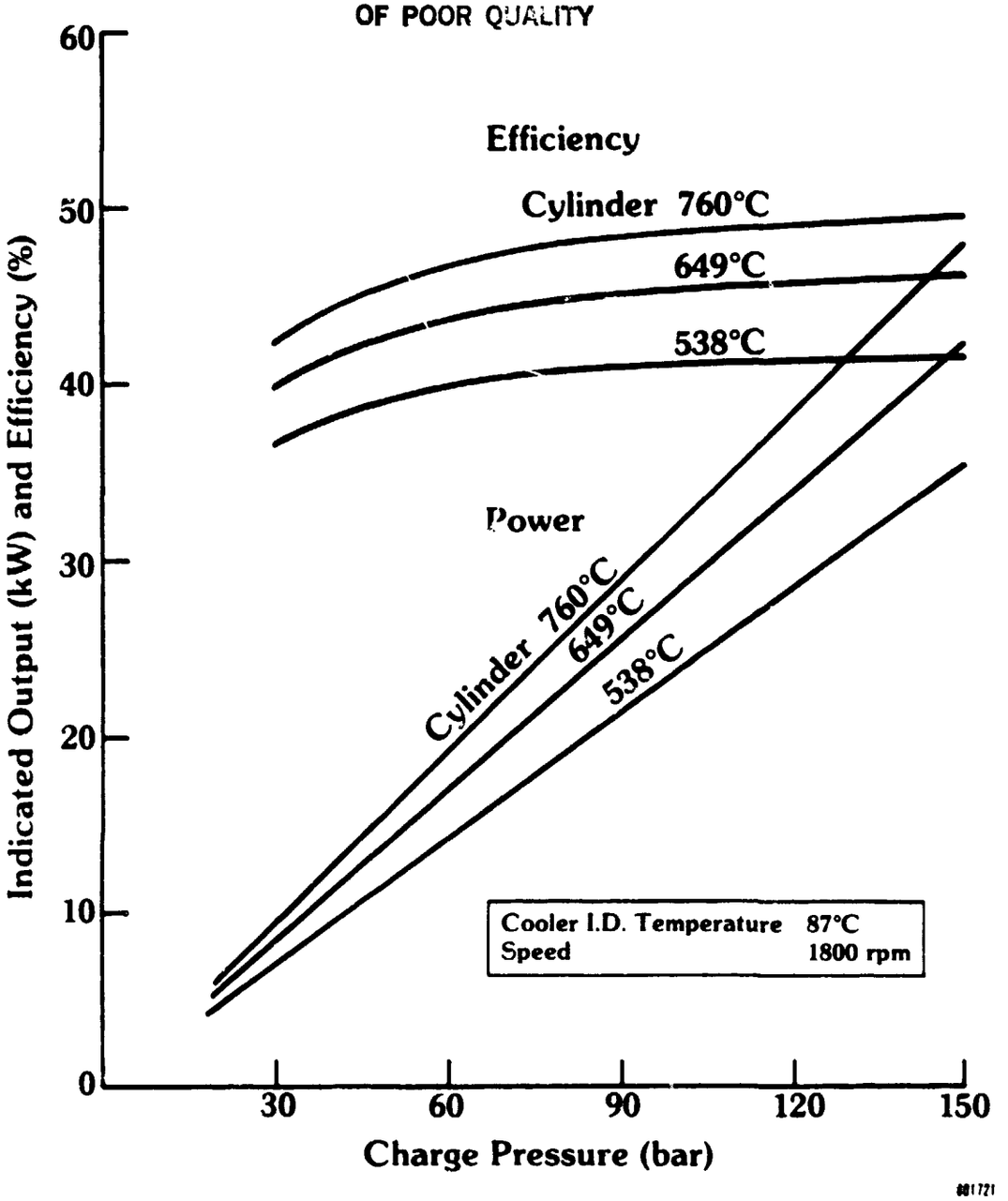

Fig. 2.2-11 H_2 Reference Engine, Indicated Power and Cycle Efficiency vs Charge Pressure, Cooler Temperature = 87°C

These maps (Figures 2.2-6 to 2.2-11) show the sensitivity of power and efficiency to heater and cooler temperature variations and permit system studies to assess the performance of the Automotive Reference Engine at various operating conditions. These curves were generated using hydrogen as the working gas only. In Figure 2.2-6 the 50,000-hour creep life criteria is exceeded whereas the cylinder life is displayed in Figures 2.2-7 and 2.2-8 at higher set temperatures as a function of charge pressure. Figure 2.2-7 highlights the base design point at 123 bar, 649°C cylinder temperature. By comparison, Figure 2.2-8 illustrates gains in efficiency at the higher cylinder temperature, but with considerable loss in life.

2.2.8 Summary

The ASE Reference Engine was downrated to meet the 50,000-hour creep life criteria.

Improvements in the external system are possible due to the lesser volume constraints in the stationary application.

The engine produced 30.6 kW brake output power at a brake efficiency of 35.5 percent using hydrogen as a working gas. If helium is selected as a working gas, brake power is 28.8 kW at a brake efficiency of 33.9 percent.

2.3 Optimized Reference Engine

2.3.1 Introduction

In the previous section, the direct use of the ASE Reference Engine for stationary engine application was explored. It determined the use of the Reference Engine at a derated operating point was feasible.

In this section, the requirement for "direct substitution" is relaxed to allow changes in materials and engine dimensions. The engine, in effect, becomes a tailored "Reference Engine" for the stationary application. The optimization procedure is limited to the upper end of the engine and considers only the particular component dimensions rather than basic structure. The lower drive end (crankcase, crankshaft, etc.) is not changed. The engine speed (1800 rpm) and design life (50,000 hours) are held fixed.

The philosophy to retain maximum commonality with the automobile production hardware is still maintained.

2.3.2 Conceptual Design

Because of the need to operate with the same engine drive, major modifications of the engine dimensions was not practical. The piston diameter was allowed to vary only by a limited extent due to drive geometric and constructural constraints. This provides also common block castings with the Automotive Reference Engine. The layout, which resembles closely the baseline engine, is shown in Figure 2.3-1.

The present ASE Reference Engine selects Climax Molybdenum XF818 for the cylinder and regenerator housings. The seamless heater head tubes are drawn from Sandvik 12RN72 (an iron-based alloy). For the optimum Reference Engine these materials were replaced with Inconel-625, which is a nickel-based alloy with better creep rupture properties than the Sandvik 12RN72. Inconel-713LC replaced the original

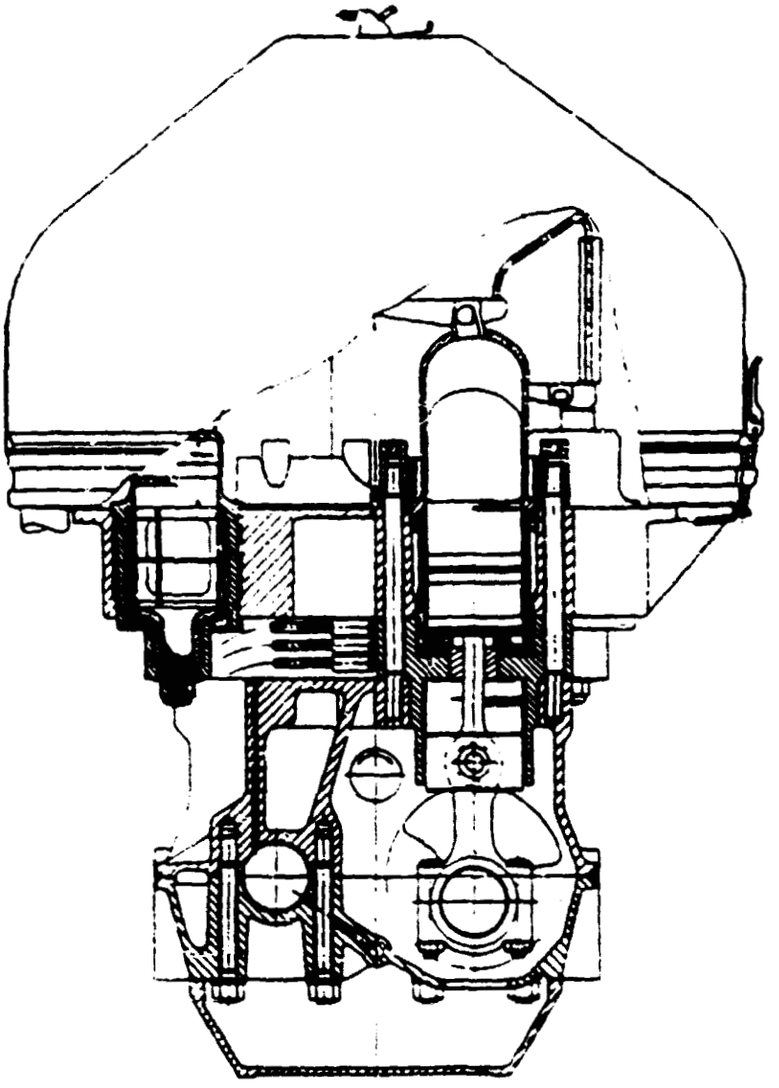

Fig. 2.3-1 Optimum Engine - Cross Section

XF818 used in the regenerator and cylinder castings. These material changes allowed operation at higher working gas temperatures giving better overall engine efficiency.

2.3.3 Cycle Analysis and Optimization

With the life, power, speed, and lower end selected in Section 2.2 on the derated Reference Engine, the cycle optimization effort concentrated on optimizing component sizes and materials.

A comparison of reference and optimized engine hot side materials is given in Table 2.3-1, where again the Larson-Miller parameter was utilized as a qualitative tool for each material.

With the materials chosen, an iterative study was conducted to determine the highest efficiency for variations in charge pressure, cylinder temperature, and piston diameters. Figure 2.3-2 summarizes these results. The sensitivity of efficiency to temperature, pumping, and conduction losses at higher pressure result in a maximum efficiency around 700°C. The corresponding variation in piston diameter is also illustrated in Figure 2.3-2 and, with consideration of keeping the overall block dimensions the same, the overall optimization point was selected to be:

- 1800 rpm
- 100 bar charge pressure
- 724° heater head temperature
- 37.5 kW indicated power
- 704° cylinder temperature
- hydrogen as the working gas

Helium gas was substituted for hydrogen in this optimization effort and again certain dimensions were allowed to vary. The results of both hydrogen and helium optimizations on component dimensions are given in Table 2.3-2.

The overall performance of both hydrogen and helium engines at 100 bar operating pressure is shown in Figure 2.3-3. Table 2.3-3 summarizes the performance difference of a 1.7 point efficiency loss at constant power if the hydrogen working fluid is replaced by the helium and the engine reoptimized.

2.3.4 Engine Component Evaluation and Optimization

Structurally the heater head was satisfactory with its original dimensions and the main change in this area was the selection of the Inconel-625 tube material in place of the Sandvik 12RN72, resulting in a small reduction in tube outer diameter.

The combustor and preheater improvements incorporated in the Reference Engine (Section 2.2) were included in the optimum engine.

Regenerator dimensions were changed as indicated in Table 2.3-2 and cooler dimensions remained unchanged.

TABLE 2.3-1

MATERIAL CHANGES FOR OPTIMUM ENGINE

Component	Reference Engine	Optimum Engine
Heater Tubes	Sandvik 12RN72	Inconel-625
Cylinder Wall	XF818	713LC
Regenerator Housing	XF818	713LC

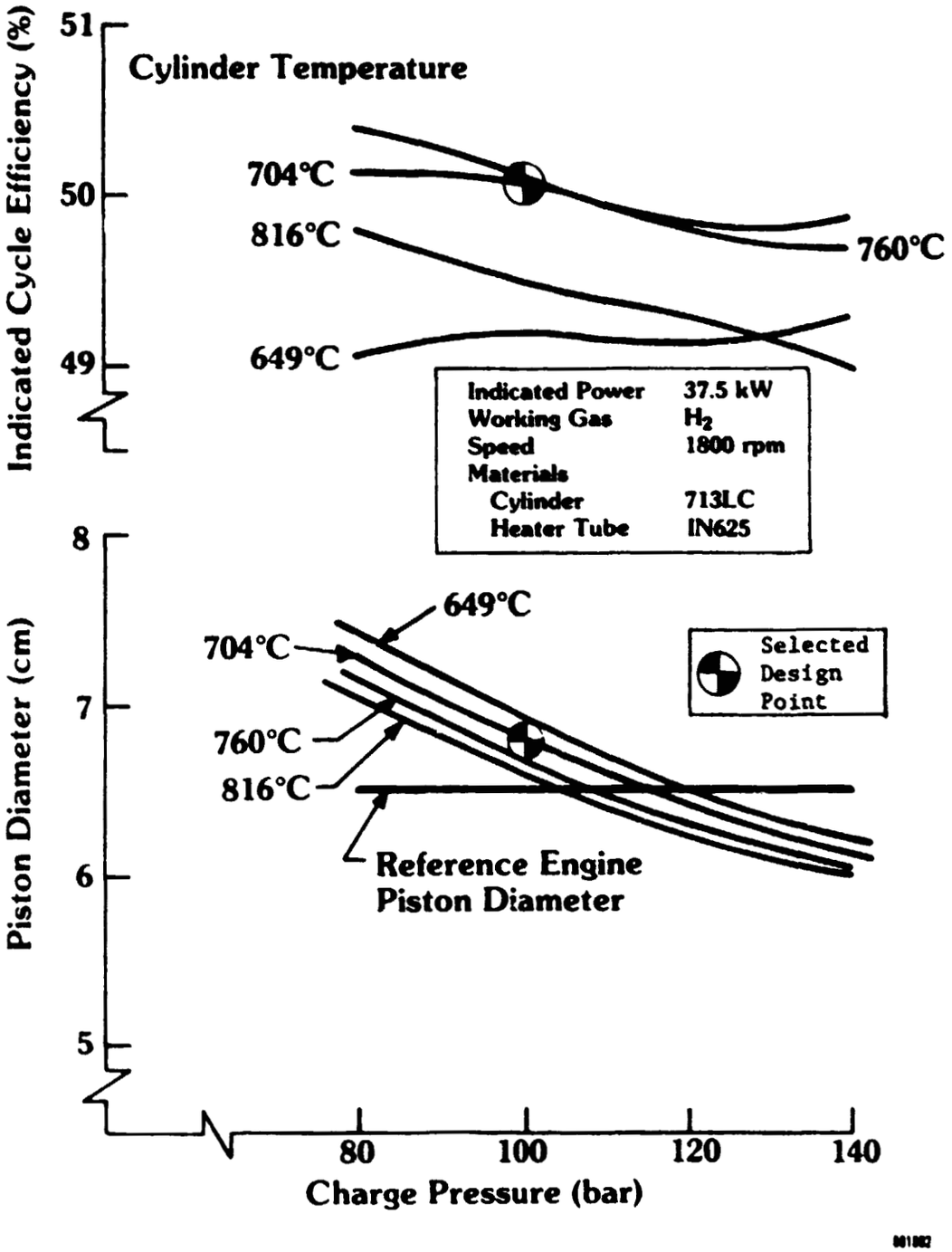

Fig. 2.5-2 Charge Pressure, Piston Diameter, Efficiency Combinations

TABLE 2.3-2

CYCLE ANALYSIS AND OPTIMIZATION

Summary of Optimum Engine Geometry

	Dimension	Reference (H_2)	Optimum (H_2)	Optimum (He)
Piston	Piston Diameter (mm)	65.1	67.5	67.82
	Rod Diameter (mm)	13.0	13.5	13.55
	Crank Radius (mm)	17.0	17.0	17.0
	Swept Volume (cm^3)	113.0	121.58	122.84
Regenerator	Diameter (mm)	67.0	57.7	59.2
	Top Area (cm^2)	35.25	26.18	27.57
	Length (mm)	48.0	55.33	45.6
	Wire Diameter (mm)	0.05	0.05	0.05
	Filling Factor (%)	32.9	32.9	25.57
Cooler	Number of Tubes	400.0	400.0	400.0
	Tube I.D. (mm)	1.0	1.0	1.0
	Tube Length (mm)	69.0	69.0	69.0
	Effective Length (mm)	57.0	57.0	57.0
Heater Tube	Tubes/Cylinder	22	22	22
	Tube I.D. (mm)	3.0	3.0	3.0
	Tube O.D. (mm)	4.5	4.2	4.2
	Tube Length (mm)	259.0	259.0	259.0
	Effective Length (mm)	224.0	225.0	224.0

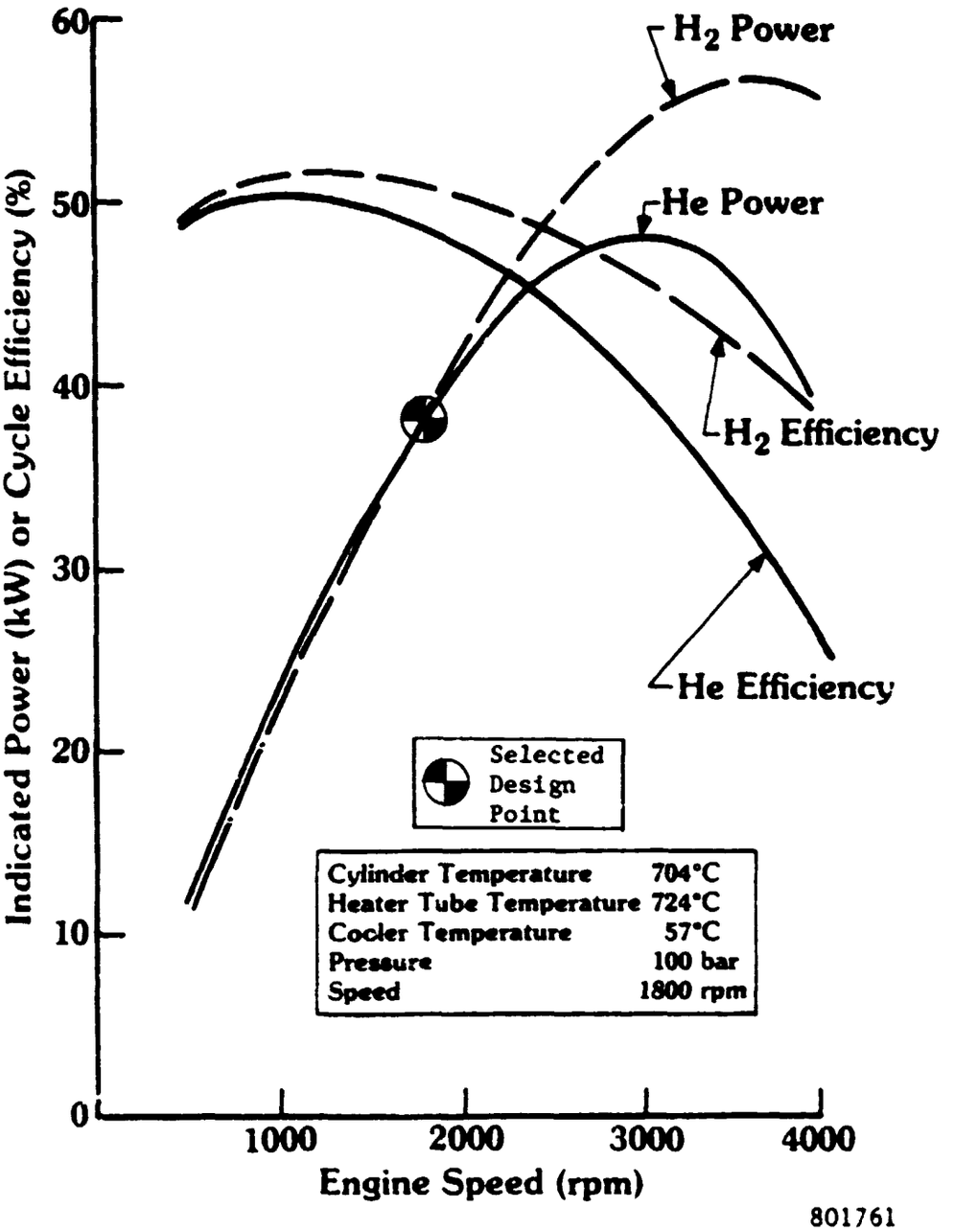

Fig. 2.3-3 The Influence of Working Gas on Optimum Engine Performance

TABLE 2.3-3

H_2/He OPTIMIZATION

- Engine Optimized for Both Gases
- Same Operating Point (704°C, 100 bar, 1800 rpm)
- Differences Found:

	H_2	He	Δ Change
Cycle Efficiency (%)	50.70	48.52	-2.2
Indicated Power (kW)	37.50	37.50	0
Brake Power (kW)	31.56	31.56	0
Brake Efficiency (%)	38.44	36.75	-1.7

The optimized engine required less power to overcome friction and auxiliary loads due to:

- lower operating pressure - reduced from 123 to 100 bar
- redesigned water pump

The impact is summarized in Table 2.3-4 where auxiliary and friction loads are reduced from 6.88 to 5.95 kW (a 13.5 percent reduction).

2.3.5 Performance Map Generation

Performance maps (Figures 2.3-4 to 2.3-9) were generated for the helium gas version of the engine. The selected range of heater and cooler temperatures is given in Table 2.3-5.

The indicated torque characteristics of the two optimized engines and the Reference Engine are given in Figure 2.3-10. The corresponding brake torques are shown at 1800 rpm.

2.3.6 Summary

The ASE Reference Engine has been downrated for utilization in a long-life (50,000 hours) stationary engine application and a second configuration was optimized using both hydrogen and helium working fluids. A summary of the operating and performance parameters of the four engines is given in Table 2.3-6, and shows the optimized engine is approximately three points higher in brake efficiency for both hydrogen and helium gases. The helium design imposes a two point efficiency penalty over hydrogen. A significant portion of the efficiency improvement in the optimized engine is due to reduced frictional drive losses. As a guideline on the impact of efficiency gains, a plot of fuel consumed as a function of efficiency has been prepared. Figure 2.3-11 illustrates a three point gain in optimizing the engine saves 30,000 Kg of fuel during the life cycle.

TABLE 2.3-4

ENGINE COMPONENTS - AUXILIARY POWER CONSUMPTION AT DESIGN POINT

System	Reference Engine	Optimum Engine	Explanation
Drive Friction	4.64	3.8	Lower Pressure
Cooling			
Water Pump	0.18	0.09	Optimized Geometry
Fan	0.98	0.98	Fixed Ratio Drive
Combustor			
Air Blower	0.52	0.52	
Atomizing	0.34	0.34	
Lube Oil Pump	0.22	0.22	
Total Power (kW)	6.88	5.95	

TABLE 2.3-5

PERFORMANCE MAP GENERATION - OPTIMUM ENGINE

- Optimized for He
- Matrix of Data for He N = 1800 rpm

Cylinder Head Temperature (°C)	Heater Tube Temperature (°C)	Cooler Temperature (°C)
593	613	27
704	724	57
816	836	87

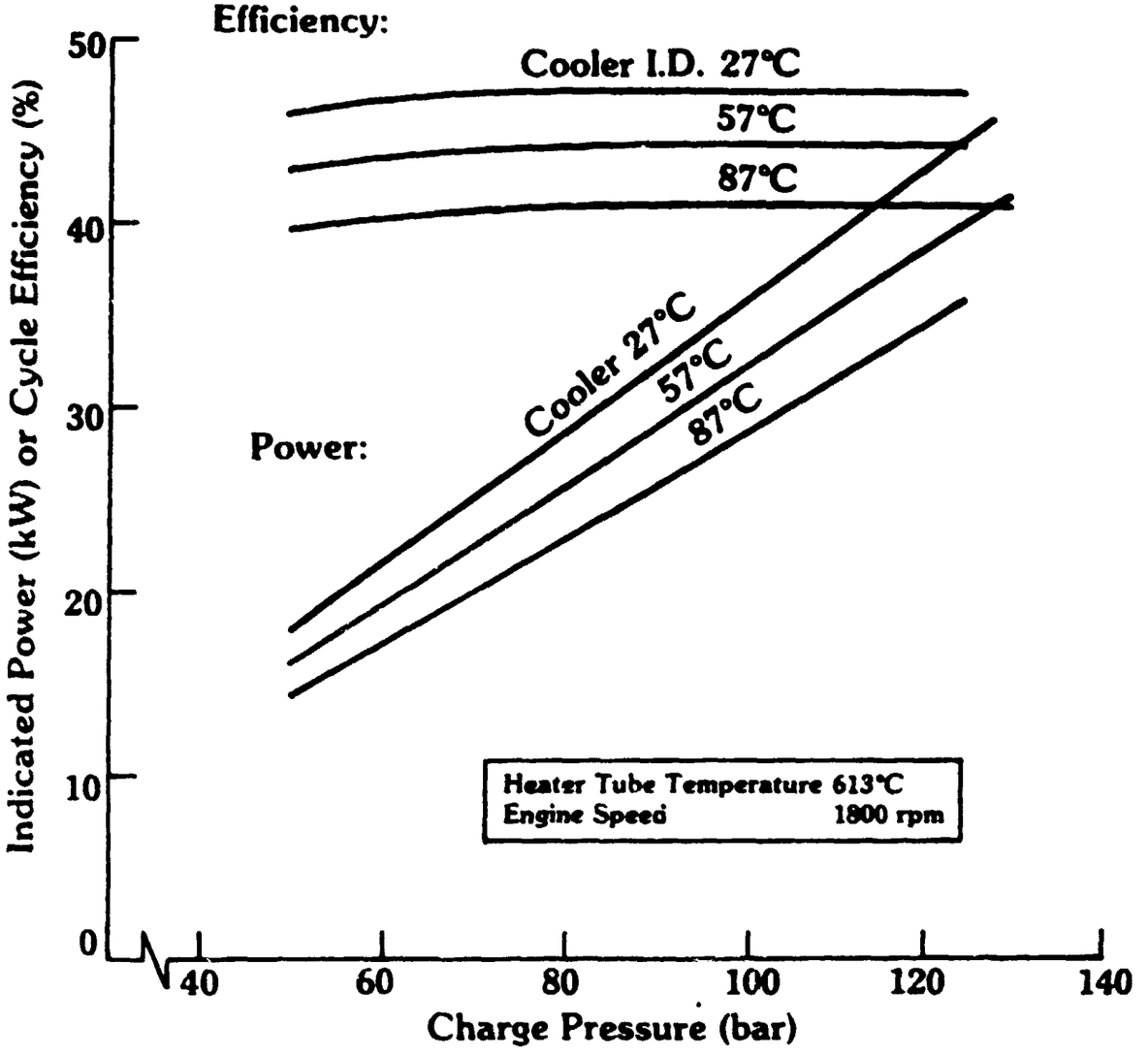

Fig. 2.3-4 Optimum He Engine Performance @ 593°C Cylinder Temperature

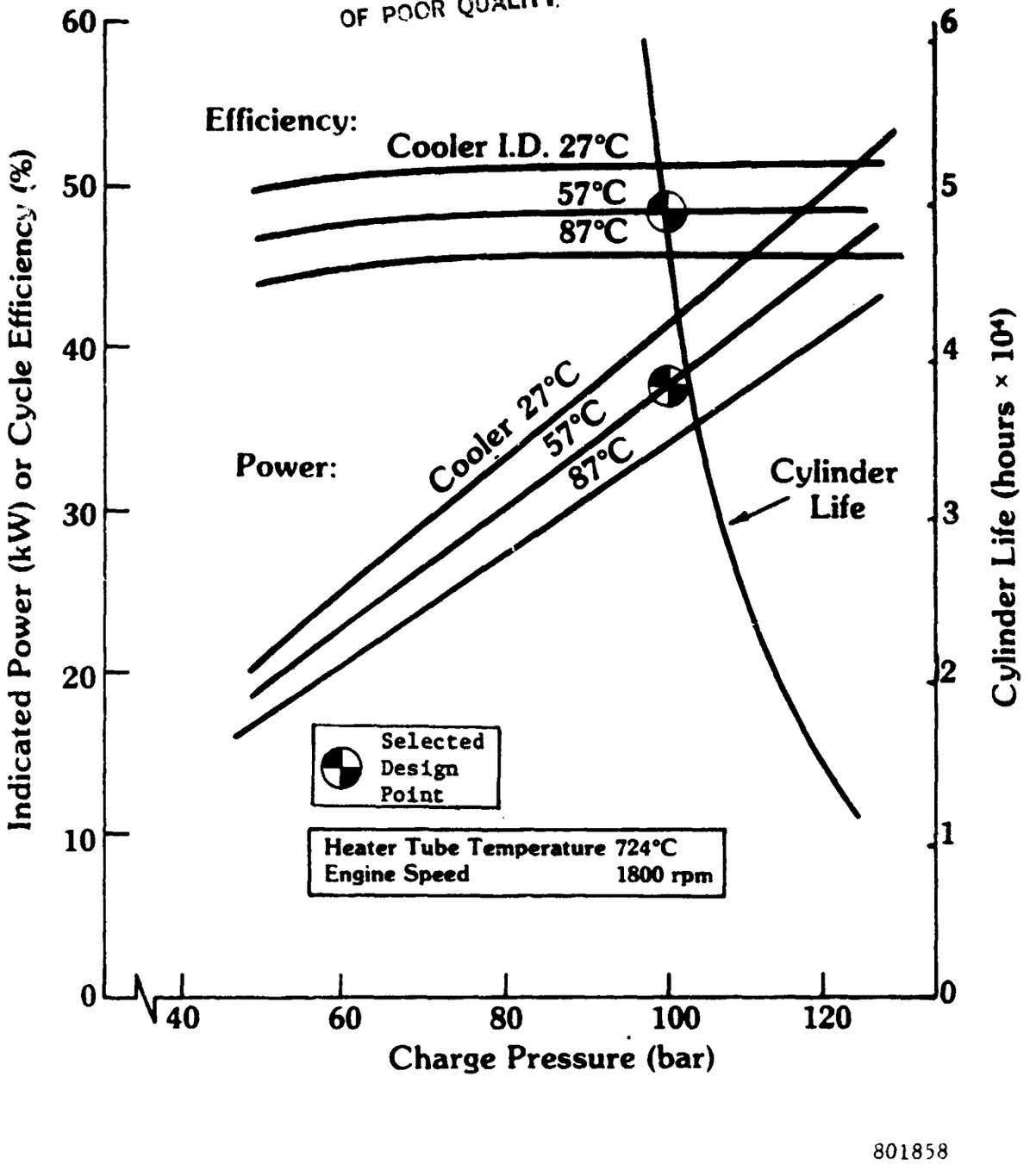

Fig. 2.3-5 Optimum He Engine Performance @ 704°C Cylinder Temperature

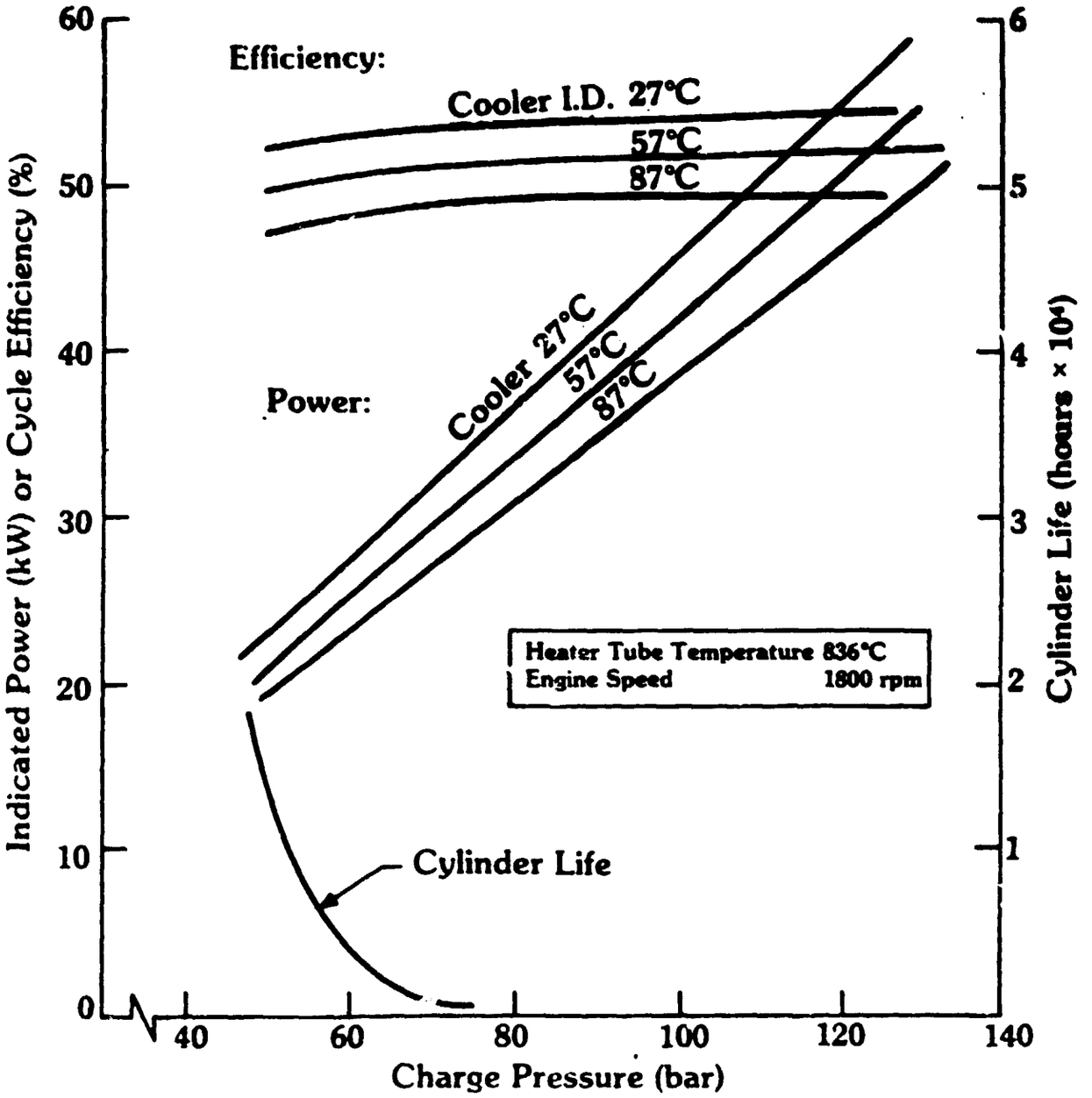

Fig. 2.3-6 Optimum He Engine Performance @ 816°C Cylinder Temperature

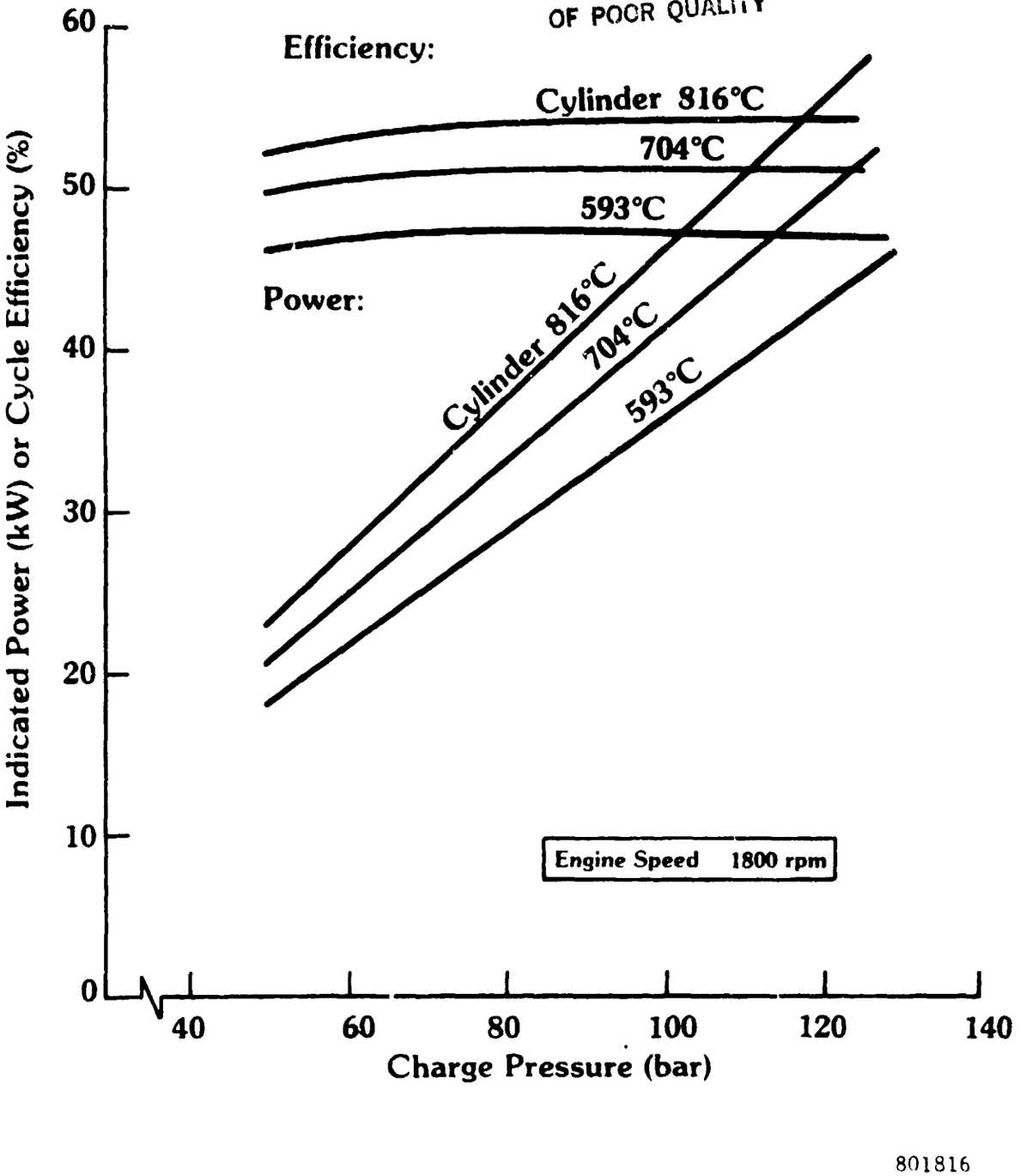

Fig. 2.3-7 Optimum He Engine Performance @ 27°C Cooler Temperature

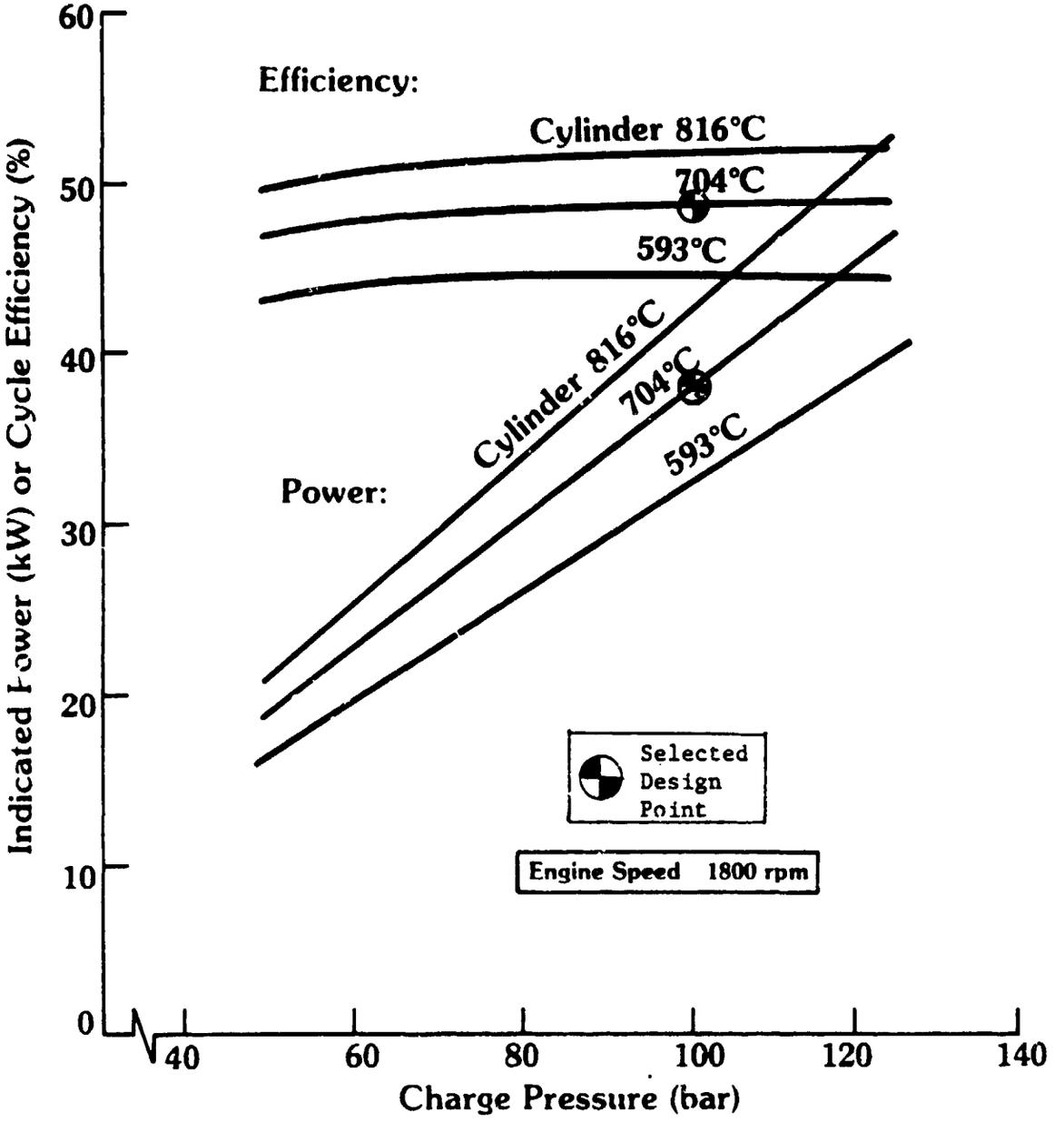

801830

Fig. 2.3-8 Optimum He Engine Performance @ 57°C Cooler Temperature

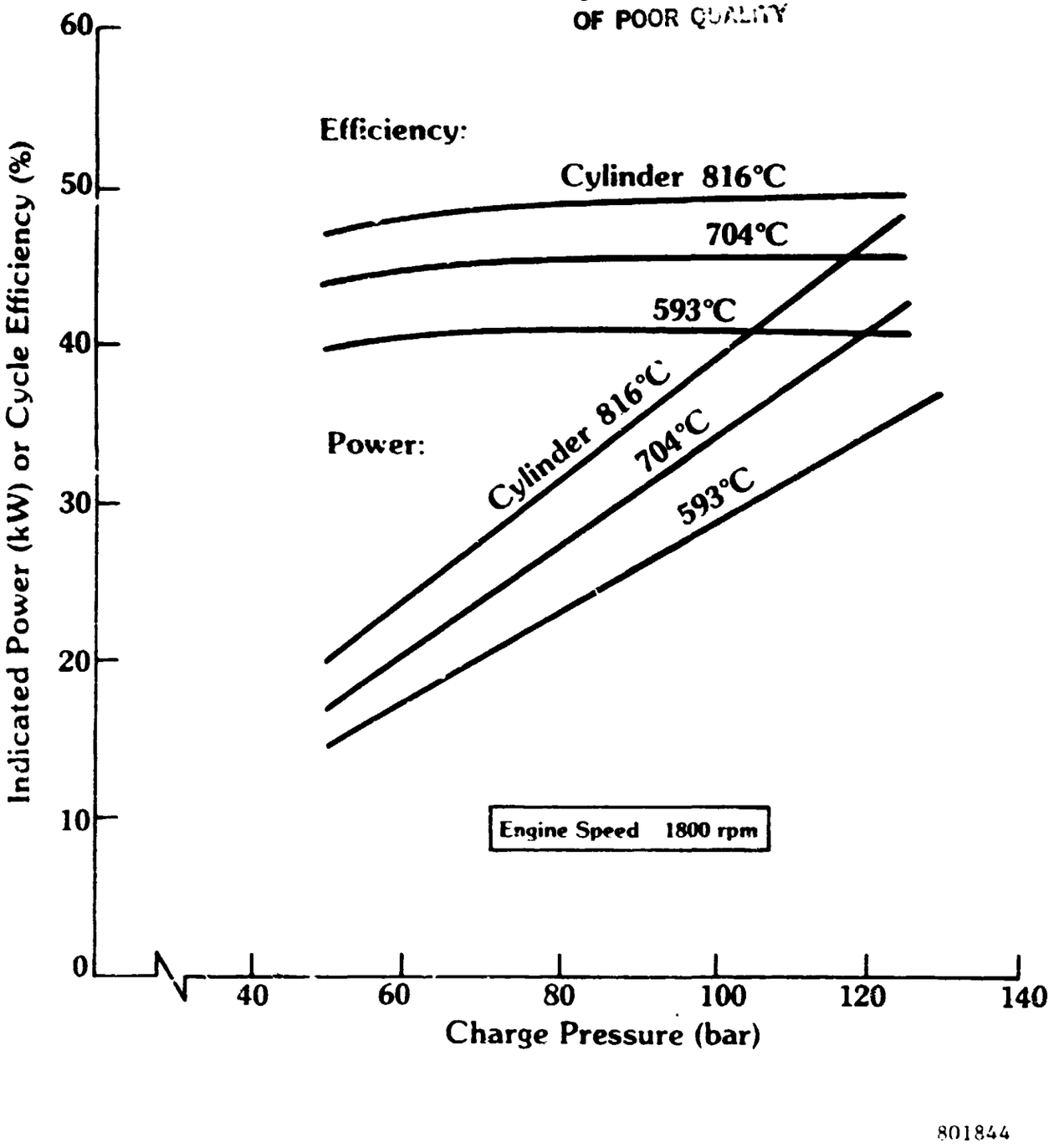

Fig. 2.3-9 Optimum He Engine Performance @ 87°C Cooler Temperature

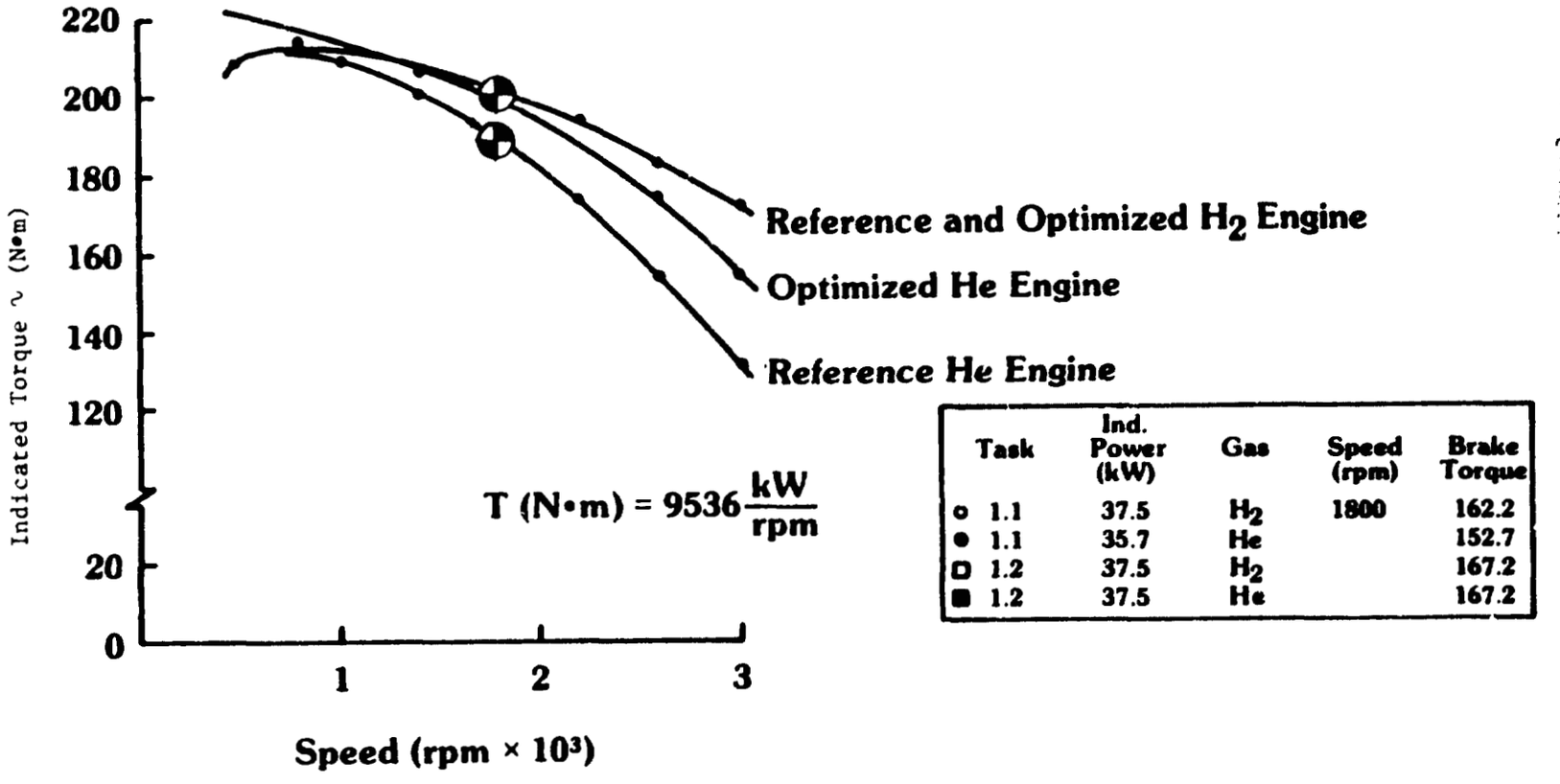

Task	Ind. Power (kW)	Gas	Speed (rpm)	Brake Torque
o 1.1	37.5	H_2	1800	162.2
● 1.1	35.7	He		152.7
□ 1.2	37.5	H_2		167.2
■ 1.2	37.5	He		167.2

Fig. 2,3-10 Indicated Torque Curve

TABLE 2.3-6

REFERENCE AND OPTIMUM ENGINE SUMMARY

Task		Reference (Section 2.2)		Optimized (Section 2.3)	
Engine Type		Kinematic	Kinematic	Kinematic	Kinematic
Working Fluid		H_2	He	H_2	He
Temperature Heater	°C	669	669	724	724
Temperature Cylinder	°C	649	649	704	704
Temperature Cooler	°C	57	57	57	57
Pressure	bar	123	123	100	100
Speed	rpm	1800	1800	1800	1800
Displacement Engine	cm^3	453	453	486.67	491.30
No. of Cylinders		4	4	4	4
Indicated Power	kW	37.50	35.71	37.5	37.5
Auxiliary Power	kW	2.25	2.25	2.15	2.15
Drive Power	kW	4.64	4.64	3.8	3.8
Brake Power	kW	30.61	28.82	31.56	31.56
Indicated Efficiency	%	48.33	46.61	50.7	48.52
Brake Efficiency	%	35.51	33.87	38.44	36.75
Combustion Efficiency	%	90.0	90.0	90.0	90.0
Heater Head Material		12RN72	12RN72	In-625	In-625
Cylinder Material		XF818	XF818	713LC	713LC
Heat Input	kW	86.2	85.09	82.1	85.9
BSFC $\frac{kg}{kW}$		0.24	0.25	0.22	0.23
Brake Torque	(Nm)	162.2	152.7	167.2	167.2

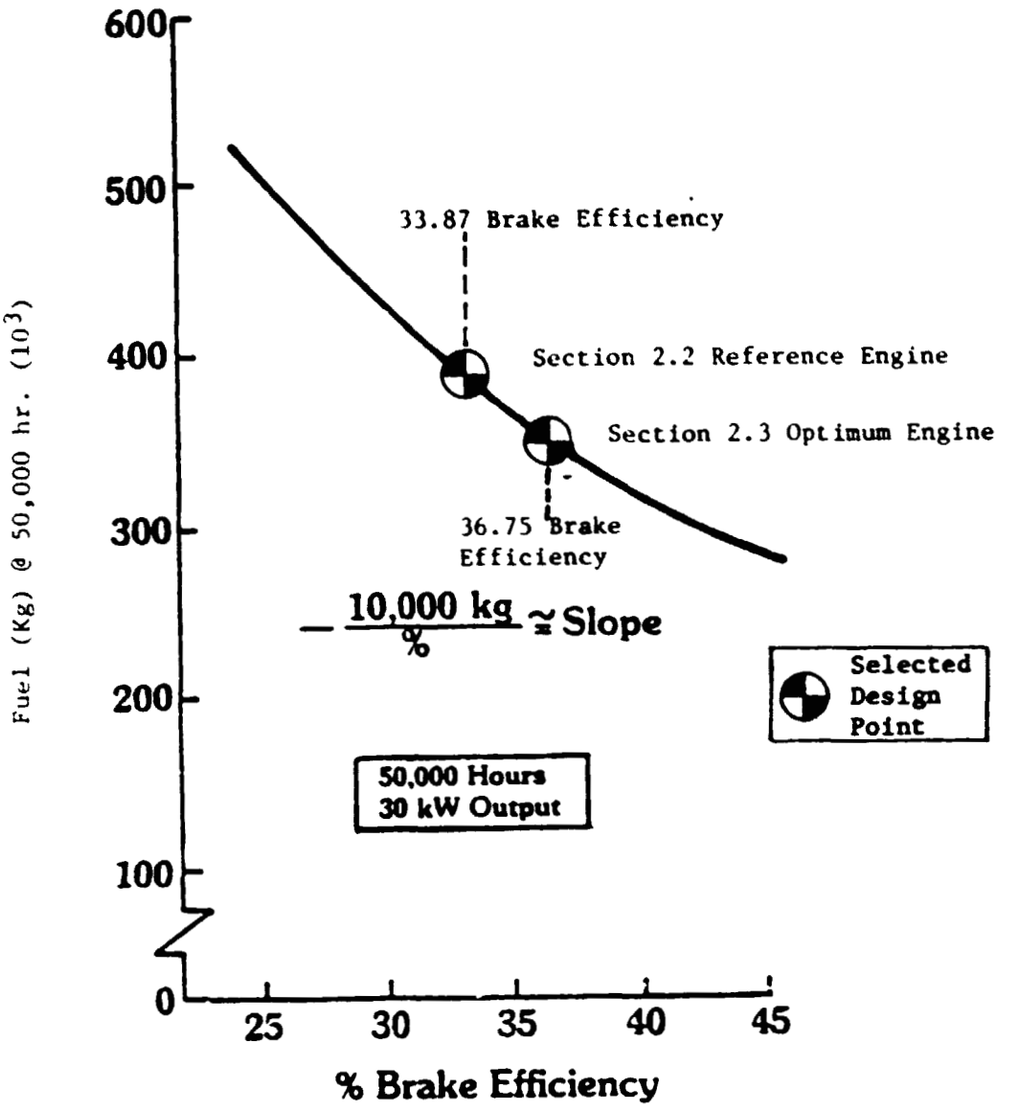

Fig. 2.3-11 Results - Effect of Brake Efficiency on Fuel Consumption

3.0 400 kW KINEMATIC ENGINE (TASK 2 ENGINE)

3.1 Introduction

The objective of Task 2 was to develop a conceptual design for a high-efficiency 400 kW engine which is not burdened by prior automotive constraints. Ease of fabrication, durability and cost were considered in the selection of overall design, design features, and materials. The cycle optimization effort includes alternate heater head materials and working fluids.

The performance was established for an Inconel-625 heater tube, helium gas engine with the same operating temperatures and speed as the optimized 37.5 kW engine (see Section 2). An alternate case, using Udimet-700 heater tube materials and H_2 gas, reached a brake efficiency level of 45 percent, the highest efficiency level achieved under this study. Primary credit for this improvement derived from a significant reduction in the drive system friction losses.

3.2 Conceptual Layout

The conceptual layout of the 400 kW kinematic engine is based on the same four-square, double-acting (Rinia) configuration as the automotive engine. The 50,000-hour life and 1800 cycles/minute speed values were maintained. The layout incorporates three improved features: the variable-stroke Z-crank, concentric regenerators (rather than canister type), and individual cylinder head combustors in place of one large central combustor. Figure 3.2-1 illustrates the overall engine layout.

3.2.1 Variable-Stroke Z-Crank

The variable-stroke Z-crank is a significant departure from the conventional crankshaft reciprocal-to-rotary motion system. A simplified schematic of the Z-crank system is shown in Figure 3.2-2. While somewhat similar to the wobble plate system used on the Phillips/Ford automotive engine, the Z-crank avoids the deficiencies found in both systems.

The Z-crank concept has been under study at MTI for some time and a number of patents have been filed. A description of its mechanical operation can be found in Reference 4.

Adapting the Z-crank to the 400 kW stationary engine proved attractive for the following reasons:

- Significant (>50 percent) reduction in drive system friction loss.
- Increased volumetric and geometric power densities.
- Elimination of gears for reduced noise and cost.
- Simplification of power controls. The fact that the subject engine is a constant-speed machine does not imply constant load. The variable-stroke feature allows power to be controlled at constant engine pressure. This system replaces the more complicated mean pressure control system used in the automotive engines.

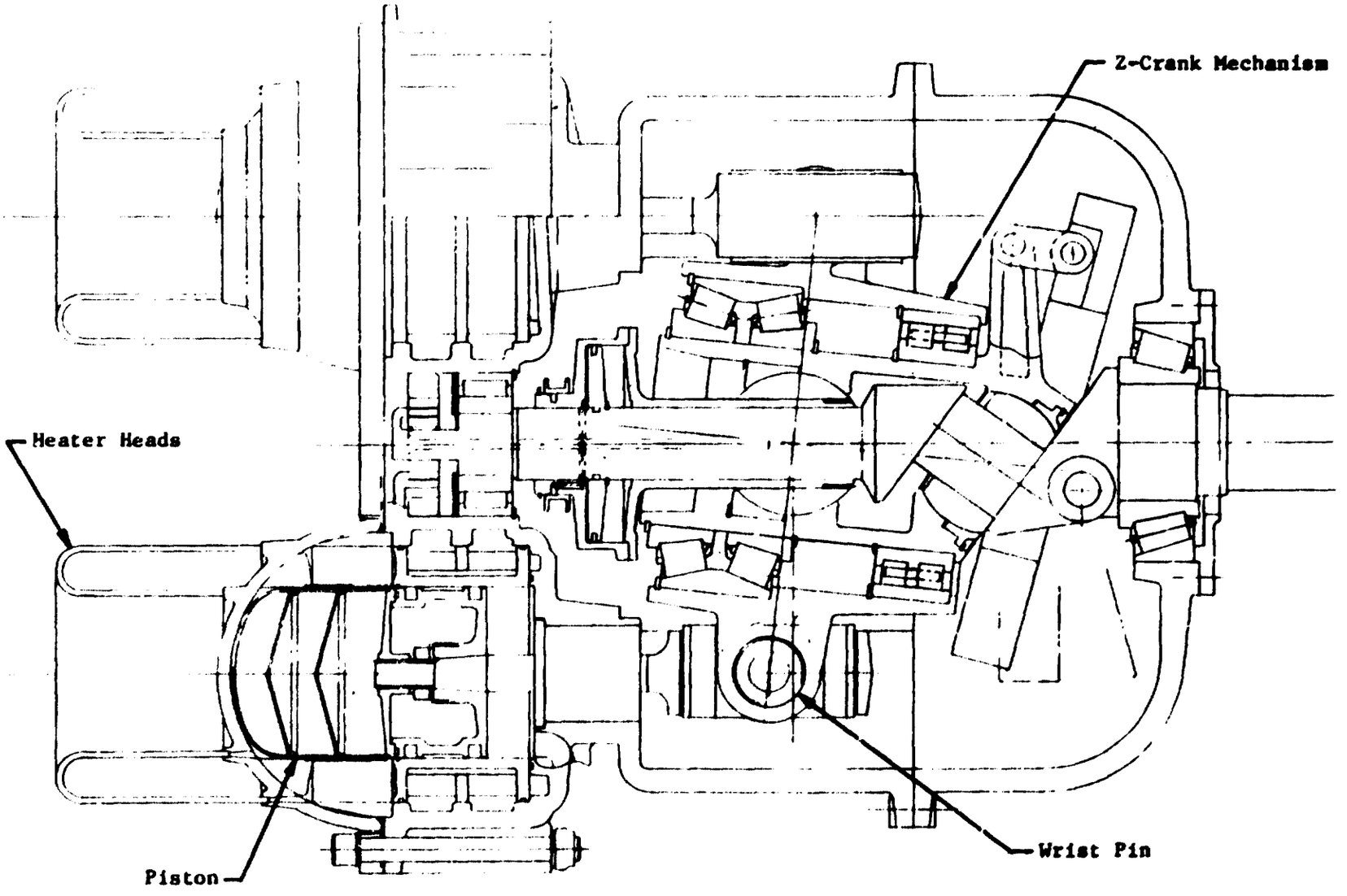

Fig. 3.2-1 400 kW Kinematic Stirling Engine

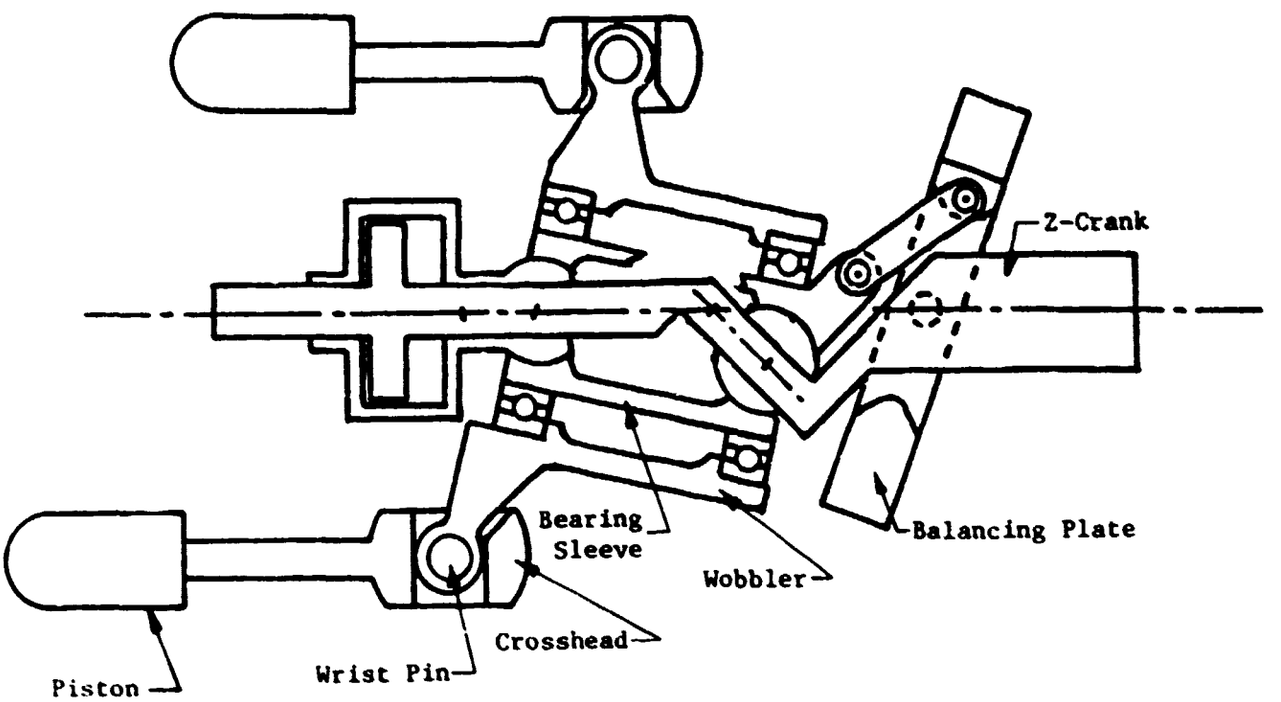

Fig. 3.2-2 MTI Z-Crank Mechanism

811672

- Simplicity. Fewer overall parts are required for this system than for a conventional Stirling crankshaft system.

3.2.2 Concentric Regenerator

A regenerator stores and reclaims cycle heat as the working gas reciprocates between the engine's expansion and compression volumes. This reclaiming of heat is vital to the high efficiency performance of the Stirling engine, which requires a large temperature difference to maintain a high Carnot efficiency (Reference 4), i.e.

$$\eta = k \frac{T_E - T_C}{T_E}$$

where: k = function of engine design

T_E = expansion space temperature

T_C = compression space temperature

For the reference and optimized engines of Section 2.0, canister-type regenerators were used (see Figure 2.2-1). These regenerators create pressure losses which result from ducting the working fluid from the quadrant design of the heater head tubes to the circular canister.

A concentric regenerator design was selected in the 400 kW kinematic engine, which has the same heat conduction loss rates as the canister design, but minimizes the pumping loss and reduces dead volume. The engine design has four concentric regenerators, one for each cylinder. Figure 3.2-3 illustrates the concentric regenerator location relative to other system components.

3.2.3 Individual Combustors

Design values for heat transfer and heat release rates dictated that heater tube lengths must be short. Further, the concentric regenerators, described in Section 3.2.2, require that the tubes be directed from the expansion space of the cylinder to the regenerator, concentric to but at a larger radius than each cylinder. For this tube configuration, it is convenient to use four combustors of 125 kW each, one on each cylinder centerline. The alternative of one central combustor results in a geometry which makes uniform heat distribution difficult. The combustor is discussed in detail in Section 3.4.

3.3 Cycle Analysis and Optimization

3.3.1 Optimization Summary

Cycle analysis and optimization results were incorporated into the conceptual layout. The performance code was held to the constraints listed in Table 3.3-1 and dimensions were optimized without exceeding the given limits. A total of three optimizations were accomplished - all with an indicated power level of 500 kW. Table 3.3-2 contains the different material/working gas combinations, the displacement and indicated efficiency of each engine. A dimensional comparison of the three optimum engines is given in Table 3.3-3 and a summary of heat energy input, output, and efficiencies is given in Table 3.3-4. An explanation of the displayed heater tube materials is given in the following Section 3.3.2.

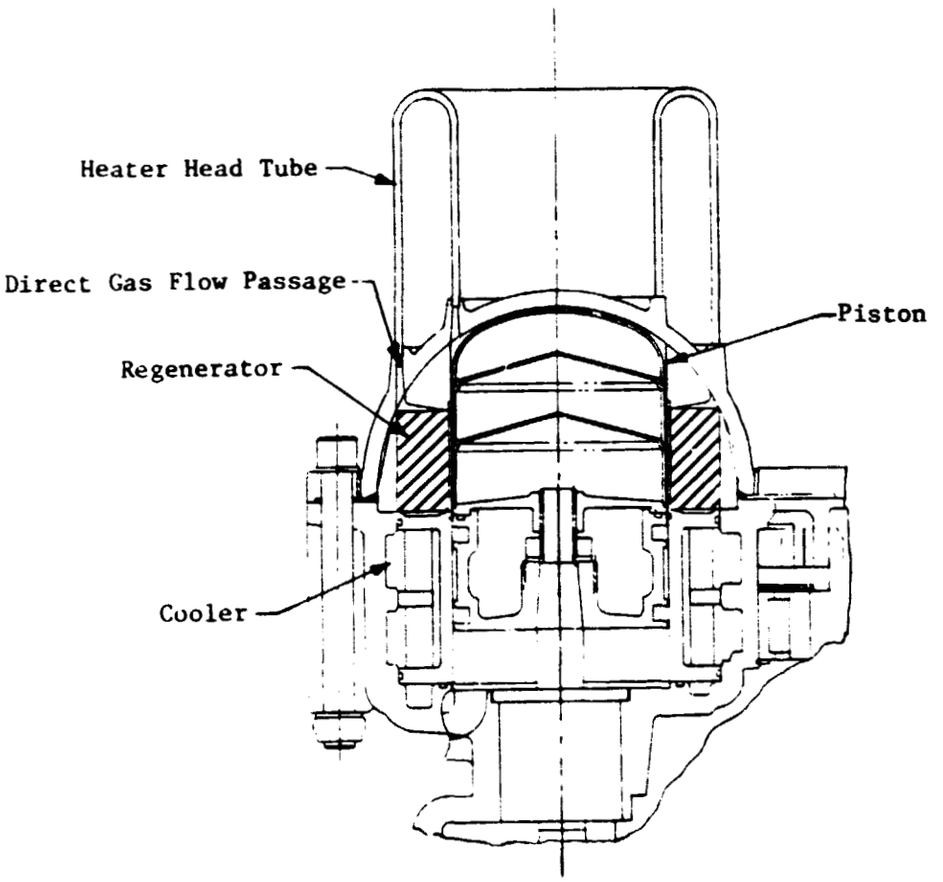

Fig. 3.2-3 Concentric Regenerator

811719

TABLE 3.3-1

CYCLE ANALYSIS AND OPTIMIZATION

Cycle Constraints

- Speed: = 1800 rpm
- Temperature, Heater Tube: $\leq$ 800°C
- Temperature, Cooler: = 57°C
- Pressure: $\leq$ 150 bar

TABLE 3.3-2

400 kW KINEMATIC ENGINE OPTIMIZATIONS

Heater Tube Material	Working Gas	Engine Displacement (cm^3)	Indicated Efficiency
Udimet 700	H_2	4915	58.7I
Udimet 700	He	5400	54.51
Inconel 625	He	6089	52.4

TABLE 3.3-3

GEOMETRY COMPARISON: H_2 and He

			H_2	He	He
Piston	Crank Radius	(mm)	23.81	23.81	23.81
	Piston Diameter	(mm)	181.27	190.00	201.74
	Displacement	(cm^3)	4915.77	5400.66	6088.68
Heater	Tube I.D.	(mm)	5.15	5.15	3.32
	Tube O.D.	(mm)	7.21	7.21	4.64
	Effective Length (per cylinder)	(mm)	331.8	348.57	252.51
	Number of Tubes (per cylinder)		63	66	218
	Material		U-700	U-700	In-625
Regenerator	Frontal Area	(cm^2)	313.17	340.32	356.25
	Wire Diameter	(mm)	0.0762	0.0762	0.0762
	Filling Factor	(%)	34.34	30.63	34.09
	Effective Length	(mm)	83.14	71.91	53.72
Cooler	Tube I.D.	(mm)	3.45	3.99	3.94
	Number of Tubes		400	400	400
	Effective Length	(mm)	100.00	105.3	119.00
Operating Pt.	Temperature		800°C	800°C	724°C
	Pressure		150 bar	150 bar	120 bar

TABLE 3.3-4

400 kW KINEMATIC ENGINE SUMMARY

TASK				
Type			Variable Z-Crank	
Working Fluid		H_2	He	He
Temperature Heater	°C	800	800	724
Temperature Cylinder	°C	780	780	704
Temperature Cooler	°C	57	57	57
Pressure	bar	150	150	120
Speed	rpm	1800	1800	1800
Displacement Engine	cm^3	4915.77	5400.66	6088.68
Number of Cylinders		4	4	4
Indicated Power	kW	500	500	500
Auxiliary Power	kW	35.8	35.8	41.36
Drive Power	kW	32.2	32.2	29.04
Brake Power	kW	432	432	429.6
Indicated Efficiency	%	58.71	54.51	52.4
Brake Efficiency	%	45.65	42.41	40.5
Combustion Efficiency	%	90.0	90.0	90.0
Heater Head Material		U-700	U-700	I-625
Cylinder Material		713-LC	713-LC	713-LC
Heat Input	kW	946.2	1018.8	1060.6
sfc	kg/kW	0.17	0.20	0.21
Torque	Nm	2289	2289	2278

3.3.2 Material Change

The optimization process requires an iteration of the code results until convergence to a satisfactory solution. Such was the case when Inconel-625 material replaced Udimet-700 in the heater tubes. A number of 50,000-hour life solutions were generated based on the Larson-Miller parameter for the Inconel-625 material, but because Inconel-625 has significantly different high temperature properties than Udimet-700, it was necessary to drop head temperature, resulting in a lower indicated efficiency. Multiple runs of the optimization code were performed to minimize this decrease. It should be noted Udimet-700 is considered not practical for this application, but was included to show the gains of performance at a higher temperature.

Figure 3.3-1 summarizes the relationship of charge pressure, temperature, factor of safety, and indicated cycle efficiency for the Inconel-625 material heater tube version of the engine. The locus of cycle efficiency achievable at the minimum safety limit of 1.65 (same as Section 2) is shown. This chart concludes optimum efficiency occurs at 724°C heater tube temperature with a charge pressure around 120 bar pressure. Figure 3.3-2 illustrates a two point reduction in cycle efficiency at 1800 rpm when the material was changed from Udimet-700 to Inconel-625, which requires a reduction in operating temperature and pressure to maintain 50,000-hour life.

3.3.3 Working Gas Change

This study was initiated with hydrogen (H_2) working gas and extended to include helium (He) working gas for both the Udimet-700 and Inconel-625 heater tube material versions. The impact of the gas substitution is illustrated in Figure 3.3-3, which indicates a four point drop in efficiency with the substitution of working gas and reoptimization.

While performance comparisons have been held at 1800 rpm, it has been demonstrated in Figures 3.3-2 and 3.3-3, gains in brake efficiency are possible at lower rpm, at the loss of power output at full stroke. However, higher losses in efficiency occur below 50 percent stroke at the lower rpm, as described in Section 3.3.4.

3.3.4 Variable Stroke Output and Efficiency

The variable stroke feature of the 400 kW engine provides a simpler control system than the mean pressure control to modulate power at constant engine speed. A set of characteristics were generated for power and indicated efficiency as a function of both speed and percent of stroke for the helium engines.

The stroke is controlled by a hydraulic actuator system incorporated into the variable angle Z-crank design. Reducing stroke to 50 percent reduces power output by 70 percent, with an advantageous efficiency gain of 2 points; efficiency drops off much more rapidly below 50 percent stroke. A reduction to 25 percent stroke resulted in an approximate 10 point drop in cycle efficiency. Figures 3.3-4 and 3.3-5 illustrate the characteristics for the variable stroke Udimet-700 and Inconel-625 helium engines, respectively.

3.4 Engine Components Analysis and Optimization

Cycle optimization is performed for the engine itself, excluding the external components such as the combustion and cooling systems. This section now reviews these systems in relation to the specific requirements and logistic advantages of the stationary engine in the 400 kW power class.

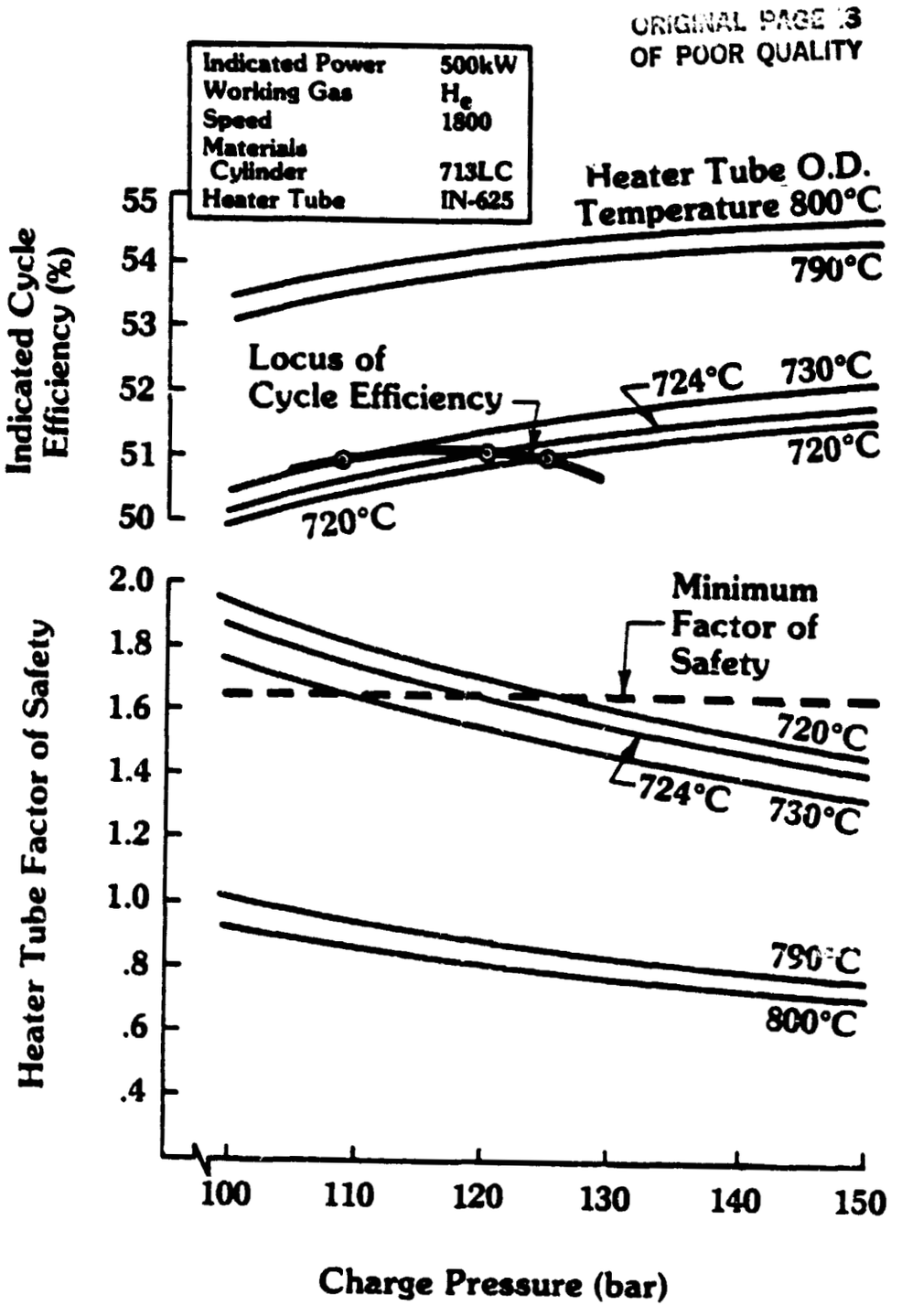

Fig. 3.3-1 Charge Pressure, Factor of Safety/Efficiency Combinations

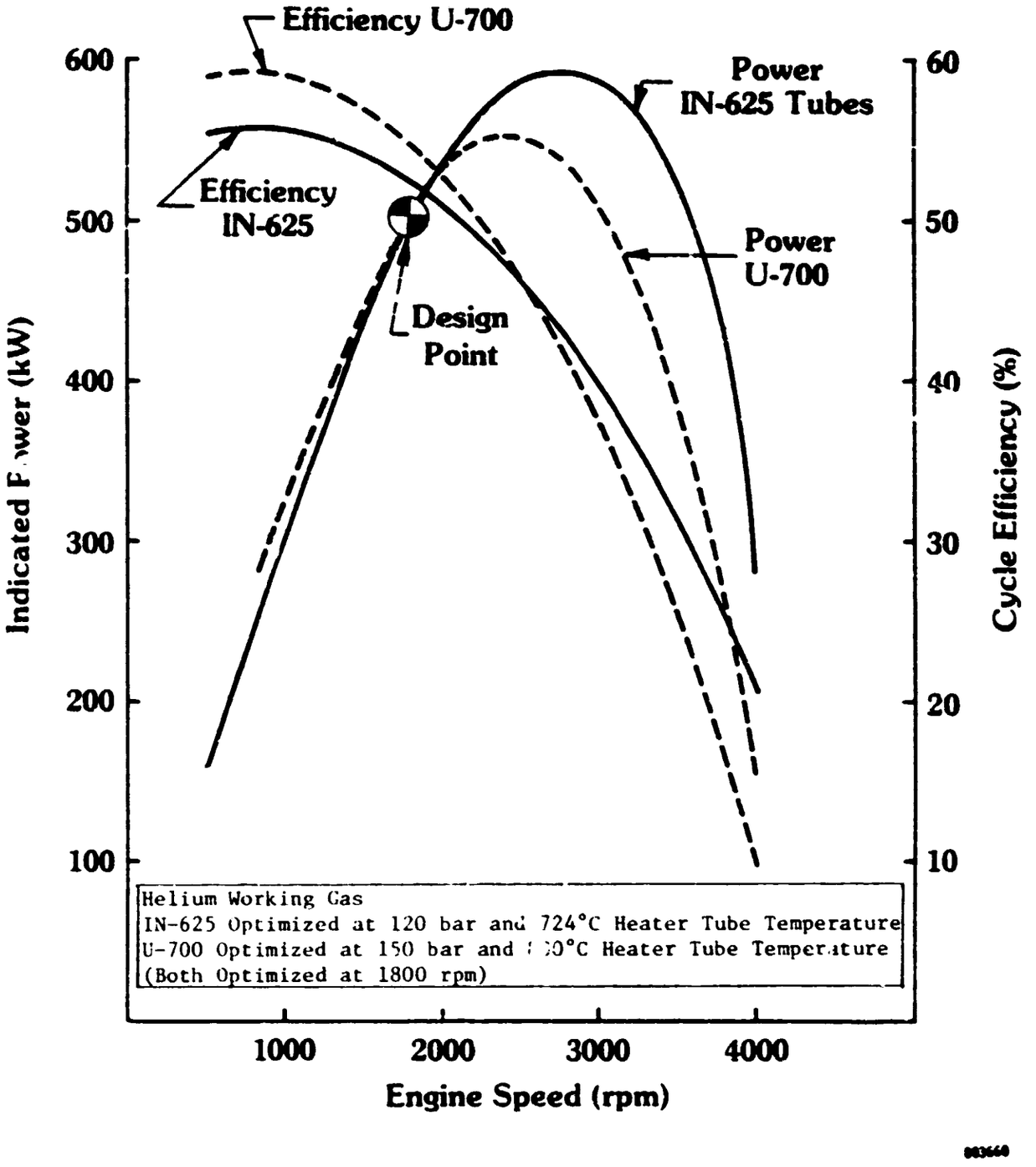

Fig. 3.3-2 Comparison of Heater Tube Material in a 400 kW Engine

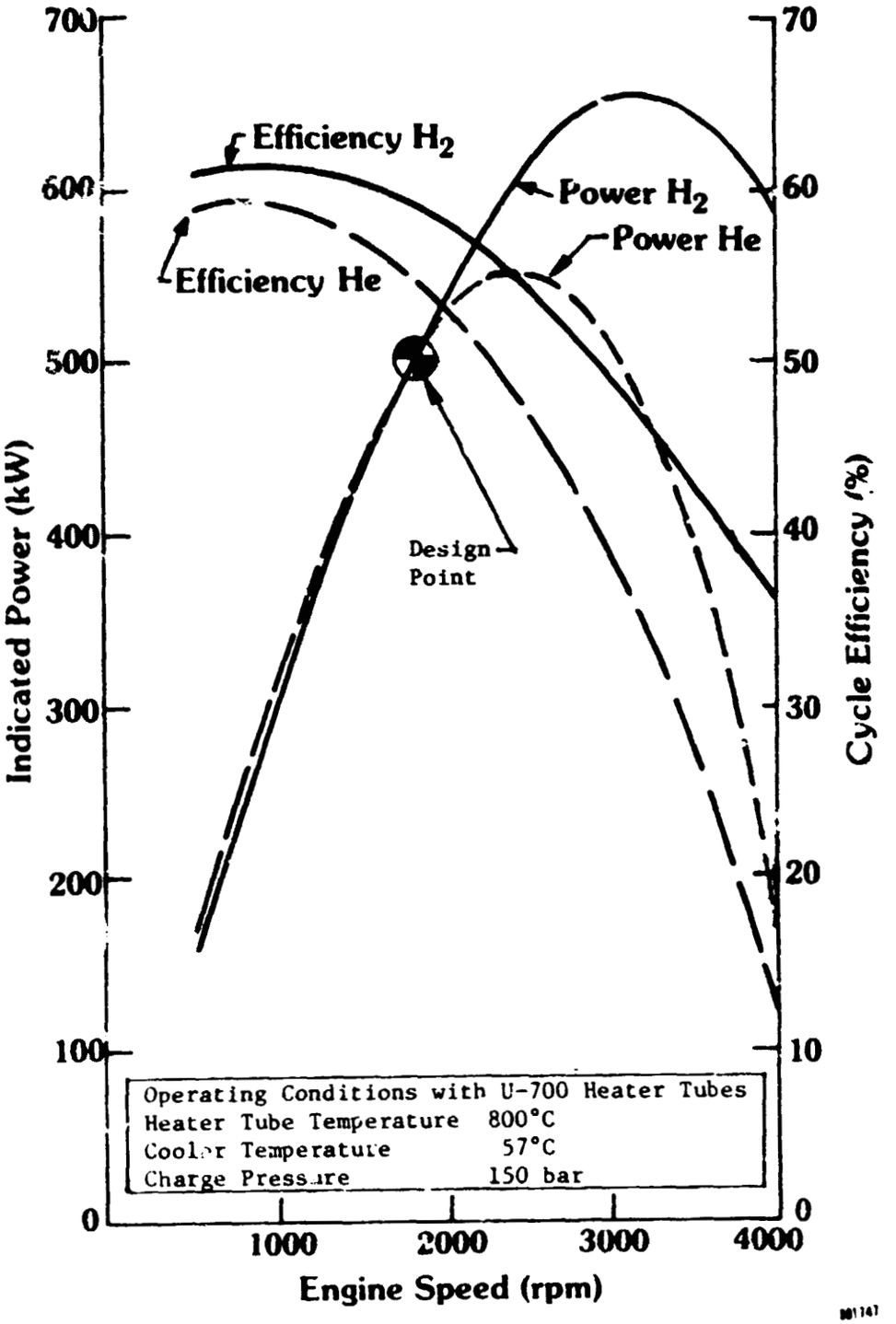

Fig. 3.3-3 Performance Comparison Between Optimized He and H_2 in a 400 kW Engine

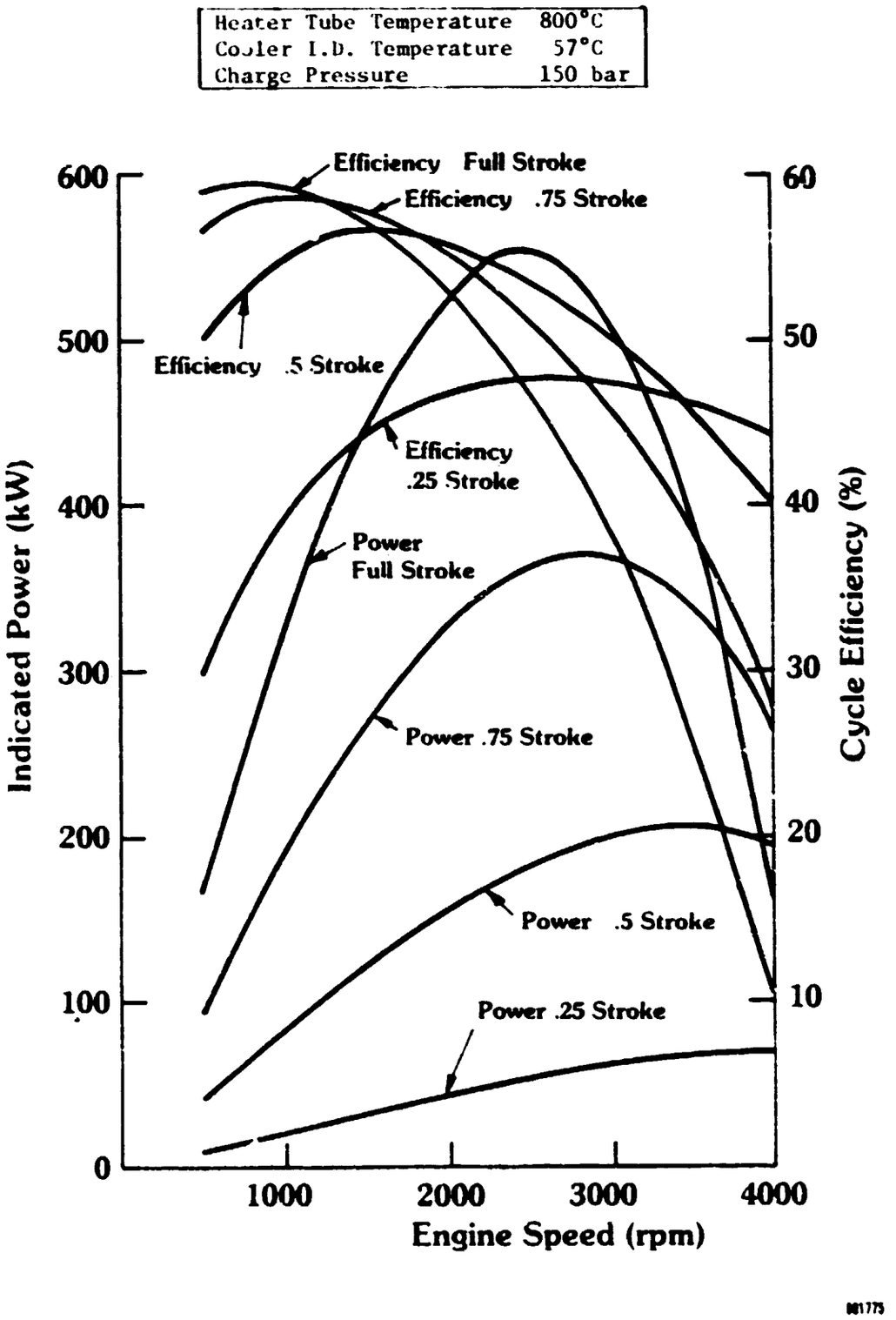

Fig. 3.3-4 400 kW Helium Engine Performance with Varied Stroke, P-700 Material

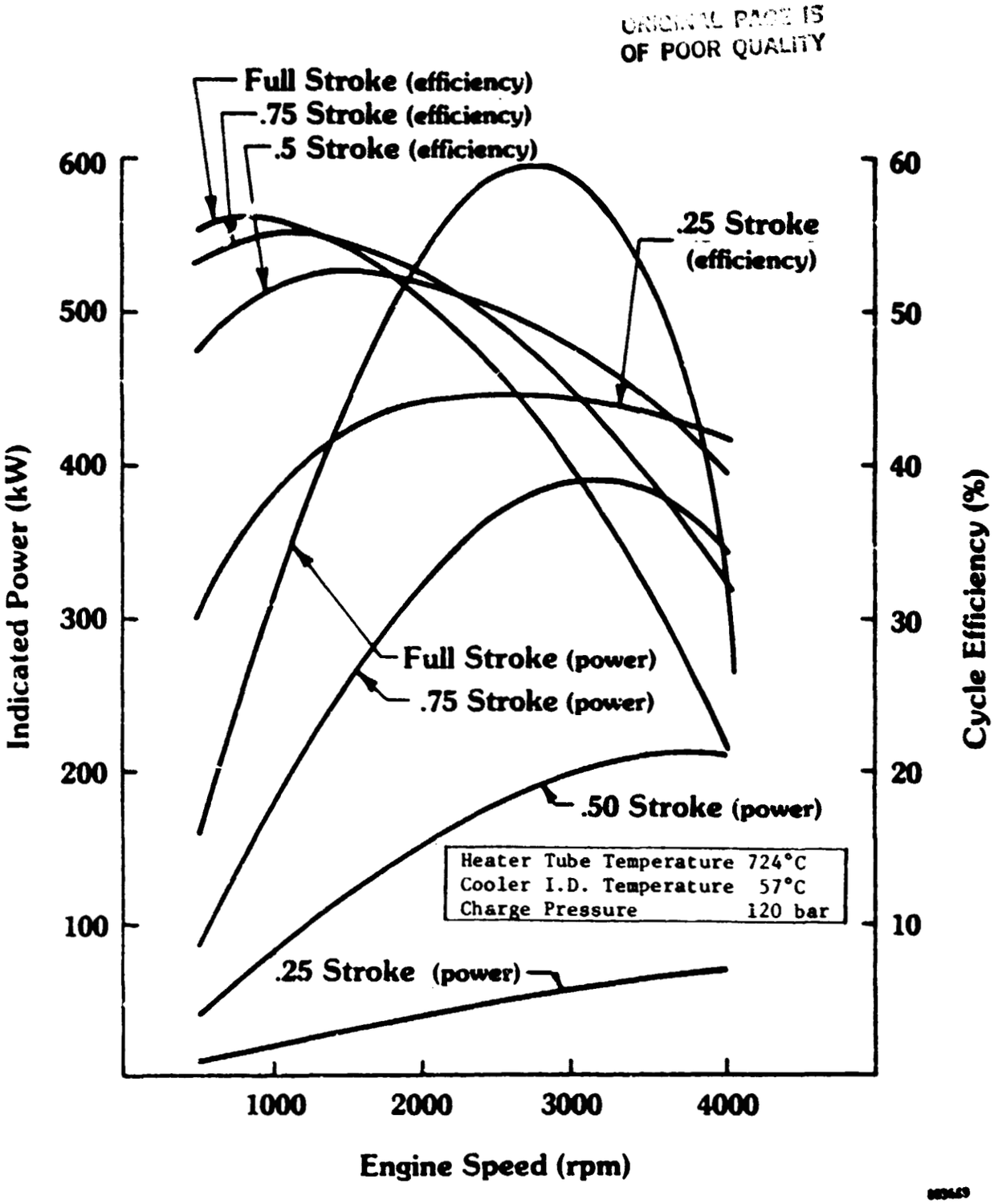

Fig. 3.3-5 400 kW He Engine Performance with Varied Stroke and IN-625 Material

3.4.1 Combustion System

As described in Section 3.2.3, the combustion system consists of four separate combustors. Two combustor designs were generated: the first, a more conventional single-pass design; and the second, a more complex but potentially high-performing double-pass design. Both designs were generated for the following:

- allowance for fuel vaporization and mixing;
- sufficiently long residence time in the main combustion zone to effectively consume the hydrocarbon components of the fuel, yet without producing large quantities of NOx or CO;
- combustor loading volume design within limits of current Stirling engine combustors;
- improved aerodynamics in the combustor and diffuser leading to the heater tubes to obtain optimum heat transfer at the tubes;
- preheater heat transfer rate similar to the ASE Reference Engine;
- adequate combustor wall cooling; and, incorporation of swirl in the primary zone to improve mixing and produce a flame stabilization zone.

3.4.2 Single-Pass Combustor

The single-pass combustor shown in Figure 3.4-1 satisfies the stated design requirements. Its features include:

- a large combustion volume above the heater tubes to promote good fuel vaporization, adequate mixing volume, and smooth flow through the heater tubes; and,
- low-cost, low-load ceramic liner and flow divider to separate combustion from exhaust air and to direct flow through the tubes.

Because of space limitations imposed by the adjacent cylinder, the preheater was placed above the combustor. The volume of the preheater is double that of the Reference Engine for the same heat transfer loading in order to favor higher combustion efficiency. Insulation thickness is increased to about three inches to compensate for the larger exposed surface area. Turning vanes in the duct approaching the heater aid in reducing flow losses.

The combined aerodynamic and thermodynamic area diffusion ratio for this combustor is 8.7, of which approximately 2.0 can be attributed to heat release. This leaves aerodynamic diffusion at about 4, which is too large a ratio for non-separated flow. The flow passages are designed to minimize these flow separation losses, which cannot be completely eliminated.

Although a double-pass combustor design was considered, it was decided to use the single-pass combustor due to its simplicity, lower potential cost, and good efficiency level. This level was estimated, somewhat conservatively, at 90 percent.

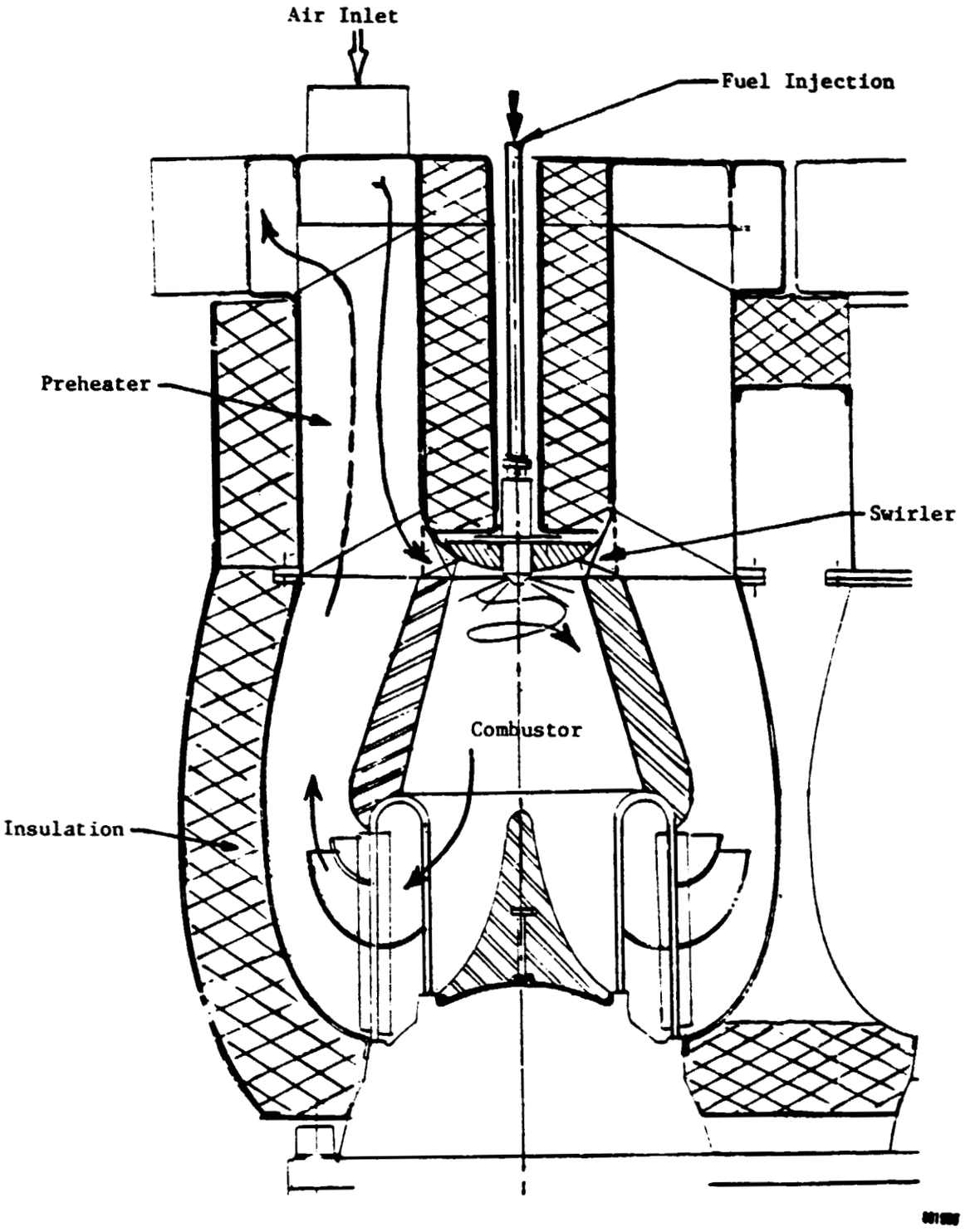

Fig. 3.4-1 Combustor for the 400 kW Stationary Stirling Engine

A final consideration for the combustor system is the method of controlling the heat input to each cycle. Because of the Stirling engine's high thermal inertia, a relatively simple, slow-rate system could be utilized to monitor heat required and to adjust fuel and airflows to provide tube temperature control as the power level varies and as the engine and combustor degrade with time. This system has the advantage of allowing the engine to keep operating at high output if one combustor or cycle deteriorates.

3.4.3 Cooling System

A well designed cooling system is critical to achieve good engine performance. For example, Carnot efficiency (the maximum efficiency a Stirling engine is theoretically capable of achieving) is more sensitive to cold end temperature change than hot end temperature. For a heater temperature of 650°C (923k) and a cooler temperature of 50°C (323k), Carnot efficiency is 65 percent. If the heater temperature is increased 10°C, Carnot efficiency increases about 0.4 points. However, if cooler temperature is decreased 10°C, Carnot efficiency rises about 1.1 points. Thus, at these temperatures, a degree change in the cold chamber has over a two-fold effect over a degree change in the hot chamber.

Stationary applications are not overly restricted by size, weight, engine compartment pressure, and styling of a vehicular installation. This is counterbalanced by the lack in readily available ram cooling airflow.

It is assumed the stationary application is either a self-contained cooling package installation or an external coolant source.

In a self-contained cooling system, a radiator with fan will be required. At a standard ambient temperature of 20°C, Table 3.4-1 summarizes the performance characteristics of the radiator and fan cooling system.

Scaled from the 40 kW engine, the radiator has a frontal area of 3.71 m^2. A conservative estimate of water-side pressure drop would be equal to the 40 kW engine, or 3.73 psi. The hydraulic power is then:

$$3.73 \times 240 \times 583 \times 10^{-6} \times .746 = .39 \text{ kW}$$

It is assumed the radiator core raises cooling air temperature to one-half of the difference between the coolant inlet temperature (37°C) and the cooling air (21°C), therefore giving an 8°C rise.

If an external water supply, such as a river, pond, or cooling tower, is available, a lower than ambient temperature coolant will increase engine efficiency. Cooling ponds could cool 12 to 18 pounds of water per hour: 10° for each square foot of pond surface area.

The pressure drop losses through the radiator would be replaced by those of a strainer; furthermore, with brackish or salt-water cooling, a liquid-to-liquid heat exchanger is recommended to protect the engine.

Analyses of the 400 kW engine in this report assumed the more general radiator/fan configuration rather than the cooling pond.

3.5 Performance Map Generation

A full set of performance maps was generated for the Udimet 700 helium

TABLE 3.4-1

PERFORMANCE OF A RADIATOR WITH FAN (21°C AMBIENT TEMPERATURE)

Indicated Power Output	500 kW	
Indicated Efficiency	58.7 percent	
Total Heat Input	852 kW	(2.906×10^6 Btu/hr.)
Heat Rejected to Radiator	352 kW	(1.2×10^6 Btu/hr.)
Cooler Tube Wall ΔT	2.2°C	(4°F)
Coolant Temperature	42°C Out, 37°C In	(108°F Out, 98°F In)
Coolant Flow H_2O	15.1 Kg/sec.	(240 GPM)
Hydraulic Power	.39 kW	(0.522 HP)
Pump Efficiency	50 percent	
Pump Power	.78 kW	(1.04 HP)
Radiator Cooling Air ΔT	8°C	(14°F)
Cooling Air Flow Required	2700 Kg/min.	(5954 lb/min.)
Air Density (84°F)	1.17 Kg/m^3)	(.073 $lb/ft.^3$)
Volume Flow	2309 m^3/min.	(81,565 cfm)
Radiator Frontal Area	3.71 m^2	(40 $ft.^2$)
Face Velocity	10.4 m/sec.	(34 ft/sec.)
ΔP	12.7 mm H_2O	(0.5 H_2O)
Fan Efficiency	0.5	
Fan Power	9.6 kW	(12.85 HP)

working gas engine. The required operating matrix points about the original design point are given in Table 3.5-1. The full set of performance curves is given in Figures 3.5-1 through 3.5-3, where the abscissa is a percentage of full stroke rather than charge pressure. Indicated power and cycle efficiency are shown along lines of constant cooler temperature.

This data set is augmented by additional curves of the Inconel 625 helium configuration engine (Figures 3.3-5 and 3.5-4).

3.6 Summary and Comparison - 400 kW Kinematic Engine Summary

Table 3.3-4 provides a convenient summary of the engines explored under this task. The programs highest efficiency of 45.6 percent is achieved with the Udimet 700 heater tube material and the H_2 working gas. The engine has a displacement of only five liters and operates at a high brake specific output of 87.9 kW/ℓ or 117 bhp/ℓ. Brake specific fuel consumption was a very attractive 0.17 kg/kW-hr. U-700 however, as mentioned earlier, is a strategic material with fabrication limitations. Therefore, such a material is considered impractical for this application.

The Inconel 625 heater tube/He working gas engine provides a bsfc of 0.21 kg/kW-hr and a brake output power of 429.6 kW. External dimensions between the engines did not vary significantly and the weight of this engine and drive system has been estimated at 1000 kg (2200 lbs.) The brake efficiency is 40.5 percent.

A comparison was made on a brake output basis between the two engines of Section 2.0 and the Udimet 700 heater tube material engines of Section 3.0. Table 3.6-1 compares the hydrogen (H_2) working gas engines and also includes a column for a 400 kW engine with Z-crank and a U-crank (automotive engine type) drive system. Table 3.6-2 is a similar comparison for the helium working fluid engines. The large difference between the optimum 37.5 kW engine and the 400 kW engine is essentially due to the Z-crank drive system efficiency and higher operating temperature.

TABLE 3.5-1

PERFORMANCE MAP GENERATION

- Optimized for He
- Matrix of Data

Material	Cylinder Head Temp. (°C)	Heater Tube Temp. (°C)	Cooler Temp. (°C)	Pressure (bar)
U-700 Heater Head	668	688	27	150
	780	800	57	150
	891	911	87	150
Inconel 625 Heater Head	704	724	57	120

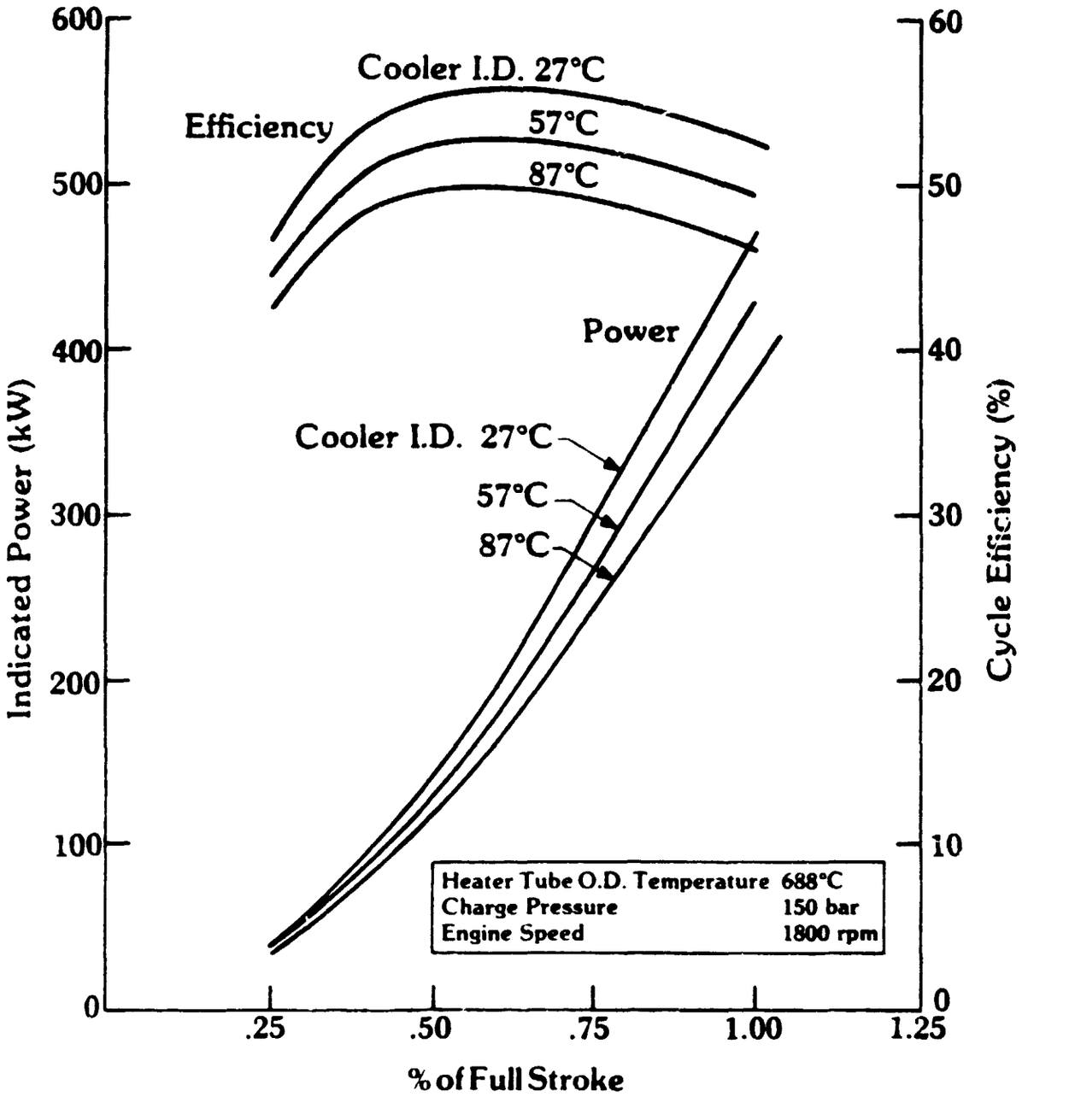

Fig. 3.3-1 He Gas, Cylinder Temperature = 668°C
400 kW Kinematic

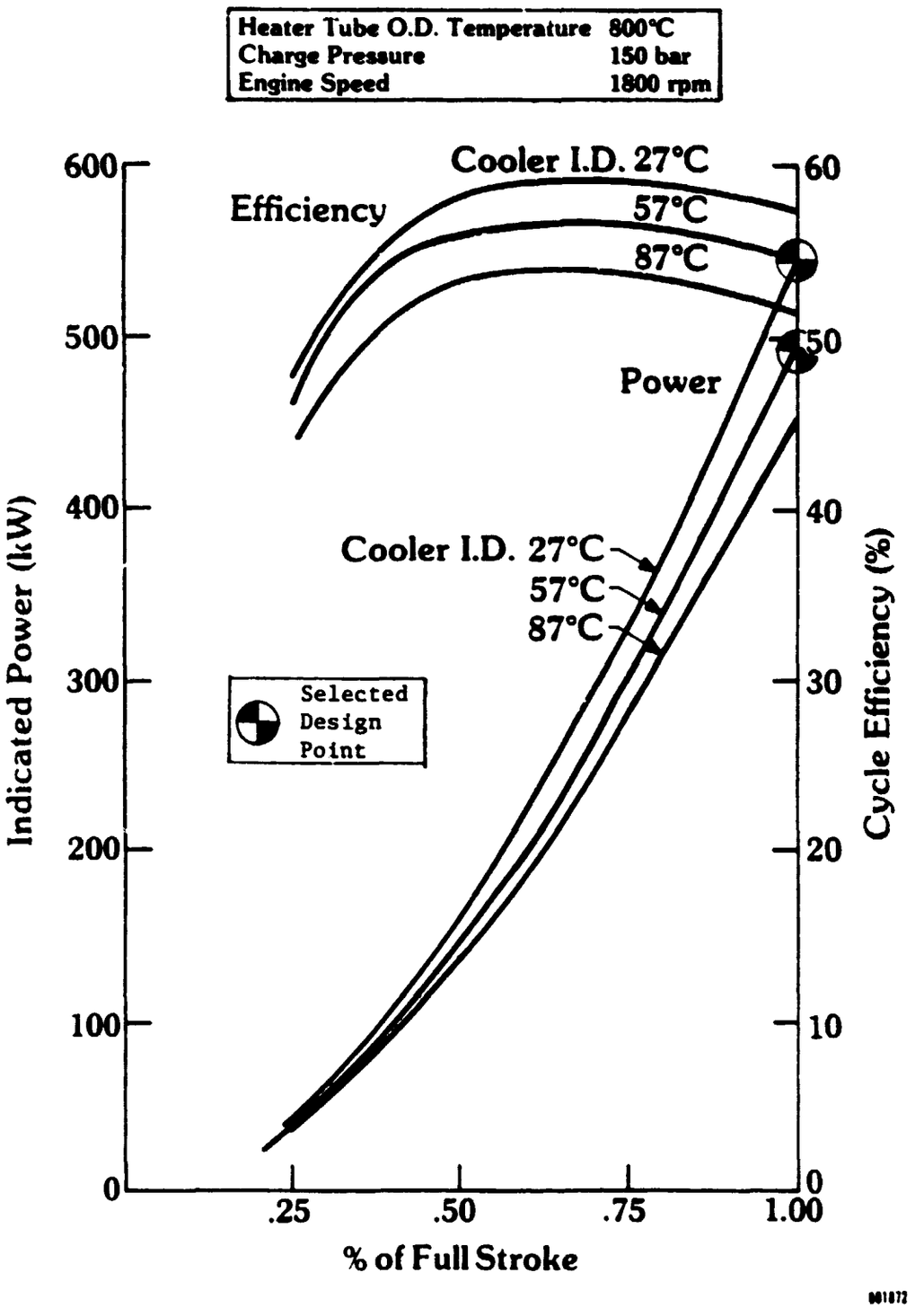

Fig. 3.5-2 He Gas, Cylinder Temperature = 780°C
400 kW Kinematic

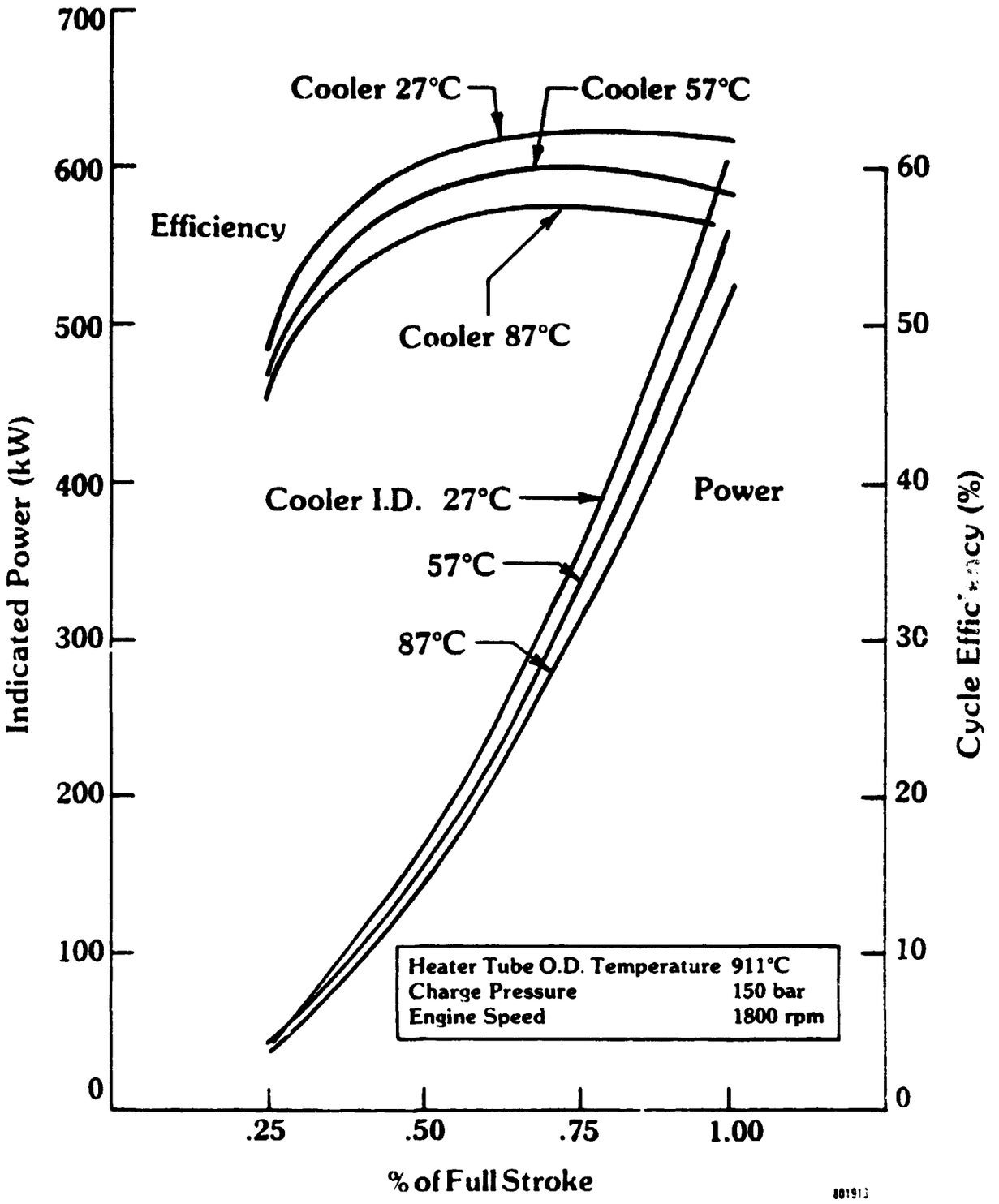

Fig. 3.5-3 He Gas, Cylinder Temperature = 891°C
400 kW Kinematic

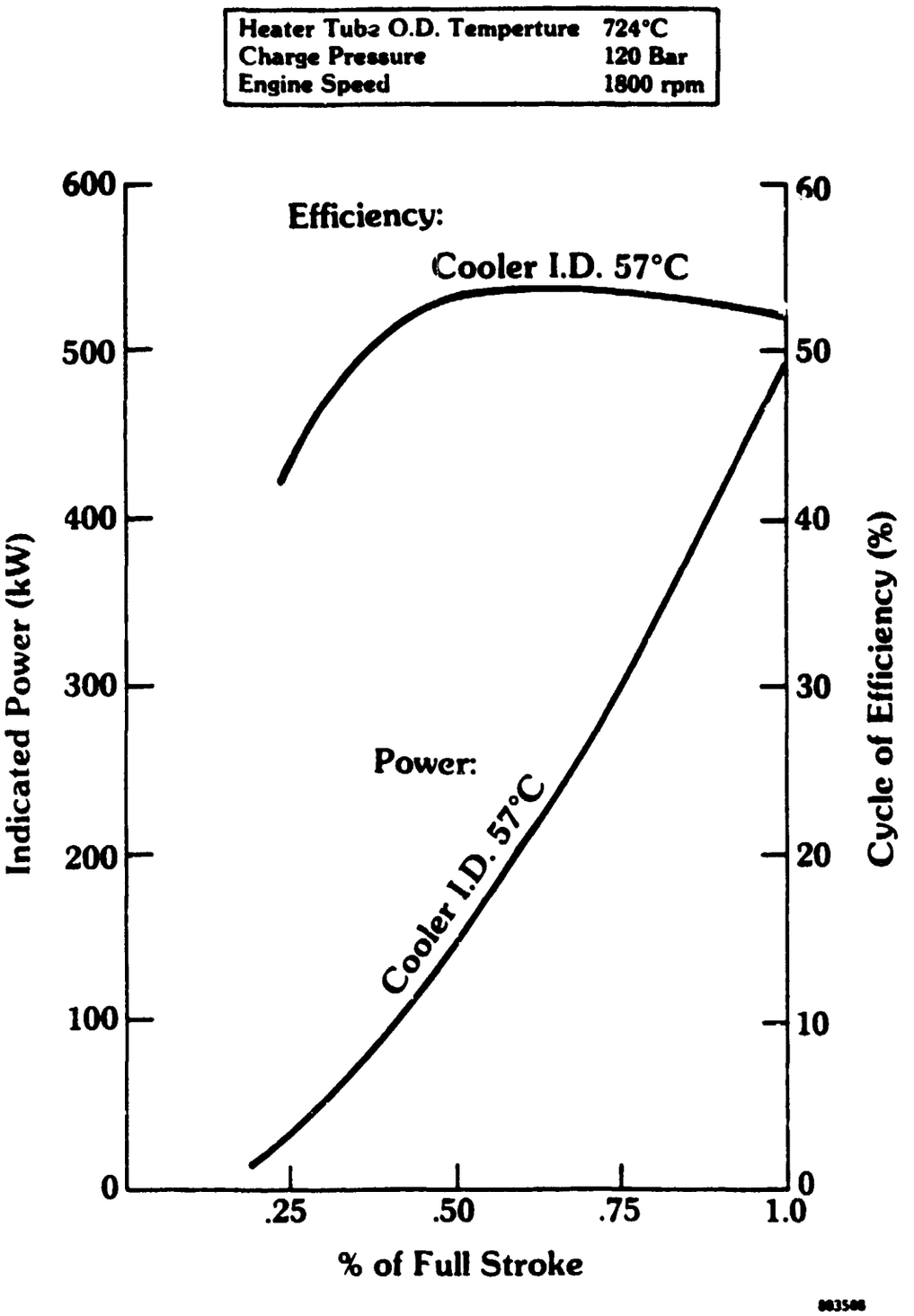

Fig. 3.5-4 In-625 Heater Tube Material, He Gas
400 kW Kinematic

TABLE 3.6-1

400 and 37.5 kW KINEMATIC ENGINE COMPARISON (H_2 GAS)

Operating Conditions	Engines			
	Reference (H_2)	Optimum (H_2)	400 kW (H_2)	
			"2" -Crank	"U" -Drive
Pressure (Bar)	123	100	150	
Water Tube Temperature (°C)	669	724	800	
Cooler Tube Temperature (°C)	57	57	57	
Engine Speed (rpm)	1800	1800	1800	
Indicated Power (kW)	37.5	37.5	500.00	
Heat Input to Heater Tubes*	2.55	2.34	1.97	
Heat Rejection*	1.23	1.06	0.72	
Pumping Loss*	0.08	0.09	0.09	
Drive System Power*	0.15	0.12	0.07	0.14
Auxiliary Power*	0.06	0.07	0.08	
Brake Power (kW)	30 61	31.56	432.00	404.5
Indicated Cycle Efficiency (%)	48.33	50.74	58.71	
Brake Efficiency (%)	35.51	38.44	45.65	42.75

*Per Brake kW Power

TABLE 3.6-2

400 AND 37.5 kW KINEMATIC ENGINE COMPARISON (He CAS)

Operating Conditions	Engines			
	Reference (He)	Optimum (He)	400 kW (He) "Z"	400 kW (He) "U"
Pressure (bar)	123	100	150	
Heater Tube Temperature (°C)	669	724	800	
Cooler Tube Temperature (°C)	57	57	57	
Engine Speed (rpm)	1800	1800	1800	
Indicated Power (kW)	35.71	37.5	500	
Heat Input to Tubes*	2.68	2.45	2.12	
Heat Rejection*	1.25	1.13	0.79	
Pumping Loss*	0.18	0.13	0.18	
Drive System Power*	0.16	0.12	0.07	0.16
Auxiliary Power*	0.09	0.07	0.08	
Brake Power (kW)	28.58	31.56	432	398.6
Indicated Cycle Efficiency (%)	46.61	48.52	54.51	
Brake Efficiency (%)**	33.58	36.75	42.2	39.1

* Per Brake kW Output.

** 0.9 Combustor Efficiency Included

4.0 SMALL FREE-PISTON (37.5 kW) WITH HYDRAULIC OUTPUT (TASK 3 ENGINE)

4.1 Introduction

This section describes the design and analysis of a single-cylinder free-piston Stirling engine (FPSE), which provides 37.5 kW of power for stationary applications. Since existing FPSE single-cylinder designs are an order of magnitude smaller than the target size, a scaling algorithm is developed to allow use of proven design technology. The starting point for scaling was the optimum engine described in Section 2.0. After converting from kinematic to free-piston, the task effort concentrated on developing a matching hydraulic output system. A selection process resulted in development of a hydraulic pumping unit compatible with the output power characteristics of the FPSE. Performance curves for the engine, comparisons to the original Task 2 engine, and a description of the hydraulic system are included in this discussion.

4.2 Free-Piston Engine Size Scaling

The design of this FPSE engine was scaled from an existing engine system to generate the initial engine layout. Numerous scaling algorithms were reviewed; each had its particular advantages, capabilities, and limitations. However, four scaling algorithms, identified in Table 4.2-1, were considered for the definition of the initial 37.5 kW hydraulic free-piston engine. Finally, algorithm 1 was selected, since it provided the most direct scale-up in the range required. The sequence of the scaling and subsequent design refinement are laid out in Table 4.2-2. The algorithm was applied in Step 4 to generate the FPSE design that was then optimized by the same procedures applied to the kinematic optimum engine. The conceptual layout process described in Section 4.3 ensures that dimensional constraints (wall thicknesses, allowance for cooling flow, structural integrity) were properly taken into account.

4.3 Conceptual Layout - Engine

Although the engine design shown in Figure 4.3-1 was "scaled" from the optimized kinematic 37.5 kW engine of Section 2.3, the two engine layouts bear little geometric resemblance. The major differences between the designs are as follows:

- single-cylinder design (current FPSE's are all single-cylinder)
- gas springs to replace kinematic (crankshaft) linkages
- concentric regenerators and coolers rather than canister type (current FPSE state of the art)
- freedom of stroke rather than fixed piston stroke
- 37.5 kW power diaphragm to replace the engine rod seal
- additional dead volume to allow overstroke of displacer during power transients

TABLE 4.2-1

HYDRAULIC FPSE SCALING ALGORITHMS

Objective - Determine practical limits of scaling up a FPSE while maintaining constant efficiency.

D = Displacer H = Heater R = Regenerator C = Cooler

Case I Combined multiple cylinders into 1 cylinder

Add regenerator and coolers in parallel

Limit: Geometry

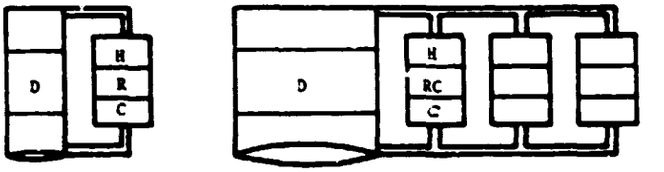

Area = X Area = NX

Stroke = Constant

Case II Curv Geometry and Operating Point (P, T, Frequency)

Hold constant component effectiveness

Hold constant losses/unit output

Limit: Scalable to single cylinders below 1 MW

Case III Multiple Scaling Factors

SF_1 = Engine Geometry

SF_2 = Heat Exchanger Dimensions

SF_3 = Number of Passages in Heat Exhanger

Limit Good only below 50 kW

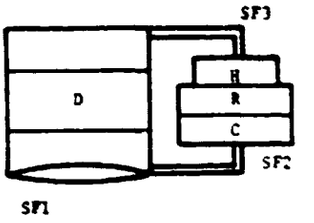

Case IV Geometry and Gas Spring Scaling

Geometry $\frac{P}{P_{ch}} = Y X^{1.8}$

$\frac{P}{P_{ch}}$ = Power Output Ratio

Y = Charge Pressure Ratio

X = Engine Geometry Factor

Limit: Tube transfer area and regenerator frontal area

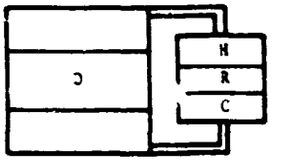

TABLE 4.2-2

37.5 kW FPSE SCALING PROCESS STEPS

	Engine Type	No. of Cylinders	Output	Comment
Start	Kinematic	4	37.5 kW	Optimum Engine, Section 2.3 (Task 1.2)
Step 1	Kinematic	1	9.375	Optimum Engine, Section 2.3 (Task 1.2) Per Cylinder
Step 2	Free-Piston	1	9.375	Nonoptimized
Step 3	Free-Piston	1	9.375	20 Percent Overstroke* and then Optimized (100 percent Stroke = 10.16 cm)
Step 4	Free-Piston	1	37.5	Combined Paralleled Heaters, Regenerators, Coolers
Step 5	Free-Piston	1	37.5	Optimized

*Overstroke is an extension of the piston amplitude beyond design to allow margin for transient conditions when amplitudes may exceed design.

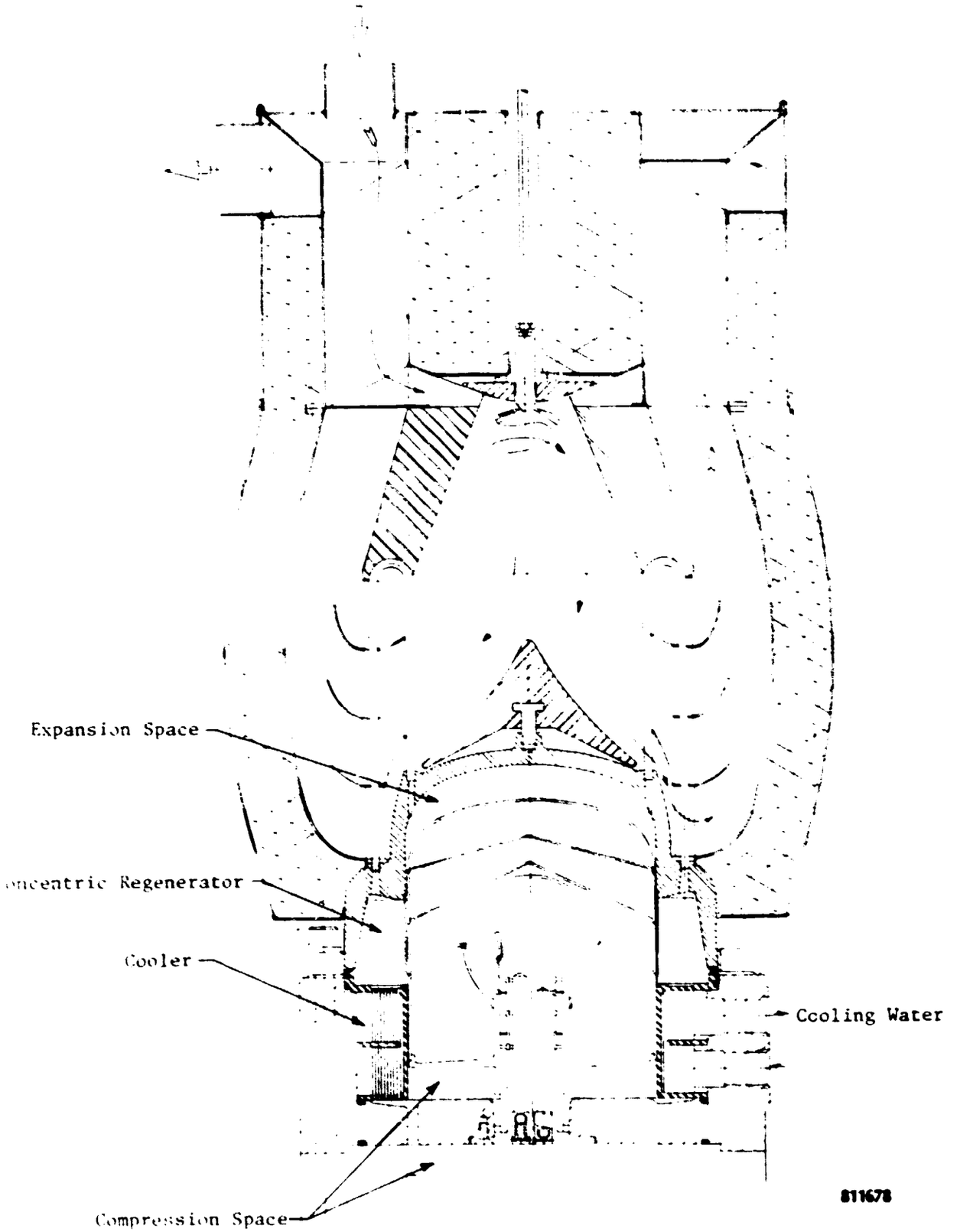

Fig. 4.3-1 37.5 kW FPSE w/Preheater and Combustor (Power Diaphragm Not Shown)

The design constraints and freedoms imposed during the optimization process are given in Table 4.3-1. This table contains a listing of the critical dimensions of the new engine and a comparison of the equivalent dimension in the optimum engine.

Additional features of the engine are:

- External Combustion System - The combustor developed in Section 3.2.3 was scaled down for use in this engine.

- Heater Head - A single row of heater tubes was found to be adequate. The tubes vector the working gas directly into the concentric regenerator.

4.4 Conceptual Layout - Hydraulic Motor

The output of the conceptualized 30-Hertz FPSE engine acts through a reciprocating metallic diaphragm. The power available at the diaphragm interface is approximately 33 kW. To convert this energy into hydraulic output, a new power conversion unit was designed to satisfy the following requirements:

- compatibility with FPSE power/frequency characteristics, i.e. stability

- maximum design efficiency

- 50,000-hour life

- manufacturability

- scalability

The selection process considered different versions of three hydraulic power unit families: vane type, piston type, and gear type. Eight preliminary layouts based on these schemes were generated. A listing of the schemes is given in Table 4.4-1.

An assessment of each scheme was conducted for mechanical constraints and performance qualities. Each performance attribute was given a weighting factor based on its relative importance. This process resulted in the selection of the cam-driven piston design shown in Figure 4.4-1. A list of diaphragm pump dimensions is given in Table 4.4-2 and the operating sequences for the pump are described in Table 4.4-3.

Some mechanical features of the hydraulic pump are given [illegible] .4-4. It is important to stress certain additional features of the system, namely:

- The chosen design has a high fill rate that requires a supercharging system. This can be achieved by pressurizing the supply tank or by use of some of the hydraulic pump output to provide a pressure head to the supply line.

TABLE 4.3-1

COMPARISON OF ENGINE GEOMETRY AND PERFORMANCE BETWEEN
37.5 kW FREE-PISTON ENGINE AND SECTION 2.3 KINEMATIC ENGINE

Engine Type		Free-Piston	Kinematic
Operating Condition			
Charge Pressure	bar	100	100
Maximum Cylinder Temp.	°C	704	704
Maximum Heater Tube Temp.	°C	724	724
Output	kW	37.5	37.5
Number of Cylinders		1	4 combined
Displacement	cm^3	1349.2	491.3
Displacer Dia/Cyl	mm	205.2	67.82
Displacer Area	cm^2	330.7	144.5
Displacer Amplitude	mm	20.4*	17.00
Displacer Rod Diameter	mm	60.04	13.54
Piston Amplitude	mm	27.7*	17.00
Phase Angle	°	45	90
Engine Speed	rpm	30 Hz	1800
Heater Tube I.D.	mm	5.63	3.0
Heater Tube O.D.	mm	7.87	4.2
Tube Effective Length	mm/tube	1069	224
Number of Tubes		65	88
Regenerator Frontal Area	cm^2	409	110.0
Regenerator Length	mm	44.1	45.6
Regenerator Wire Diameter	mm	0.05	0.05
Regenerator Filling Factor	%	23.1	25.56
Cooler Tube I.D.	mm	1.945	1.0
Tube Effective Length	mm	81.38	57
Number of Tubes		1600	1600
Heat Input @ Heater Tubes	kW	77.46	77.3
Indicated Cycle Efficiency	%	48.41	48.52
Brake Output	kW	36.0**	33.74***
Brake Efficiency	%	46.5	43.6***
Brake Efficiency with Combustor (90% Efficiency)	%	41.8	39.24

*With 20% overstroke
**Indicated power less power loss at the capillary tube and gas springs
***Indicated power less lower end drive friction only

TABLE 4.4-1

PRELIMINARY HYDRAULIC OUTPUT SCHEMES

CHOICES

VANE	PISTON	GEAR
Single	Stepped	Interrupted
Multi	Cam-Driven	
	Concentric	

SELECTED

Cam-Driven Piston

FEATURES

Stability
Simplicity
Efficiency
Scalability

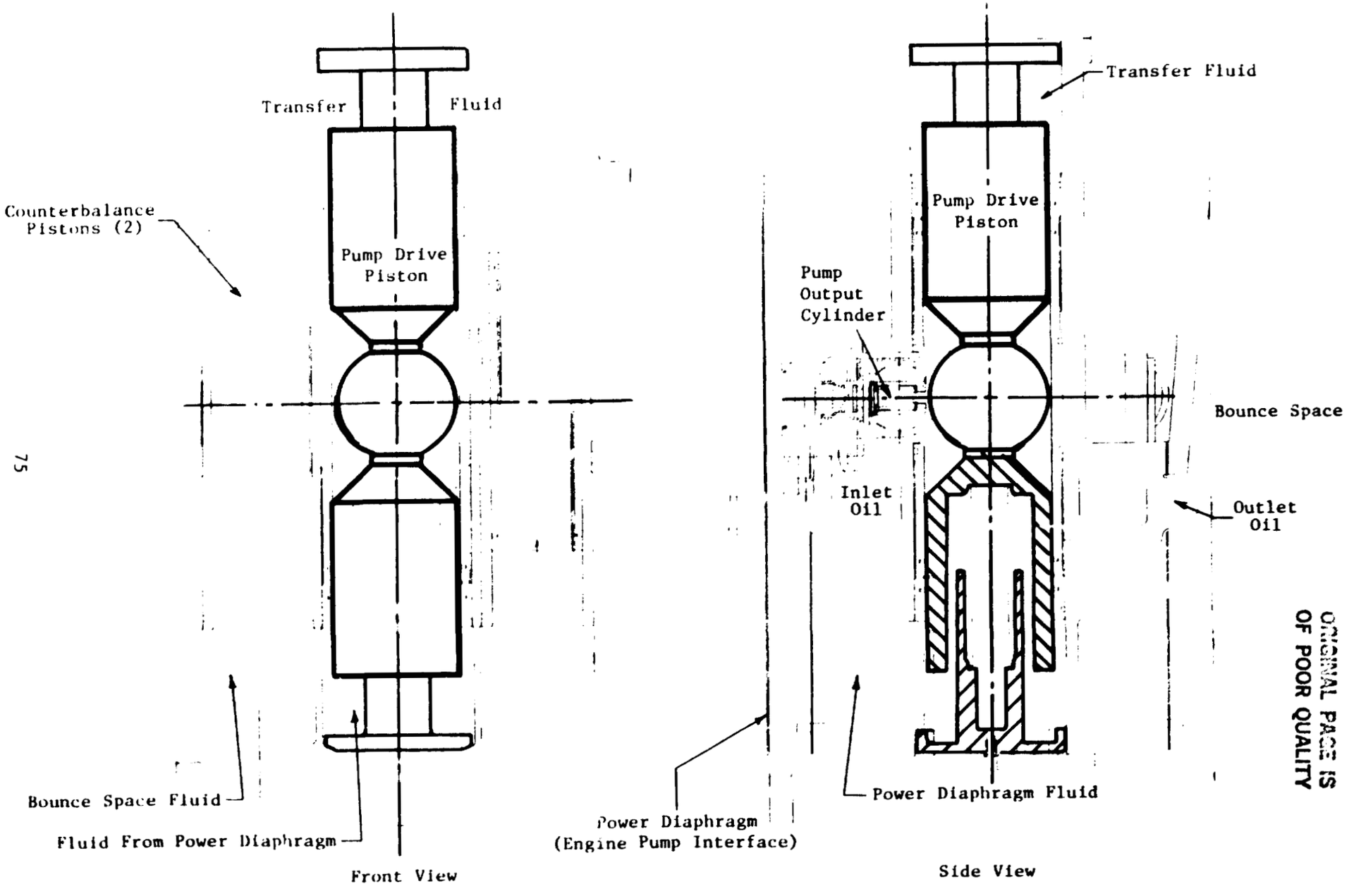

Fig. 4.4-1 37.5 kW FPSE Hydraulic Output

811679

TABLE 4.4-2

HYDRAULIC PUMP DIMENSIONS

Power Diaphragm Diameter	19 in.	48.26 cm
Pump Drive Piston Bore	4.3 in	10.92 cm
Pump Drive Piston Stroke	Variable	
Pump Output Piston Bore	1.125 in	2.85 cm
Pump Output Piston Stroke	Variable	
Overall Length	28 in.	71.1 cm
Overall Height	50 in.	127 cm
Width	23 in.	58.42 cm
Overall Volume	18.6 ft^3	526.7 ℓ

TABLE 4.4-3

HYDRAULIC PUMP OPERATING SEQUENCE

Start Action at Extreme Limit of Power Diaphragm	Effect
1. Power Diaphragm is displaced.	• Energy transferred to power diaphragm fluid forcing motion of Pump Drive Piston (PDP). • As PDP moves toward mid-point of stroke, four Pump Output Pistons move to decrease volume in pump output cylinders. Output fluid leaves cylinders at desired pressure. • As PDP moves away from mid-point, volume in the pump output cylinders increases. Check valves open to allow filling by supercharged input fluid.
2. Pump Drive Piston (PDP) is displaced.	• Incompressible fluid connections transfer some of energy through PDP to transfer fluid on other side. • Transfer fluid moves counterbalance pistons to offset inertia of PDP.
3. Counterbalance Pistons are displaced.	• Incompressible bounce space fluid responds to counterbalance piston movement by displacing another diaphragm against a gas spring (compressible fluid).
The bounce space now has stored the energy not absorbed going through the pump. The power diaphragm, having passed one-half amplitude, is now being displaced by a negative pressure differential across it (engine pressure lower than pump pressure). The bounce space pressure becomes the highest in the system and the gas spring diaphragm begins to move.	
4. Gas Spring Diaphragm is displaced.	• Bounce space fluid moves two counterbalance pistons
5. Counterbalance Pistons move.	• Transfer fluid acts upon pump drive piston. • Pump output pistons, pump until mid-stroke point of PDP. • After mid-point, pump output cylinder volume decreases; filling process.
6. PDP motion.	• Transferred via power diaphragm fluid to power diaphragm. Process repeats.

TABLE 4.4-4

IMPORTANT FEATURES OF FPSE HYDRAULIC PUMP

- One FPSE Cycle → One Hydraulic Pump Drive Piston Cycle → Two Hydraulic Pump Output Cycles, i.e., 30 Hz input frequency → 60 Hz output frequency
- Incompressible fluid transfer energy with minimum losses.
- Three Separate Fluid Volumes:
  - Power Diaphragm Volume (power diaphragm to pump drive piston).
  - Transfer Fluid (pump drive piston to counterbalance pistons (2)).
  - Gas Spring Fluid (counterbalance pistons to gas spring diaphragm).
- Power transfer fluids are not part of output flow system. They are a separate self-contained system.
- Four output pump pistons which balance loads on pump drive piston globe (3-dimensional cam) for long life and low wear.
- Two diaphragms.

- The dynamics of the chosen pump design provide a stable interaction with the Stirling engine, i.e. the rate of change of pump power demand as a function of stroke is greater than that of the engines output. Thus, a change in stroke (whatever the cause, i.e. drop in engine power, etc.) produces a reaction driving the system to the stabilized operating point. See Figure 4.4-2.

4.5 Cycle Analysis and Optimization

The requirement that the FPSE engine be as comparable as possible with the optimum kinematic engine was satisfied by applying the chosen scaling process to one cylinder of the optimum engine. This starting point was used in the five-step process, shown in Table 4.2-2, to achieve an optimized engine. The optimization process of Step 5 produces a final pressure and temperature very close to the base kinematic optimum engine. Hence, the same operating parameters were chosen. The results of this final optimization are given in Table 4.5-1, which compares the FPSE to all 37.5 kW kinematic engines developed in this study.

- Similarities

  - operating temperature
  - mean pressure
  - frequency

- Differences

  - Larger displacement in FPSE. This is required to provide overstroke margin (20 percent) to prevent displacer contact during transients, to provide space for the displacer gas spring volume and to provide space for gas to distribute across the face of the power diaphragm. The gas volume for these needs increases dead volume and, thus reduces engine pressure amplitude, which must be offset by an increase in total engine displacement.

  - Higher drive power required for the FPSE. This is counterbalanced by the fact that a hydraulic pump is included. To be consistent, a hydraulic pump would need to be added to the optimum kinematic engine drive system. This would raise its drive power requirements by approximately 3 kW.

4.6 Hydraulic System

A full hydraulic system utilizing the FPSE/hydraulic pump design as a component is shown in Figure 4.6-1. This system drives a hydraulic motor at a location remote from the engine/pump. The motor output is considered to be a rotating shaft. The chosen configuration provides a consistent basis for comparing the FPSE/hydraulic pump with the optimum kinematic engine. A typical application for the system might be in earth-moving or loading equipment. Other applications include fluid pumping through pipelines or within industrial facilities. Use of the hydraulic motor includes the potential for application in a motor vehicle, such as a car, truck, bus or for military purposes, such as a tank.

While effort to define a full control unit for this system was not in the scope of this task, the control valve "G" and motor "H" of Figure 4.6-1 must be linked to the engine unit "D" for the system to respond to varying power demands.

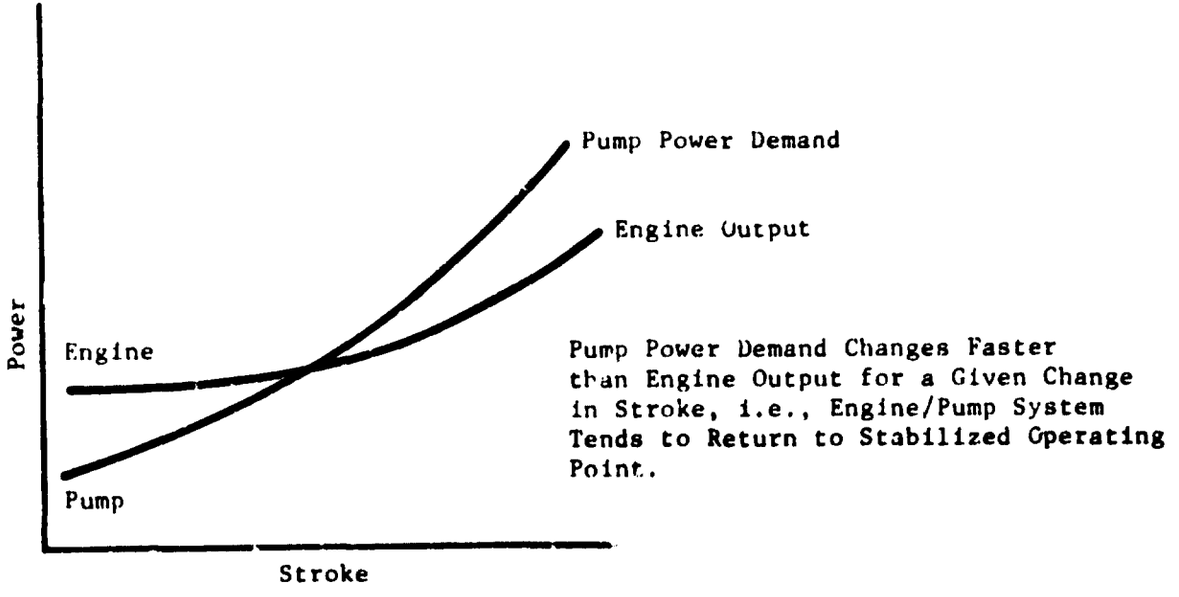

Fig. 4.4-2 FPSE/Hydraulic Pump Stability

TABLE 4.5-1

PERFORMANCE SUMMARY OF 37.5 kW ENGINES

SECTION		2.2	2.2	2.3	2.3	4.0
Type		Reference		Optimized	Reference	Diaphragm Free Piston
Working Fluid		H_2	He	H_2	He	He
Temperature Heater	°C	669	669	724	724	724
Temperature Cylinder	°C	649	649	704	704	704
Temperature Cooler	°C	57	57	57	57	57
Pressure	Bar	123	123	100	100	100
Speed	rpm	1800	1800	1800	1800	30 Hz
Displacement Engine	cm^3	452.68	452.68	486.67	491.30	1349.29
No. of Cylinders		4	4	4	4	1
Indicated Power	kW	37.5	35.71	37.5	37.5	37.5
Auxiliary Power	kW	2.25	2.25	2.15	2.15	2.15
Drive Power	kW	4.64	4.64	3.8	3.8	4.86
Brake Power	kW	30.61	28.82	31.56	31.56	30.49
Indicated Efficiency	%	48.34	46.61	50.7	48.52	48.41
Combustion Efficiency	%	90.0	90.0	90.0	90.0	90.0
Brake Efficiency	%	35.51	33.87	38.44	36.75	35.41
Heater Head Material		12RN72	12RN72	In-625	In-625	In-625
Cylinder Material		XF-818	XF-818	713-LC	713-LC	713-LC
Heat Input	kW	86.2	85.09	82.1	85.9	86.1
bsfc	kg/kW	0.24	0.25	0.22	0.23	0.23
Torque	Nm	162.2	152.7	167.2	167.2	–

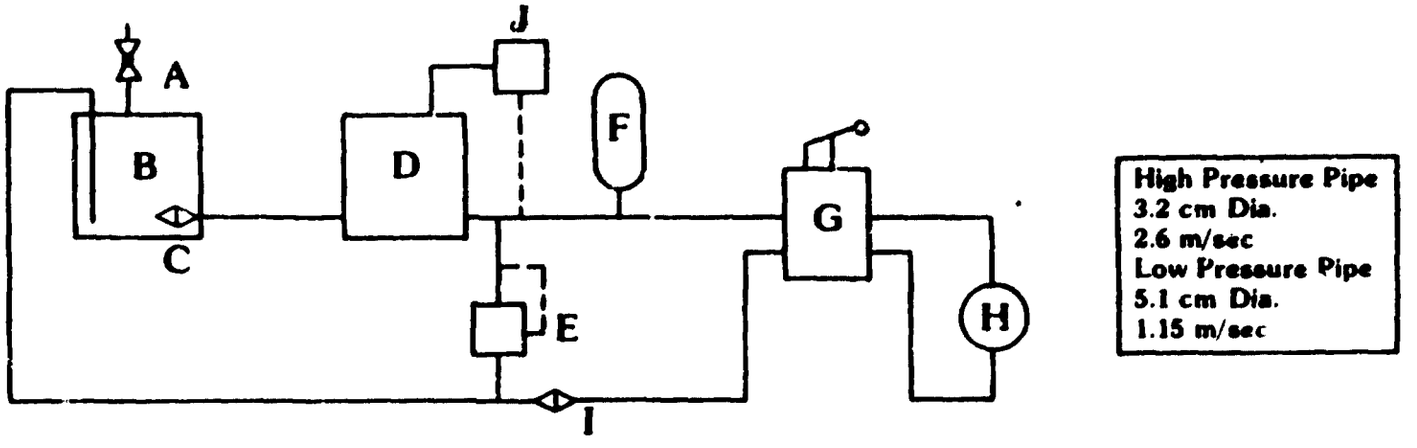

Legend

A	Pressurized Air (8 bar) Source with Check Valve
B	Reservoir (Cooler Optional)
C	Strainer
D	Engine/Pump Unit
E	Pressure Relief Valve
F	Accumulator
G	Control Valve - Start, Stop, Hold, Modulate, Reverse
H	Reversible Motor
I	Filter
J	Unloading Valve - Idles Engine Until Demand

Fig. 4.6-1 Hydraulic System

4.7 Performance Maps

A set of performance curves (Figures 4.7-1 through 4.7-6) were generated for three different levels of cylinder head temperatures (592°C, 704°C, and 836°C) and cooler temperatures (27°C, 57°C, and 87°C). The FPSE engine described in this section varies in frequency directly as the square root of charge pressure.

The result of this pressure to frequency interaction is shown in the behavior of the efficiency lines. While cycle efficiency was essentially insensitive to pressure changes in the kinematic engine, efficiency shows a significant drop-off as pressure increases on the FPSE system. This is a result of the increase in frequency which increases pumping losses. The kinematic engine holds constant speed as pressure increases and does not suffer this frequency (speed) related loss. The effect could be diminished by controlling the displacer dynamics, through the control of the displacer spring or damping to maintain near-constant frequency.

4.8 Comparison with Kinematic Engines (See also Section 2.0)

Table 4.5-1 provides a summary of operating point characteristics for all 37.5 kW output machines covered by this study. Comparison is limited to size and efficiency considerations especially since working fluid, indicated power, and materials are the same for the optimum engines. A further comparison is made on the following items:

- Control systems
- Seal life
- Ease of manufacture
- System-to-system comparison

4.8.1 Control Systems

Stirling engine control systems are a currently developing technology. In kinematic Stirling engines, the mean pressure control system (Reference 5) has been proven effective in the highly transient automotive application. The system, however, is complex. A stationary Stirling engine could use a simplified version of this system.

The FPSE engine/hydraulic pump would require development of a control system suited to the intended application. Such a system would integrate the combustor, engine, pump, and motor to handle transient requirements and to maintain stability. Start-up, shutdown, and emergency procedures would be included in the system plan.

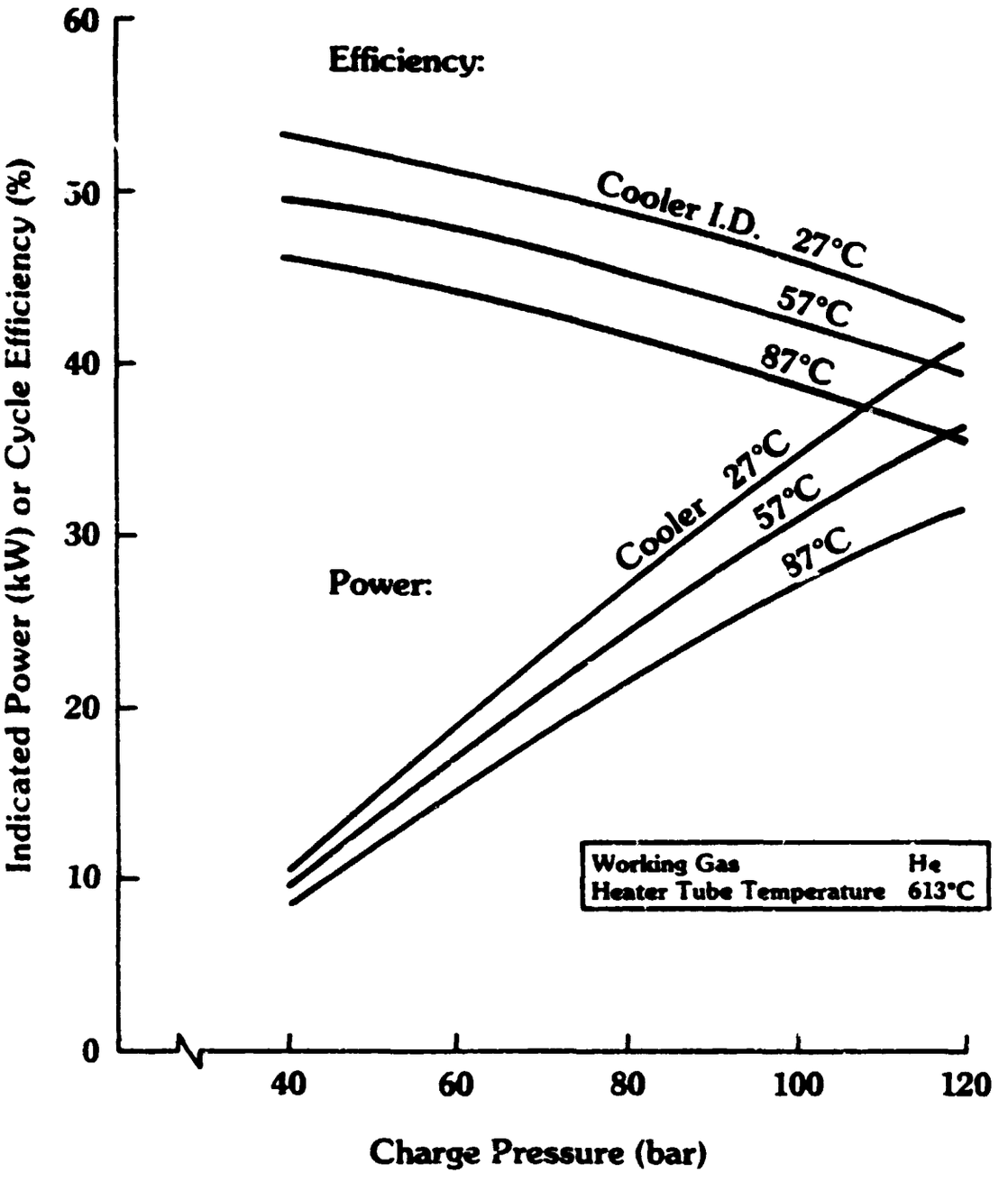

Fig. 4.7-1 37.5 kW FPSE Performance @ 593°C Cylinder Temperature

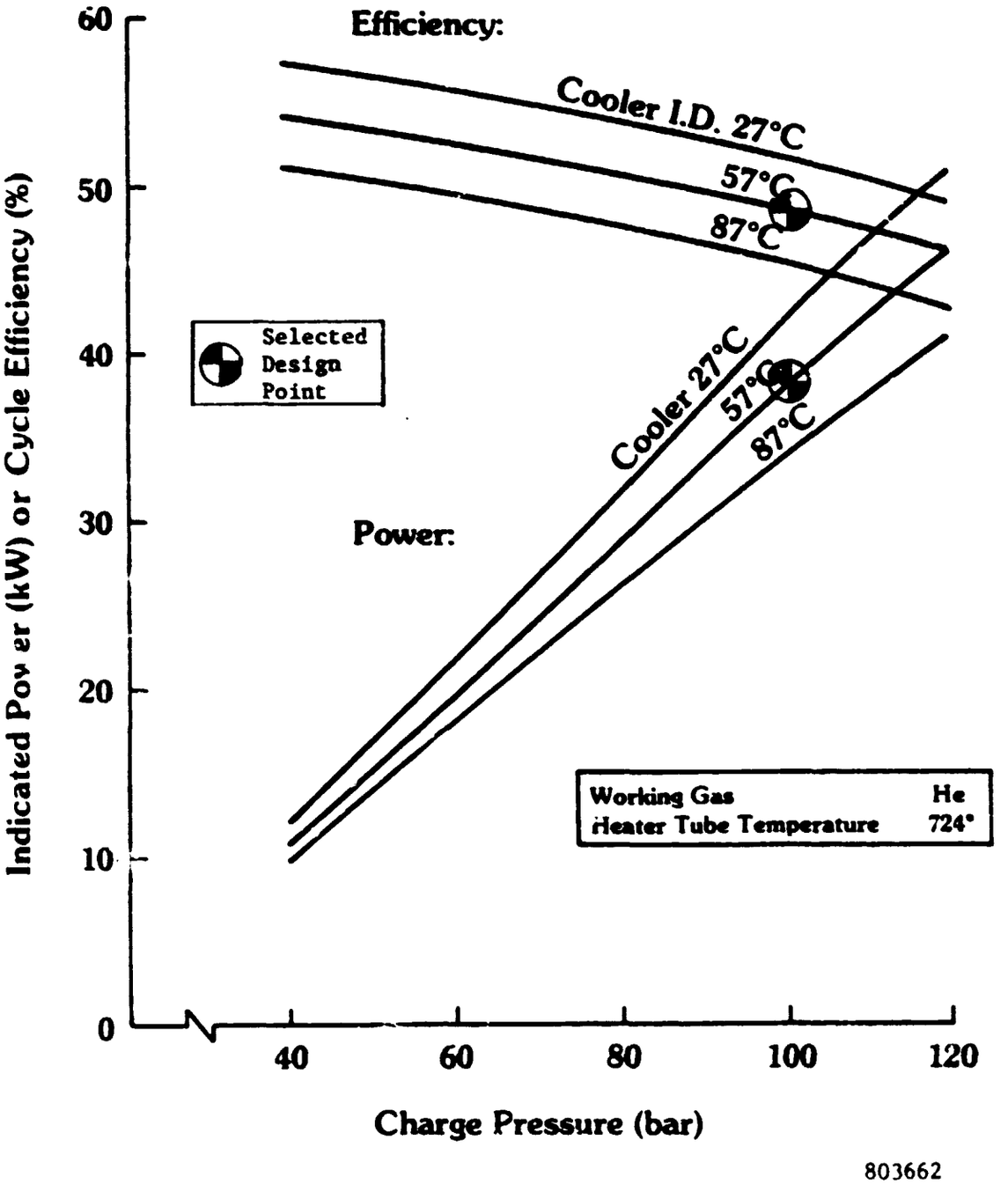

Fig. 4.7-2 37.5 kW FPSE Performance @ 704°C Cylinder Temperature

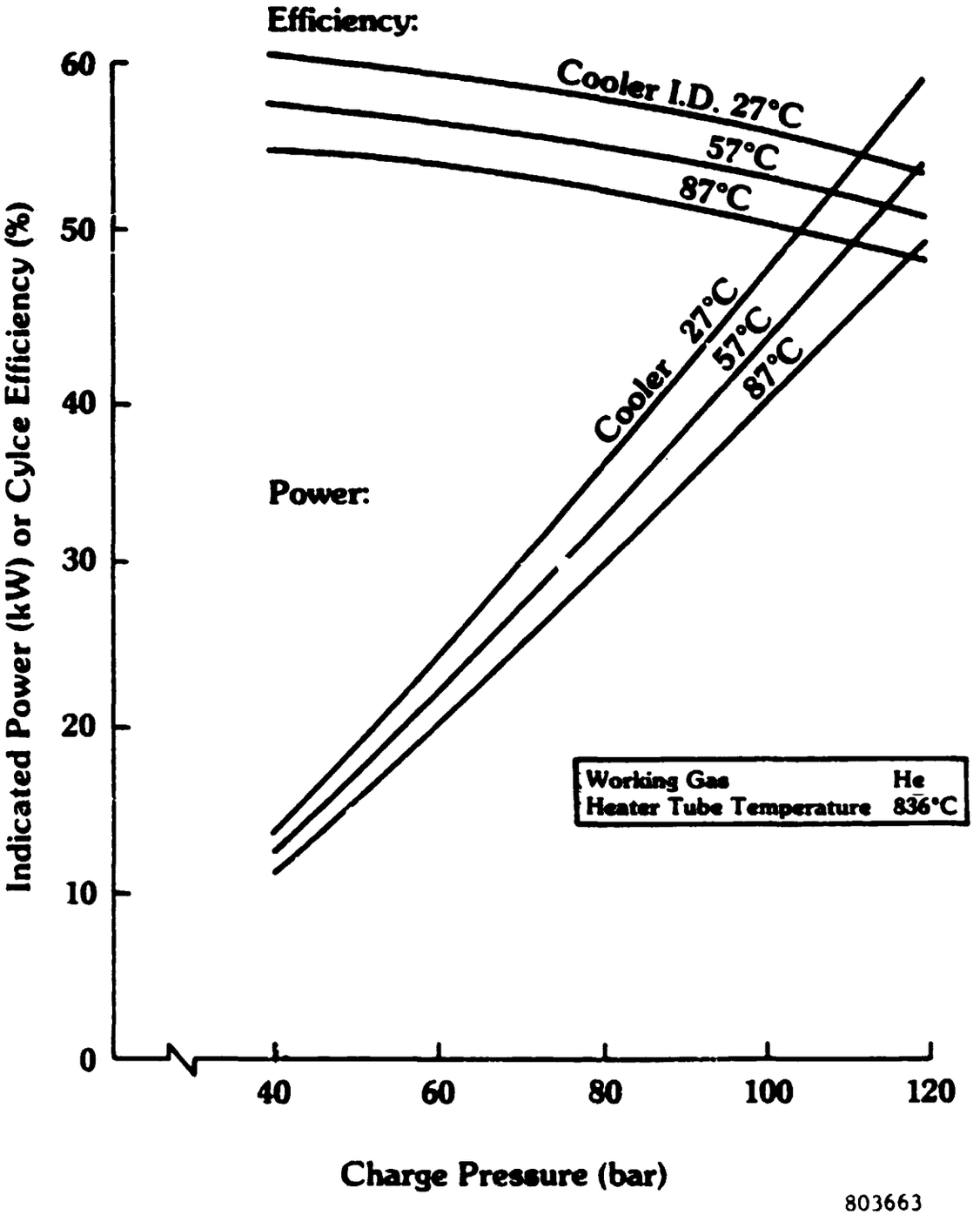

Fig. 4.7-3 37.5 kW FPSE Performance @ 816°C Cylinder Temperature

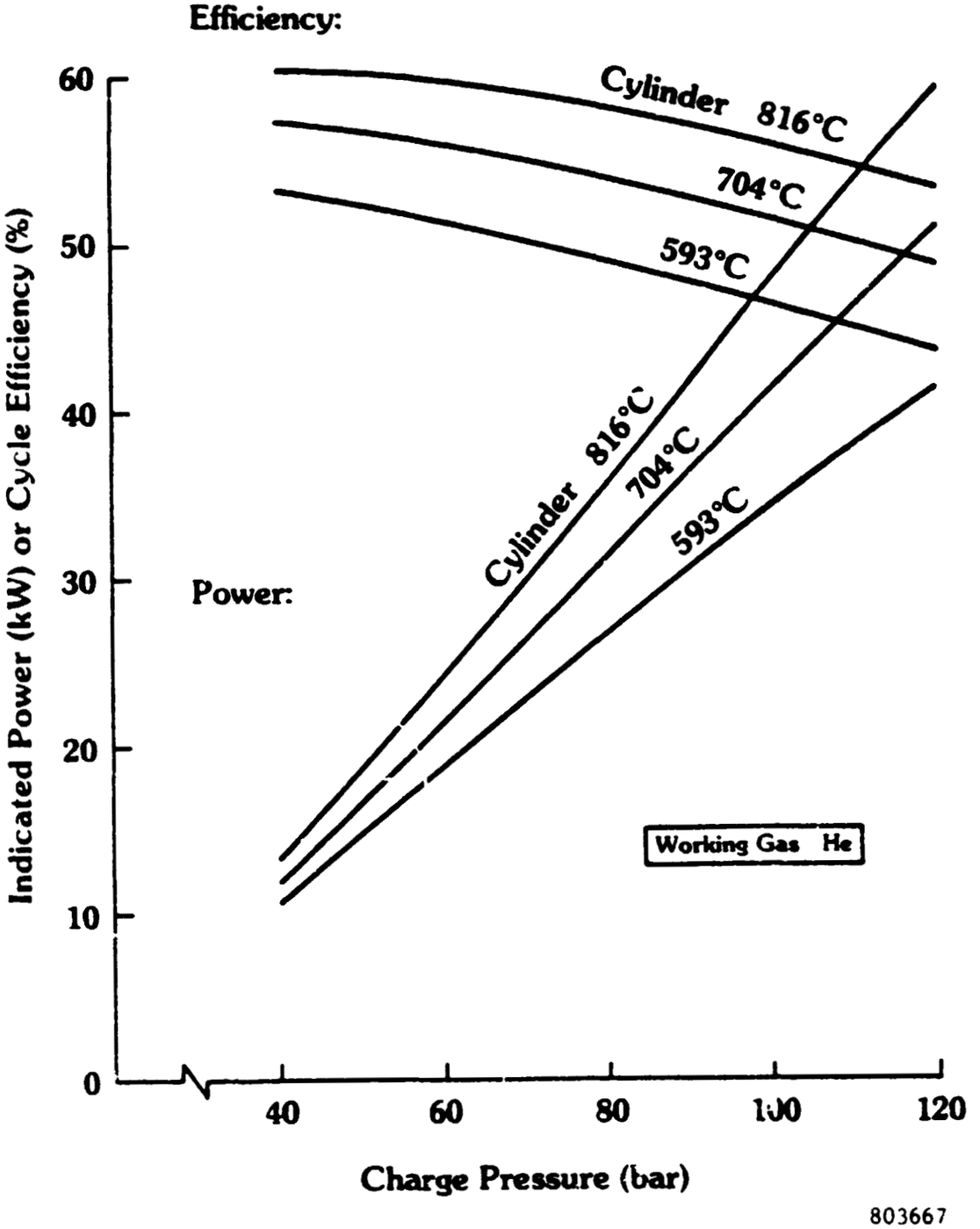

Fig. 4.7-4 37.5 kW FPSE Performance @ 27°C Cooler I.D. Temperature

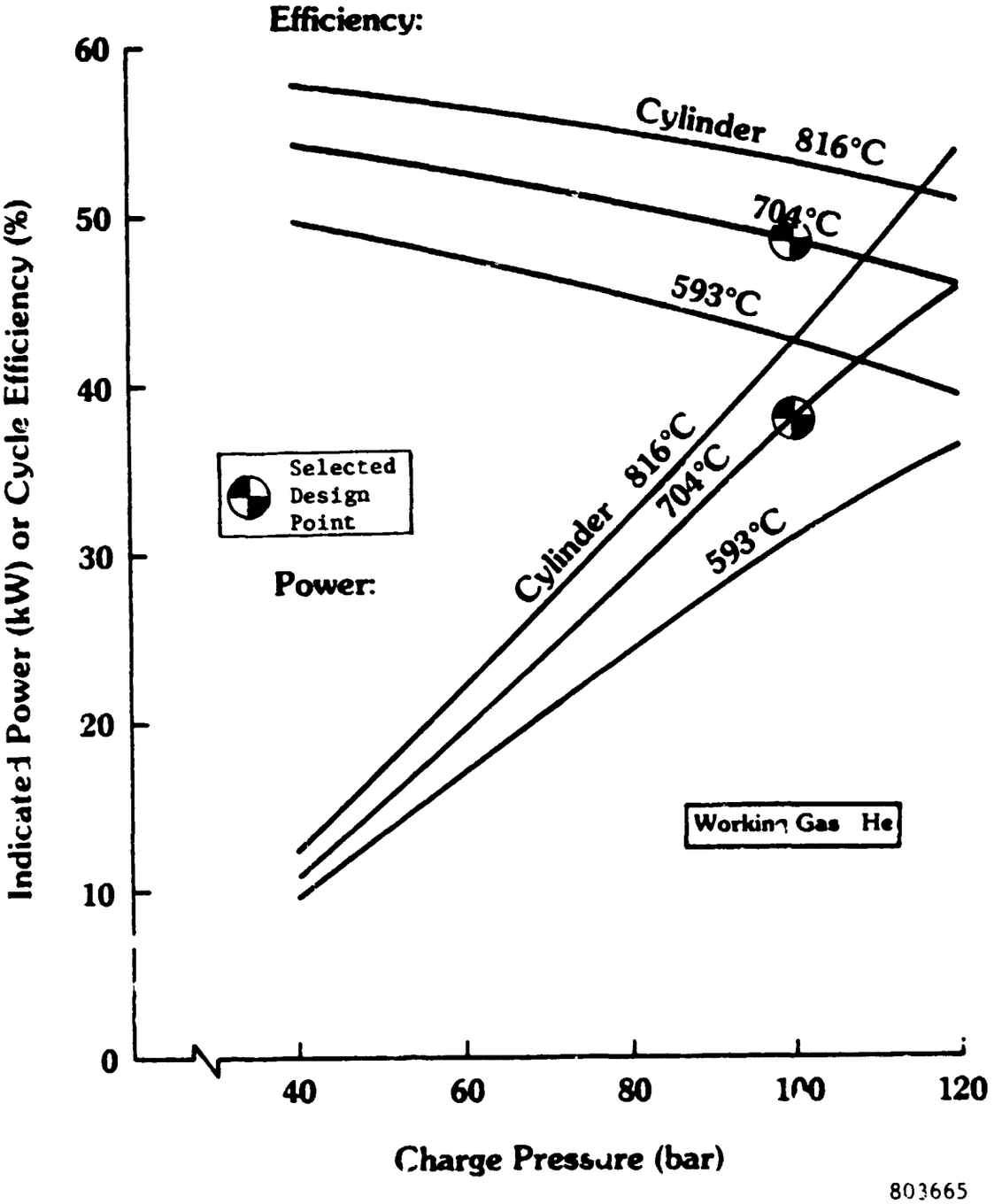

Fig. 4.7-5 37.5 kW PSE Performance @ 57°C Cooler I.D. Temperature

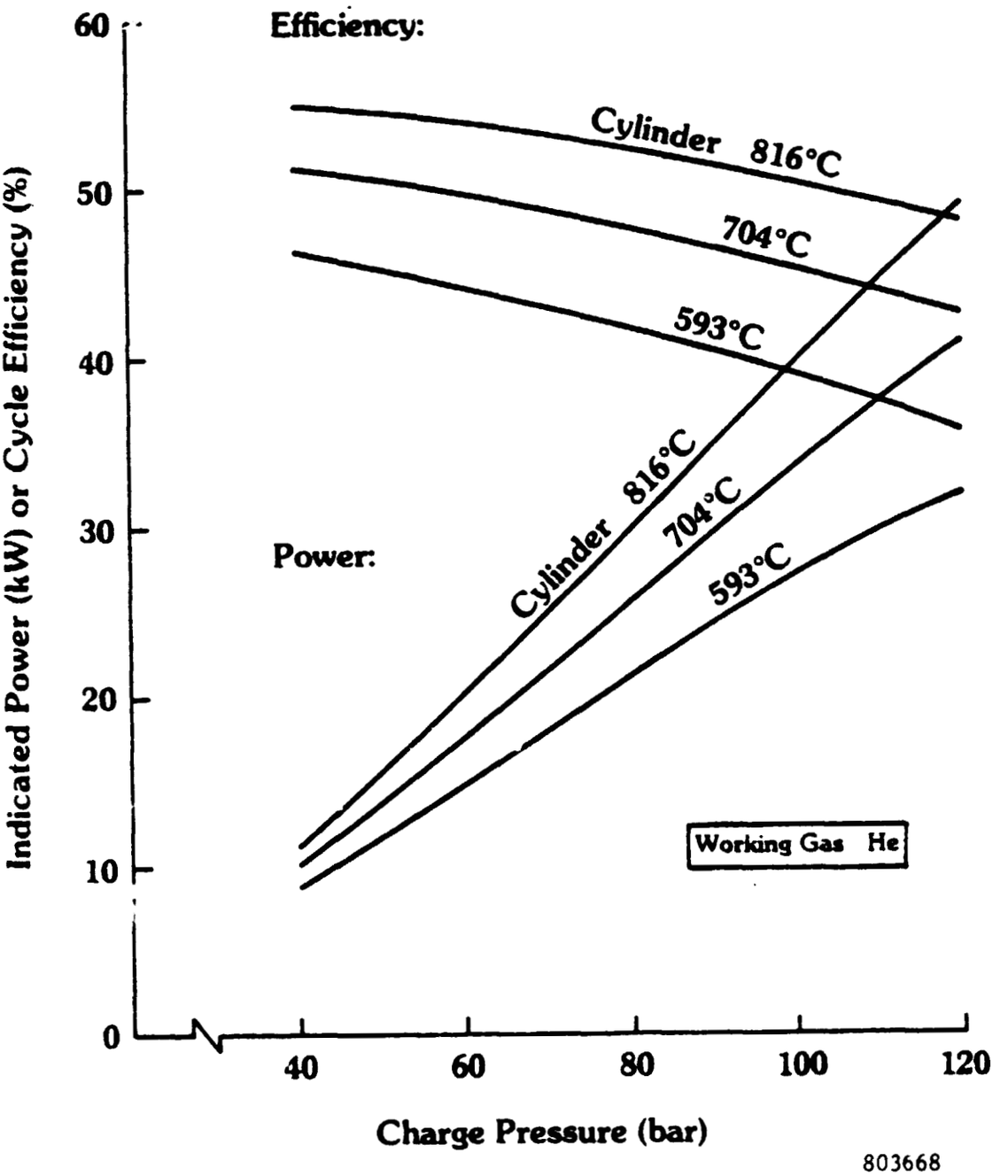

Fig. 4.7-6 37.5 kW FPSE Performance @ 87°C Cooler I.D. Temperature

4.8.2 Seal Life

The kinematic engine portion of the study proceeded on the assumption that the lower piston speed and steady-state operation of a stationary engine would extend seal life to the 50,000-hour life. The rod seals must withstand very high pressure differentials while allowing relative motion between the seal and the connecting rod. The piston seals, separating the expansion and compression volume, experience significantly lower pressure differentials, but both sets of seals are susceptible to damage and wear. There is a minimum of four of each type of seal in a kinematic engine and the loss of one would seriously affect engine performance.

The single-cylinder, diaphragm free piston engine eliminates these seals. The rod seal is replaced by a flat oil-backed power diaphragm. Such diaphragms are presently used in very high frequency compressors. Recent experimental work at MTI aimed at evaluating the high cycle fatigue capabilities of such diaphragms has been very encouraging. The piston seal is replaced by a non-contacting displacer clearance seal. The ability to use a clearance seal is based on the fact that the pressure across the displacer in a displacer-type engine is approximately ten percent of that across the piston in a Rinia engine. The reduction in pressure differential is critical since clearance seal loss varies as the square of the differential.

4.8.3 Ease of Manufacture

The two engines offer different routes to ease of manufacture. The kinematic engine will benefit from its commonality with an established automotive engine production line and mass production techniques. The FPSE benefits from a simpler overall design and fewer parts. The heater head is substantially simpler, having eliminated the hot-conduit manifold, however, the FPSE requires a gas-spring-displacer-support system. The tighter tolerances required in the gas spring hardware offset some of the benefits of the overall, simpler FPSE design.

4.8.4 System-to-System Comparison

Table 4.8-1 summarizes a comparison of the two engines for specified types of output. Rotary or hydraulic fluid output, conversion of kinematic drive shaft output to hydraulic flow through a pump, or conversion from hydraulic flow to remote rotary fluid through a motor were considered.

4.9 Summary

The results of this effort are:

- A scaling algorithm was used to allow one cylinder of an essentially proven kinematic design to be upsized by a factor of 4 into a free-piston unit.
- The dynamics of using a power diaphragm rather than a power piston were found acceptable in the conceptual design process.
- A hydraulic pump was designed which matched the output characteristics of the FPSE, thereby providing stability and a readily [illegible] hydraulic output.

TABLE 4.8-1

BRAKE POWER AND EFFICIENCY FOR ALTERNATE OUTPUT DRIVE SYSTEM - 37.5 kW ENGINES

	Kinematic		FPSE	
Location/Output	Power	Efficiency	Power	Efficiency
At the Engine: Rotary Shaft Output	31.56 kW	36.75%		
Hydraulic Fluid Output			30.49 kW	35.4%
Convert Kinematic* to Hydraulic Flow Through Hydraulic Pump	29.04 kW	33.81%		
Convert Hydraulic** Flow to Rotary Motion Remote from the Engine Through a Hydraulic Motor	27.59 kW	32.11%	28.97 kW	33.63%

* Hydraulic pump assumed 92 percent efficiency.

** Hydraulic motor assumed 95 percent efficiency.

- Using He gas, brake efficiency for the resultant FPSE engine is 35.4 percent with hydraulic output and 33.6 percent with rotary output.

Efficiency and power levels for the free-piston unit essentially matched those of its kinematic counterpart, i.e., the optimum engine of Section 2.3.

5.0 400 kW Free-Piston Engine with Hydraulic Output (Task 4 Engine)

5.1 Introduction

In an attempt to more clearly define the size limitations associated with free-piston engines, a 400 kW design was explored. The resulting engine design was derived by scaling the engine thermodynamics from the 400 kW kinematic design described in Section 3.0. A four-cylinder configuration was used to provide the same per-cylinder power output as the kinematic design and to allow the use of a single hydraulic synchronization and balance system.

5.2 Conceptual Layout - Engine

Three potential conceptual design routes were considered:

- Totally new single-cylinder design.
- Scale-up of Section 4.0 engine 37.5 kW diaphragm free piston (an order of magnitude increase).
- Conversion of Section 3.0 engine 400 kW kinematic to FPSE (four-cylinder, 400 kW engine).

With the knowledge obtained in the development of a satisfactory hydraulic output system, the third route was selected as the most direct, i.e., the 400 kW kinematic engine was converted from a Rinia-type engine to a four-cylinder displacer-power-diaphragm device. The impact of this conversion on a number of engine dimensions is given in Table 5.2.1.

The adapted design, designated as a multi-cylinder, dynamically balanced, hydraulically linked free-piston Stirling engine design is shown in Figure 5.2-1, and has the following features:

- Smooth application of power to the hydraulic output system, four smaller sequenced power strokes rather than one large power stroke.
- Balanced displacers and pistons. Moving in two parallel planes, the displacers and pistons cancel any induced axial forces and moments, thus eliminating the need for other engine balancing systems. A two-cylinder unit would not provide the equivalent benefit - it would be balanced axially, but would still have a rocking couple.
- Self-Synchronizing. The four power diaphragms were linked together using a noncompressible working fluid in the hydraulic pumping section of the engine. This nonmechanical, but yet essentially fixed hydraulic linkage forces the work out of each cylinder and simplifies the control system of the engine, i.e., no one cylinder can "run away" or "act out of phase" with the others.

5.3 Conceptual Design - Hydraulic Pump

The hydraulic pumping system developed for the 400 kW engine is a modified version of the unit designed under Section 4.0. It is scaled up in size and connected in such a way to synchronize the engine and pump units.

TABLE 5.2-1

COMPARISON OF 400 kW KINEMATIC AND FREE-PISTON ENGINES

	Kinematic (Sec. 3.0)	FPSE w/Overstroke (Sec. 5.0)
Mean Pressure Bar	120	120
Max. Cylinder Temp. °C	704	704
Max. Heater Tube Temp. °C	724	724
Output kW per cylinder	125	125
Displacer Dia. mm	201.74	222.31
Displacer Amplitude mm	23.81	28.572
Displacer Rod Dia. mm	42.028	46.313
Piston Amplitude mm	23.81	38.513
Phase Angle	90°	45°
Engine Speed rpm	1800	1800
Heater Tube I.D. mm	3.316	3.647
Heater Tube O.D. mm	4.642	5.106
No. of Tubes	218	219
Tube Effective Length mm	252.5	250
Regenerator Area cm^2	356.25	457.18
Regenerator Length mm	53.718	42.572
Wire Dia. mm	0.0762	0.0762
Porosity %	65.91	60.83
Cooler Tube I.D. mm	3.945	3.945
Effective Length mm	119.	119.
No. of Tubes	400	400
Indicated Eff. %	52.416	50.76

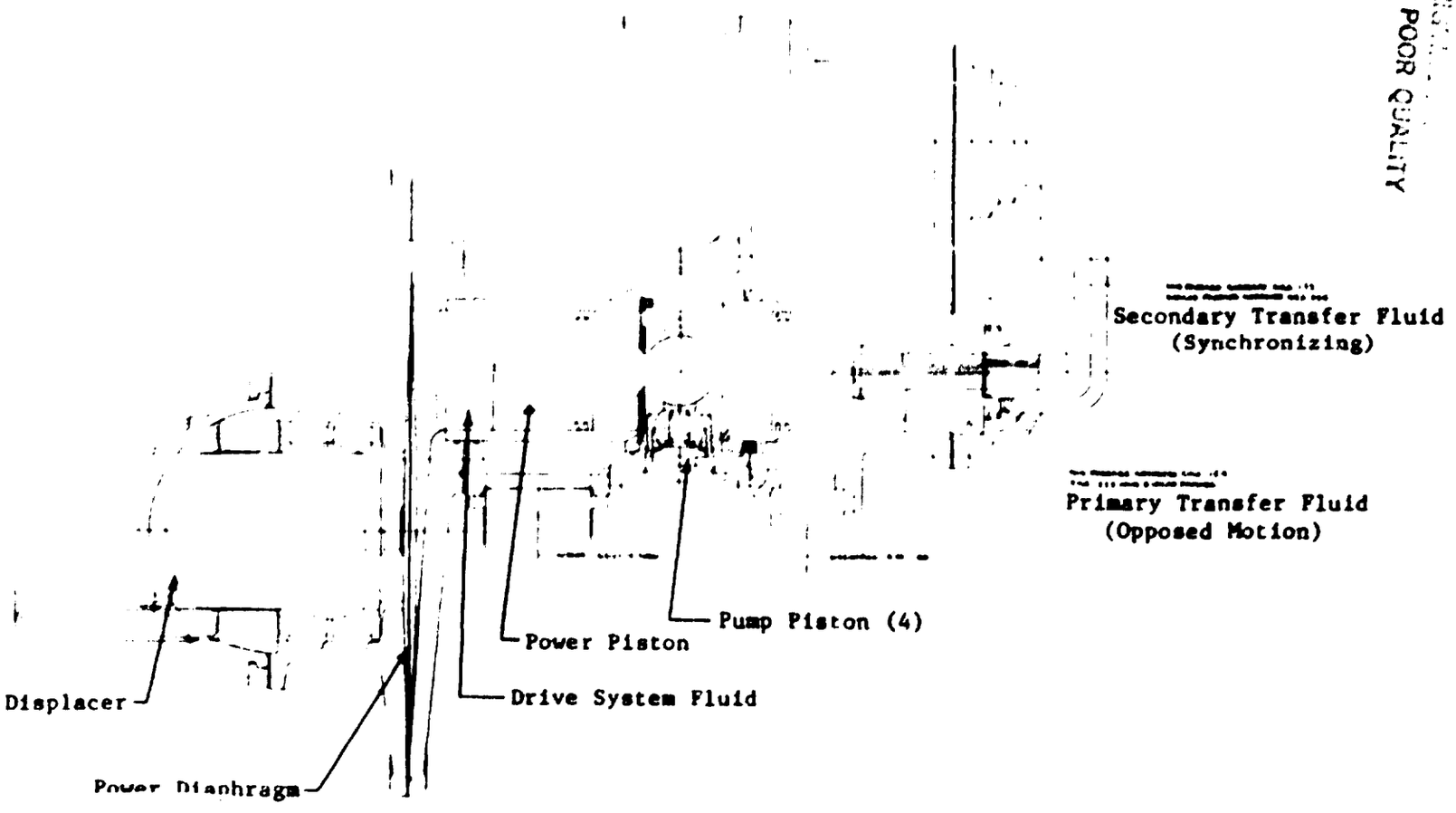

Fig. 5.2-1 400 kW FPSE With Hydraulic Output (71.9 L/SEC. @ 20.7 MPA)

The features of this overall pump design include:

- Simplified design. Relative to the pump design generated in Section 4.4, the modified design changes the pumping volume from the outside face of the four-pump piston to the volume between the pump piston and the drive piston. This allows the use of one large ring valve for each pump.

- Smoother pumping of output fluid with four pump actions per engine stroke rather than two for the single-cylinder design.

- Minimum scaling. This new design requires a scale up by a factor of four rather than ten (as would be the case with a single-cylinder 40 kW unit).

- No counterbalancing needed. As with the engine, the motion of the four pump drive pistons eliminates any system couples and, hence, the need for counterbalancing pistons (as would be the case with the Section 4.0 design). Each pump unit, with four pump output pistons, acts to counterbalance loads on each piston drive pump extending pump life.

- Separate but not incompatible fluids. As in the Section 4.0 pump system, an essentially permanent work transfer fluid is used to transfer energy from the power diaphragms to the working pumps. The fluid may be the same as the actual output fluid, or, if that is not feasible, the fluid may be optimized for the pump application. The key consideration is the criticality of any leakage or contamination. As it is, all moving components are exposed to a fluid presumed to have good lubricating, heat transfer, and wear properties. Seal degradation with time is not as critical as the case of the dry seals in the kinematic Stirling engine.

- Elimination of gas spring. The multi-cylinder incompressible fluid/counterbalance design of this unit eliminates the need for the piston gas spring used in Section 4.0 FPSE's. Instead, the displacement of one diaphragm/pump piston stroke is directly returned to an adjacent pump piston unit. Figure 5.3-1 illustrates further the hydraulic linkages between the four pump units. The primary transfer fluid provides balancing between piston numbers 1 and 4, as a set, and numbers 2 and 3. To keep the two pairs of pistons synchronized, an additional link, a secondary transfer fluid. is established between numbers 1 and 2, as a pair, and numbers 3 and 4.

5.4 Cycle Analysis and Optimization

The design process was performed via the steps outlined in Table 5.4-1. Materials were unchanged. The given four-cylinder kinematic engine was first considered as a single-cylinder, 125 kW unit. Analytically, the engine was then converted to a free-piston unit of the same size. Dead volume was increased to allow for the 20 percent displacer overstroke condition that can exist in FPSE's during transient operation. Finally, the single 125 kW was recombined to form a four-cylinder package of the desired size. The close thermodynamic relationship and material commonality with the 400 kW kinematic engine concluded the optimization point would not shift significantly. So, the optimization was omitted in this case. However, gains in efficiency can still be expected.

TABLE 5.4-1

400 kW FPSE - SCALING PROCESS

	Engine Type	No. of Cylinders	Indicated Output	Comment
Start	Kinematic	4	500 kW	400 kW Kinematic (Section 3)
Step 1	Kinematic	1	125 kW	400 kW Kinematic (Section 3)
Step 2	Free-Piston	1	125 kW	No overstroke
Step 3	Free-Piston	1	125 kW	20 percent overstroke
Step 4	Free-Piston	4	500 kW	Combined - Not final optimized

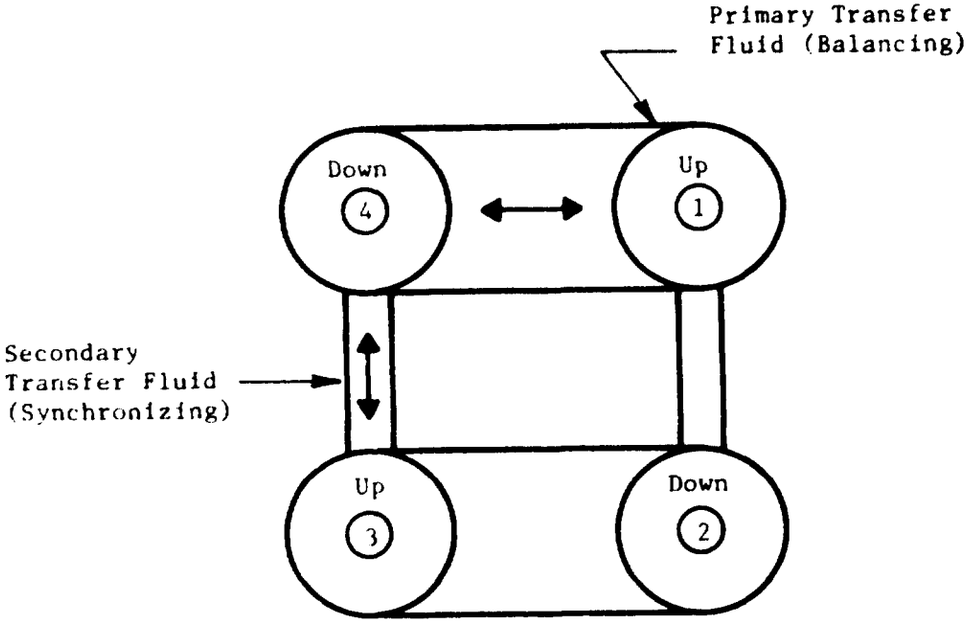

Fig. 5.3-1 Hydraulic Linkage Between Pumping Units

Table 5.4-2 lists the cycle results for the combined FPSE and compares the results to the optimized engines of Section 3.0; the closest comparison exists between the He working fluid, Inconel-625 version. Engine displacement has increased approximately 50 percent due to the need for 20 percent overstroke and volume requirements to mate with the four power diaphragms.

Estimates for auxiliary and drive power, both of which exceeded the levels of the kinematic version, resulted in a minimal decrease in brake output and brake efficiency. The anticipated heat input requirement indicates the combustion and cooling systems as sized for the kinematic version would be suitable for the free-piston engine.

5.5 Free-Piston and Kinematic Engine Comparison with Alternative Output Drives

Only a limited comparison was accomplished between the two large engines of this study. In terms of application, i.e., use of either engine for pumping or rotary power needs, the results are summarized in Table 5.5-1. Once again, as in Section 4.0, the two engine designs are sufficiently close that the efficiency advantage changes with application.

5.6 Summary

In this study, a conceptual design was developed that achieved an output exceeding 400 kW using a multiple-cylinder free-piston engine driving a hydraulic pumping unit. This conceptual design, by nature rather than size, uses a unique, simple, and compact balance and synchronization system.

Performance levels were estimated to be competitive with the kinematic version upon which the conceptual design was based. Since a full optimization of the FPSE was not accomplished, the performance advantages of the kinematic engine over the free-piston, if any, are not quantified in the higher power class.

In order to achieve the operation and efficiency of the engine unit, the proposed matching hydraulic pumping system was considered necessary. The pumping system concept described under this program offers simplicity, compatibility, and efficiency to mate ideally with FPSE's. It is, however, a new design requiring further design development.

TABLE 5.4-2

STATIONARY STIRLING ENGINE STUDY PERFORMANCE SUMMARY - 400 kW

SECTION		3.0	3.0	3.0	5.0
Type		Kinematic	Kinematic	Kinematic	FPSE
Working Fluid		H_2	He	He	He
Temperature Heater	°C	800	800	724	724
Temperature Cylinder	°C	780	780	704	704
Temperature Cooler	°C	57	57	57	57
Pressure	bar	150	150	120	120
Speed	rpm	1800	1800	1800	30 Hz
Displacement Engine	cm^3	4915.77	5400.66	6088.68	8872.35
No. of Cylinders		4	4	4	4
Indicated Power	kW	500	500	500	500
Auxiliary Power	kW	35.8	35.8	41.36	44.13
Drive Power	kW	32.2	32.2	29.04	40.00
Brake Power	kW	432	432	429.6	415.9
Indicated Efficiency	%	58.71	54.51	52.4	50.76
Combustion Efficiency	%	90.0	90.0	90.0	90.0
Brake Efficiency	%	45.65	42.2	40.5	38.0
Heater Head Material		U-700	U-700	In-625	In-625
Cylinder Material		713-LC	713-LC	713-LC	713-LC
Heat Input	kW	946.2	1018.8	1060.6	1095
bsfc	kg/kW	0,17	0.20	0.21	0.22
Torque	Nm	2289	2289	2278	–

TABLE 5.5-1

BRAKE POWER AND EFFICIENCY FOR ALTERNATE OUTPUT DRIVE SYSTEMS - 400 kW ENGINES

	Kinematic		FPSE	
Application	Output	Brake Efficiency	Output	Brake Efficiency
Rotary Power - Direct	429.6 kW	40.5%		
Rotary Power Through 95% Motor Efficiency			395.1 kW	36.1%
Hydraulic Power Through 92% Pump Efficiency	395.23 kW	37.26%		
Hydraulic Power - Direct			415.9 kW	38%

6.0 OVERALL RESULTS

The results of this study are:

- Task 1

  - With qualifying assumptions regarding seal life, an automotive Stirling engine can be adapted for stationary use by downrating output to achieve a 50,000-hour life and by removing extraneous auxiliaries.

  - The downrated engine has a brake efficiency of 35.5 percent at 30.6 kW brake output power with H_2 gas and 33.8 percent at 28.8 kW brake output power with He gas.

  - By changing materials and making small upper end dimensional changes, it is possible to optimize an automotive-based engine for the 50,000-hour stationary application. Optimized engines achieved brake efficiencies of 38.4 percent and 36.8 percent with H_2 gas and He gas, respectively, at 31.5 kW brake output power.

- Task 2

  - 400 kW kinematic engines can be designed with He working fluid and can achieve a brake efficiency of 42.4 percent with Udimet-700 heater tubes and 40.5 percent with Inconel-625 tubes with 50,000-hour operating life.

  - For the same material and working fluid (Inconel-625 and He gas), efficiency is increased relative to Task 1 optimized engine by improved geometry and reduced drive system losses associated with the variable Z-crank design.

- Task 3

  - A single-cylinder 30 kW hydraulic output FPSE can be designed for the same operating point and materials as in Task 1.2. A diaphragm is used in place of the power piston and supporting seal. Brake efficiency is 35.4 percent for hydraulic output, 33.6 percent for rotary output.

  - A "cam-driven concept" hydraulic pump, actuated by diaphragm motion, can provide stable pump and engine operation in a relatively small package.

- Task 4

  - A 400 kW, four-cylinder, free-piston diaphragm engine with hydraulic output is feasible.

  - Brake efficiency for this configuration is estimated at 38 percent for hydraulic output and 36.2 percent for rotary output by using Inconel-625 material and He gas.

  - A unique hydraulically actuated synchronization and balancing system can be easily incorporated into this design.

7.0 CONCLUSIONS

The major conclusions of this study of kinematic and free-piston Stirling engines of moderate (∿30 kW) and large (∿400 kW) size were found to be:

- 30 kW Kinematic (Task 1)
  - 50,000-hour life is feasible for the contemplated automotive Stirling engine if it is sufficiently downrated in power and speed.
  - Higher efficiencies can be achieved in such a unit if it is properly optimized for this lifetime requirement.
- 400 kW Kinematic (Task 2)
  - A Stirling engine of this size using an advanced, variable-stroke output control system is potentially viable and deserves further investigation.
- 30 kW FPSE (Task 3)
  - An FPSE design incorporating a hydraulic output system can provide operating efficiencies in the same range as a kinematic Stirling engine.
  - A hydraulic output system design compatible with an FPSE's power/stroke characteristic is feasible and deserves further investigation in a single-unit version.
- 400 kW FPSE (Task 4)
  - The conversion of a kinematic engine design into a free-piston version, while maintaining similar size and efficiency levels, was achieved through use of a new hydraulic output system that promises to have significant impact on free-piston engine designs for fluid applications.

This study characterized free-piston and kinematic Stirling engines for stationary applications from 30 kW to 400 kW load demands. Within the qualifying seal life assumptions, the proposed designs were found mechanically acceptable for the 50,000-hour life criteria and offer attractive efficiency levels from 34 to 45 percent. Further efficiency gains would be expected with extended design detailing and optimization studies beyond the scope of this study.

8.C REFERENCES

1. NASA-CR-165381 (MTI 81 ASE 164 DRZ), "Automotive Stirling Engine Reference Engine Design Report" June 1981

2. NASA-TM-D-5195 Creep Rupture Data for Welded N-155 Tubes. This was supplemented by MTI internal information.

3. NASA-CR-159588, "Design Study of a Kinematic Stirling Engine for Dispersed Solar Electric Power Systems" United Stirling, 1980

4. Engineer Report: Variable-Stroke Power Control Concept Study, 81ASE196ER18

5. Assessment of the State of Technology of Automotive Stirling Engines, September 1979, NASA-CR-159631

6. Walker, G., Stirling Engines, Claredon Press, Oxford, 1980, P. 76.

APPENDIX A

A.1 First Order Computer Code Description

The First Order Code was developed to provide:

- Basic understanding of engine operation
- Accurate predictions at reasonable cost

Its system of differential equations describing the engine can be solved to first order by assuming harmonic motion. The assumption of periodic solutions, coupled with an in-depth description of the thermodynamic cycle, has delivered satisfactory results.

A basic description of the code's calculations and assumptions includes:

- Basic Engine Layout (see Figure A-1). Note that Pistons E and C operate harmonically and that an external heat system to provide energy is not included in the code. The code also operates on alternative configuration Stirling engines.
- Continuity Equation
  - Basic Cycle Pressure Wave
  - Flow Distribution in Heat Exchangers
  - Assume:

    Harmonic displacement
    Adiabatic expansion/compression spaces
    Isothermal heat exchangers with linear variations
- Momentum Equation
  - Pressure Drop in Heat Exchangers
  - Assume:

    Harmonic flow
    Steady flow friction factors
    Periodic effects on friction
    Inertial and convective momentum
- Energy Equation
  - Temperature Amplitude and Phase in Expansion/Compression Spaces
  - Mean Temperature Distribution in Heat Exchangers
  - Heat Transfer In/Out of Working Fluid
  - Assume:

    Steady mean flow in each flow direction
    Steady flow convection heat transfer correlations

Figure A-2 displays the temperature-to-position relationship for a typical Stirling engine design as generated by the code. Figure A-3 provides a typical heat conduction network.

Fig. A-1 Basic Engine Layout for Code Analysis

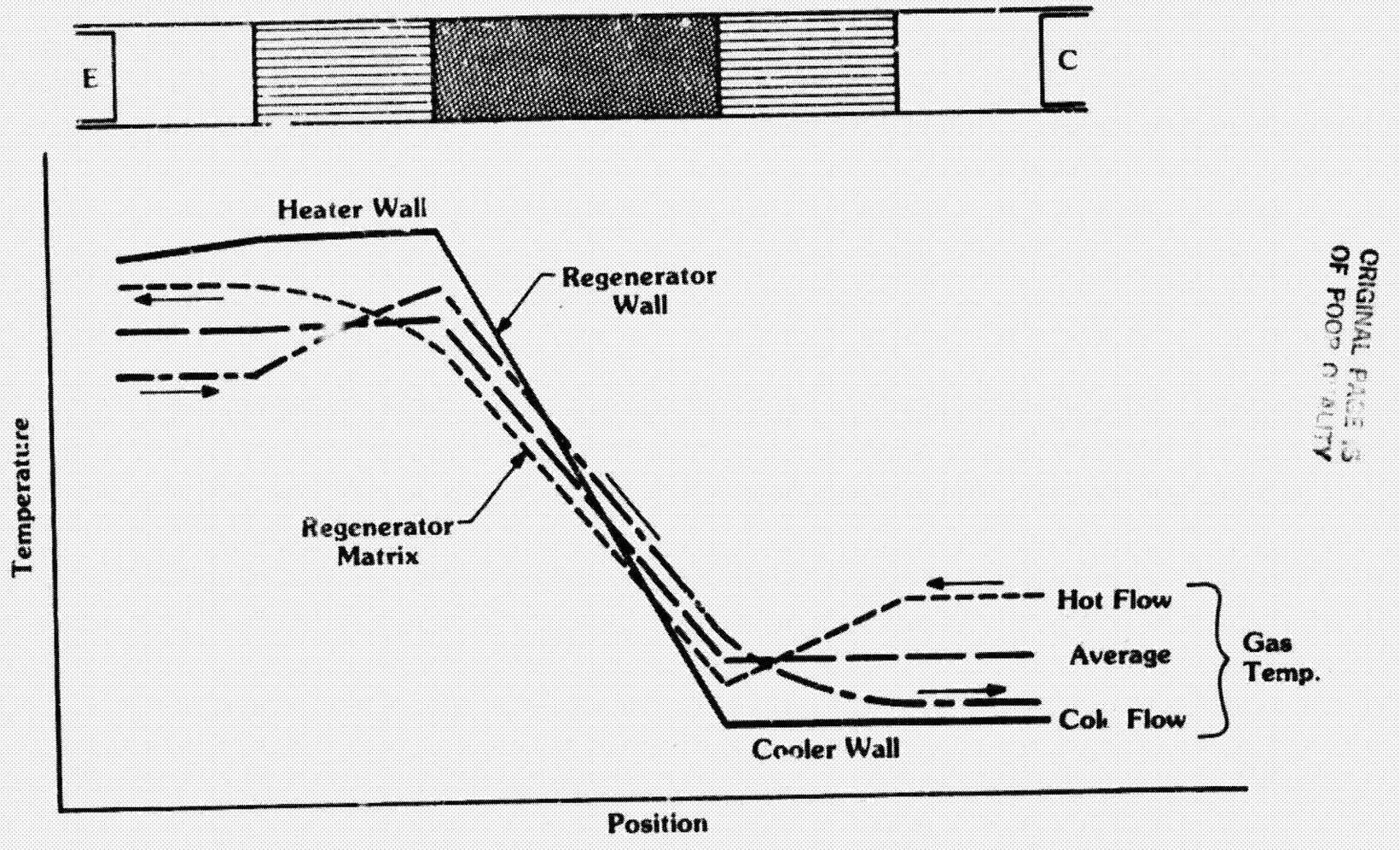

Fig. A-2 Practical Engine Temperature Distribution

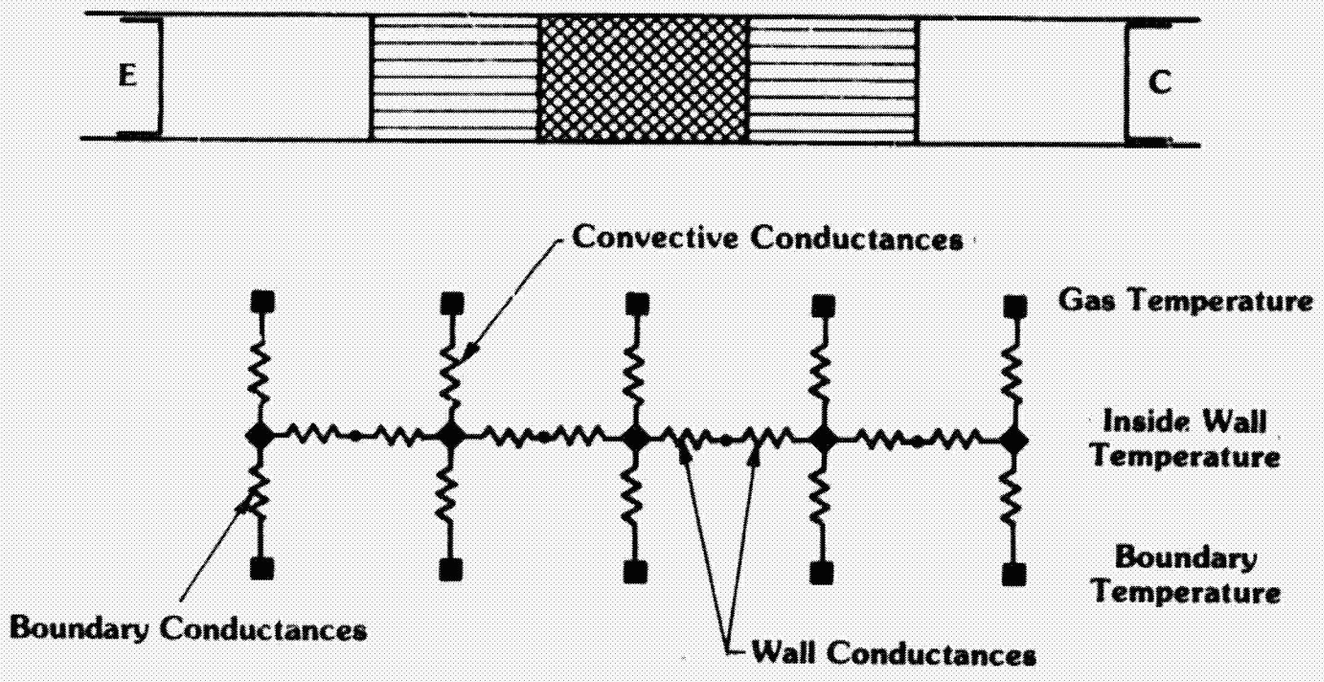

Fig. A-3 Heat Conduction Network

Parasitic losses evaluated by the code include:

- Seal leakage - coupled with thermodynamics
- Thermal hysteresis - first order
- Thermal shuttle loss - first order
- Conduction loss - coupled with boundary network

The code can operate on two-piston (alpha), relative-displacer (beta), and absolute-displacer (gamma) Stirling engines. The input requirements include a geometric description of the engines and its thermodynamic and dynamic operating levels. The output of the code includes:

- Input review
- Efficiency
- Component state and performance
- Pressure wave amplitudes and phase angles

In addition, the code also provides for optimization of key engine geometry dimensions, namely, the heater and cooler tube wall inner diameter (cm) and length/diameter ratio and regenerator frontal area, length, and porosity.

Heater tube life, required for the study, was not part of the First Order Code. To generate this information, material properties as defined by the Larson-Miller parameters were used to predict long-term creep rupture. This allowed optimization based on tube life as a function of geometry and operating point comparison with the performance effects of the tube's wall thickness and internal volume.

Since maximum pressure and thermal stresses occur at the inner surface of the heater tube, only the combined stress at this point was used to establish the criteria. Thick wall theory was applied for pressure and thermal stresses in terms of O.D./I.D. ratio as follows:

For hoop stress:

$$\sigma_p = p \frac{K^2 + 1}{K^2 - 1}$$

where:

$$K = \frac{O.D.}{I.D.}$$

p = maximum pressure

For thermal stress:

$$\sigma_E = \frac{\Delta T \alpha E}{2(1-\nu)} \left(\frac{2K^2}{K^2 - 1} - \frac{1}{\ln K} \right)$$

where:

ν = Poisson's ratio (assumed 0.3).

ΔT = Temperature gradient across tube wall.

E = Modulus of elasticity at the corresponding temperature.

α = Coefficient of thermal expansion at the corresponding temperature

Combine these two stresses. The procedure for this portion of the optimization is shown in Figure A-4.

Another modification to the code was an option to provide multiple rows of heater tubes rather than only a single row. The assumed gap between the tubes was one quarter of the diameter of the tubes in each row.

A.1.1 Validation

The main portions of the code were validated against actual data from the engines given in Table A-I. Table A-II lists the engine efficiency and indicated power at different speeds for a kinematic engine illustrating the similarity between actual and modeled data. Similar comparisons were completed for the other engine configurations.

A.1.2 Conclusions

Review of the information available resulted in the following conclusions:

- Good agreement with USS analytic prediction for Reference Engine (Basis for Stationary Stirling Study).
- Good agreement with Sunpower prediction for GASCON I Free-Piston Engine.
- Reasonable correlation with available data for USS P-40 and NASA GPU-3.

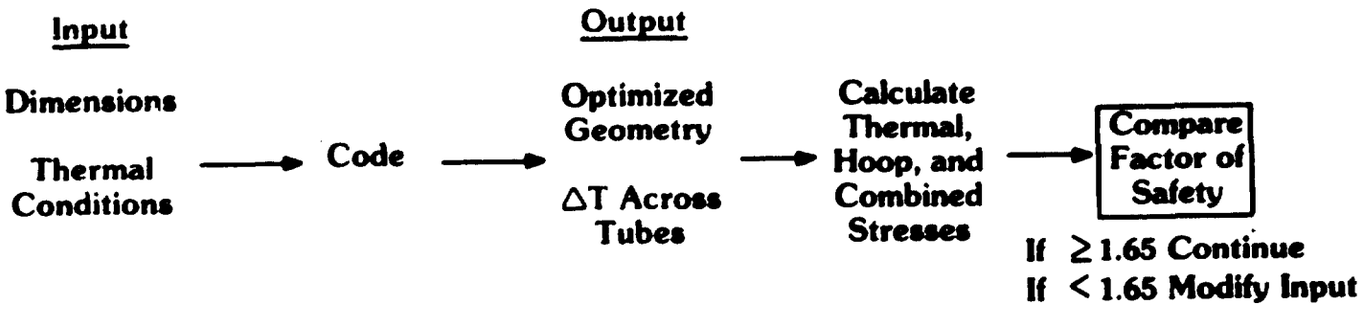

Fig. A-4 First Order Code System as Used for this Study

TABLE A-I

ENGINES USED FOR VALIDATION

- USS Reference Engine
  - Comparison of Indicated Performance with United Stirling Prediction
- GASCON I
  - *Comparison of Indicated and Component* Performance with Sunpower Prediction
- United Stirling P-40 (Engine #7)
  - Comparison of Indicated Performance with Acceptance Test Data
- NASA GPU-3
  - Comparison of Indicated Performance with NASA Initial Test Data

TABLE A-II

ACTUAL AND MODELED DATA

	Speed-rpm			
	1k	2k	3k	4k
Indicated Power (kW)				
Model (prediction)	16	31.6	44.2	50.5
Actual	14	31.6	44.2	48.3
% Change	14%	0	0	4%
Efficiency				
Model (prediction)	33.8	39.8	41.1	37
Actual	27.8	38.2	38.7	35
Δ Percent	6.0	1.6	2.4	2.0

15 mPa pressure 800°C Heater Temperature